

DISSERTATION

Submitted to the

Combined Faculties for the Natural Sciences and for Mathematics

of the Ruperto-Carola University of Heidelberg, Germany

for the degree of

Doctor of Natural Sciences

Presented by:

Dipl.-Biol. Eva Schlecker

Born in Illertissen

Oral examination: 14.07.2011

The role of tumor-infiltrating MDSC subsets in tumor progression

Referees:

Prof. Dr. Viktor Umansky

PD Dr. Adelheid Cerwenka

The work described in this thesis was started in January 2008 and completed in March 2011 under the supervision of PD Dr. Adelheid Cerwenka at the Research Group “Innate Immunity“ of the German Cancer Research Center (DKFZ), Heidelberg.

Parts of this thesis have been published in:

Nausch N, Galani I, **Schlecker E** and Cerwenka A: "Mononuclear myeloid-derived suppressor cells express RAE-1 and activate natural killer cells" *Blood*, 15. Nov. 2008; Vol. 112 No 10

Parts of this thesis have been awarded:

Schlecker E.

Oral presentation: "The two faces of myeloid-derived suppressor cells: Suppressor cells as NK cell activators" 1st Annual European Abstract Competition in Tumor Microenvironment; 11/2009; MedImmune Cambridge, UK

Conference and workshop presentations:

Schlecker E.

Oral presentation: "Chemokine networks in tumor progression: The role of tumor-infiltrating myeloid cells" Immuno-Moonsine Seminars; 02/2011; Heidelberg, Germany

Schlecker E, Stojanovic A and Cerwenka A.

Poster presentation: "Molecular characterization of tumor-infiltrating myeloid cell subsets".
Conference on Regulatory Myeloid Cells; 10/2010; Washington/Arlington, USA

Schlecker E.

Oral presentation: "Control of anti-tumor immune responses by myeloid-derived suppressor cells".
International PhD Student Conference; 05/2010; Milan, Italy

Schlecker E, Stojanovic A and Cerwenka A.

Poster presentation: "Myeloid-derived suppressor cells: reciprocal interaction with NK cells".
2nd European Congress of Immunology; 09/2009; Berlin, Germany

Schlecker E, Stojanovic A and Cerwenka A.

Poster presentation: "Crosstalk of natural killer cells with myeloid-derived suppressor cells"

4th ENII-MUGEN Summer School in Advanced Immunology; 05/2009; Capo Caccia, Italy

Nausch N, Galani IE, **Schlecker E** and Cerwenka A.

Poster presentation: "Myeloid-Derived "Suppressor" Cells express RAE-1 and activate NK cells"

EFIS-EJI Natural Killer Cell Symposium; 05/2008; Bad Herrenalb, Germany

Table of contents

1	ZUSAMMENFASSUNG.....	9
2	SUMMARY.....	11
3	INTRODUCTION.....	13
3.1	The immune system.....	13
3.1.1	The innate immune system.....	13
3.1.2	The adaptive immune system.....	14
3.2	Tumor immunology.....	14
3.2.1	Hallmarks of cancer.....	15
3.2.2	Cancer immunoediting.....	16
3.3	Monocyte and macrophage heterogeneity.....	18
3.3.1	Macrophage plasticity.....	18
3.3.2	Molecular pathways of macrophage polarization.....	20
3.4	Tumor-associated macrophages.....	20
3.4.1	Functions of TAMs.....	22
3.4.2	Therapeutic targeting of TAMs.....	23
3.5	Myeloid-derived suppressor cells.....	24
3.5.1	Historical overview.....	24
3.5.2	Origin of MDSCs.....	25
3.5.3	Mouse MDSC subset definition.....	25
3.5.4	Human MDSCs.....	26
3.5.5	Expansion and activation of MDSCs.....	27
3.5.6	MDSC-mediated suppression.....	29
3.5.7	Therapeutic targeting of MDSCs.....	33
4	AIM OF THE STUDY.....	36
5	MATERIALS AND METHODS.....	37
5.1	Materials.....	37
5.1.1	Mouse strains.....	37
5.1.2	Cell lines.....	37
5.1.3	Cell culture products.....	37
5.1.4	Cell culture media.....	38
5.1.5	Magnetic cell sorting (MACS).....	38

5.1.6	Kits.....	38
5.1.7	Antibodies	39
5.1.8	Chemicals and biological reagents.....	40
5.1.9	Solutions.....	41
5.1.10	Laboratory equipment	41
5.2	Methods.....	43
5.2.1	Cell culture methods	43
5.2.2	Mouse tumor models.....	43
5.2.3	<i>In vivo</i> treatment of mice.....	44
5.2.4	Organ dissection and preparation of single cell suspensions	44
5.2.5	Cell staining	45
5.2.6	Cell separation.....	46
5.2.7	Functional assays.....	48
5.2.8	Quantification of chemokines and cytokines.....	49
5.2.9	Gene expression profile analysis.....	49
5.2.10	Statistical analysis.....	50
6	RESULTS.....	51
6.1	Characterization of tumor-infiltrating MDSC subpopulations.....	51
6.1.1	Tumor-infiltrating MDSCs consist of a mononuclear and polymorphonuclear fraction	51
6.1.2	Phenotypic analysis of tumor-infiltrating MDSC subsets.....	53
6.1.3	Accumulation of MDSC subsets in the RMA-S tumor model	54
6.1.4	MO-MDSCs show a high proliferation rate	55
6.2	Gene expression profile of tumor-infiltrating MDSC subsets.....	55
6.2.1	Tumor-infiltrating MO-MDSCs upregulate expression of genes involved in suppression	59
6.2.2	Tumor-infiltrating MDSCs upregulate the expression of pro-inflammatory genes .	61
6.2.3	Tumor-infiltrating MO-MDSCs upregulate the expression of chemokines.....	65
6.3	Interaction of tumor-infiltrating MDSC subpopulations with immune cells	67
6.3.1	Functional properties of tumor-infiltrating MDSCs cultured with T cells	68
6.3.2	Effect of tumor-infiltrating MDSCs on NK cell function	68
6.4	TLR-4 signaling in tumor-infiltrating MDSC subsets	69
6.5	Tumor-infiltrating MO-MDSCs and their chemokine network.....	70

6.5.1	Expression of the CCR5 receptor on immune cells	71
6.5.2	Influence of exogenous CCR5 ligands on tumor progression	71
6.5.3	Influence of the CCR5 receptor on tumor progression	73
6.6	Manipulation of MDSCs <i>in vivo</i>.....	74
7	DISCUSSION	76
7.1	Tumor-infiltrating cells.....	76
7.2	Tumor-infiltrating MDSC subpopulations.....	77
7.2.1	Genetic profile of tumor-infiltrating MDSC subsets.....	78
7.2.2	Suppressive factors and their influence on immune cells	79
7.2.3	Pro-inflammatory phenotype.....	81
7.2.4	Chemokine-mediated migration	83
7.2.5	The role of CCR5 in tumor progression	84
7.3	Therapeutic implications.....	85
7.4	Concluding remarks	86
8	REFERENCES.....	87
9	ABBREVIATIONS.....	97
10	ACKNOWLEDGEMENTS.....	100

1 ZUSAMMENFASSUNG

Während der Tumorentwicklung führen eine Vielzahl an Mechanismen zur verstärkten Immunsuppression. Hierzu gehören Veränderungen in der Myelogenese, die zur Anreicherung und Rekrutierung von Suppressionszellen führen, auch bezeichnet als „Myeloide Suppressionszellen“ (MDSC = *myeloid-derived suppressor cells*). Ursprünglich wurden MDSCs in Tumorpatienten und Tumor-tragenden Mäusen als Zellen beschrieben, die in der Lage sind T-Zellantworten zu unterdrücken. Während der Tumorentwicklung akkumulieren MDSCs im Knochenmark, Blut, peripheren Lymphorganen und im Tumorgewebe. Sie bilden eine heterogene Gruppe aus myeloiden Zellen, die sich in verschiedenen Entwicklungsstadien befinden. Maus MDSCs sind durch ihre Koexpression der Oberflächenmoleküle Gr-1 und CD11b charakterisiert, die anhand ihrer morphologischen Unterschiede in zwei Untergruppen gegliedert werden. Während die mononukleären Zellen (MO-MDSC) die Marker Ly6C und F4/80 exprimieren, zeichnet sich die polymorphnukleäre Subpopulation (PMN-MDSC) durch eine Oberflächenexpression von Ly6G aus. Zusätzlich fehlt der PMN-MDSC Gruppe der Makrophagenmarker F4/80.

Ziel unserer Studie war es, die Verteilung der einzelnen MDSC Subgruppen im Blut und Tumor zu analysieren, deren Transkriptionsprofil zu untersuchen und anhand unterschiedlich exprimierter Proteine die Funktion zu bestimmen. Unsere Untersuchungen zeigten, dass nach subkutaner Injektion von RMA-S Zellen beide MDSC Populationen in den Tumor einwanderten. Genexpressionsanalysen mittels Microarray ließen deutliche Veränderungen des Transkriptionsprofils zwischen den Untergruppen im Blut bzw. im Tumor erkennen. Verglichen zu MDSCs aus dem Blut, zeigten Tumor-infiltrierende MO-MDSCs eine erhöhte Expression von Genen, die eine wichtige Rolle in Immunsuppression, Entzündungsantworten und Chemotaxis spielen. Die meisten dieser Genveränderungen auf Transkriptionsebene konnten ebenso auf Proteinebene bestätigt werden. Tumor-infiltrierende MDSCs wiesen eine erhöhte Oberflächenexpression von TLR-4, CD14, und Dectin-2 auf, was auf einen pro-inflammatorischen Phänotyp im Tumorgewebe rückschließen lässt. Stimulierung des CD14/TLR-4 Komplexes mit LPS führte zu einer erhöhten Expression des NKG2D Liganden, Rae-1, wodurch Natürlichen Killerzellen besser aktiviert werden könnten.

MO-MDSCs im Tumor zeigten eine erhöhte Aktivität von hemmenden Enzymen wie Arginase-1 bzw. iNOS verglichen zu MDSCs aus dem Blut. Zudem beobachteten wir, dass nur Tumor-infiltrierende MO-MDSCs hohe Mengen an Chemokinen produzierten. Dazu gehören drei Liganden des Chemokinrezeptors CCR5: CCL3 (MIP-1 α), CCL4 (MIP-1 β) und CCL5 (RANTES). Wiederholte Injektionen dieser rekombinanten Chemokine in den Tumor führten zur verstärkten Anreicherung von regulatorischen T-Zellen (Treg) bzw. zu einem verminderten Verhältnis von CD8⁺/Tregs im Tumor. Zusätzlich wurde das Tumorwachstum beschleunigt und die Überlebensrate der Mäuse verringert. Im Gegensatz dazu zeigten CCR5 defiziente Mäuse, die mit RMA-S Tumorzellen injiziert wurden, ein vermindertes Tumorwachstum und eine verlängerte

Überlebensrate, was mit einer erhöhten Zellzahl an CD4⁺ und CD8⁺ T-Zellen und einem Anstieg der CD8⁺/Treg Ratio im Tumor korrelierte.

Zusammenfassend zeigen unsere Daten, dass Tumor-infiltrierende MO-MDSCs eine unterstützende Rolle in der Tumorentwicklung übernehmen. Die erhöhte enzymatische Aktivität von Suppressionsfaktoren kann T-Zellantworten auf direktem Weg vermindern, während sezernierte Chemokine der Tumor-infiltrierenden MO-MDSCs indirekt das Immunsystem durch Anreicherung von Tregs im Tumor schwächt. Diese Ergebnisse beschreiben eine neue regulatorische Funktion der MDSCs in der Rekrutierung von Tregs, wodurch Behandlungen zur effektiven Tumorthherapie verbessert werden könnten.

2 SUMMARY

Several mechanisms have been proposed for profound immune impairments that accompany tumor development. Alteration in myelopoiesis that occur during tumor growth leads to the accumulation and recruitment of immunosuppressive cells, known as myeloid-suppressor cells (MDSCs). MDSCs have been characterized in cancer patients and tumor bearing mice based on their ability to suppress T cell responses. During tumor progression MDSCs accumulate in bone marrow, blood, peripheral lymphoid organs and in the tumor tissue. They represent a heterogeneous population of myeloid cells at different stages of differentiation. In mice these cells are characterized by the co-expression of the surface markers Gr-1 and CD11b. Within this population, two distinct MDSC subpopulations with clear morphological differences have been identified, comprising mononuclear cells (MO-MDSCs), which express Ly6C and the macrophage marker F4/80, and polymorphonuclear cells (PMN-MDSCs), which express Ly6G and do not display F4/80 surface expression.

The aim of this thesis was to determine the distribution of tumor-infiltrating and blood MDSC subsets as well as the molecular signature and function of genes differently regulated in MDSC subpopulations. We demonstrated that after subcutaneous injection of RMA-S tumor cells, both MDSC subsets accumulated in the tumor tissue. Gene expression profiling of blood and tumor-infiltrating MDSCs using whole genome microarrays revealed profound changes in the transcription profile between MDSC subsets in blood and tumor. Tumor-infiltrated MO-MDSCs displayed increased expression of genes involved in suppression, inflammatory responses and chemotaxis compared to blood MDSCs. We confirmed that differentially regulated genes at mRNA level were also differently expressed at protein levels and might play a significant role in MDSC function. In addition, tumor-infiltrating MDSCs showed an increased surface expression of TLR-4, CD14, and Dectin-2, suggesting a pro-inflammatory phenotype of these subsets in the tumor tissue. Stimulation of the CD14/TLR-4 complex with LPS resulted in an upregulation of the NKG2D ligand Rae-1, which might be involved in natural killer cell activation.

Compared to blood MDSCs, the activity of suppressive factors such as arginase-1 and iNOS was increased in tumor-infiltrating MO-MDSCs. In addition, we observed that only tumor-infiltrating MO-MDSCs expressed high amount of several chemokines including three ligands of the chemokine receptor CCR5: CCL3 (MIP-1 α), CCL4 (MIP-1 β) and CCL5 (RANTES). Intra-tumoral injection of these recombinant chemokines resulted in an increased accumulation of regulatory T cells and a lower CD8⁺/Treg ratio in the tumor tissue correlated with accelerated tumor growth and shortened survival of tumor-bearing mice. On the contrary, CCR5 deficient mice injected with RMA-S tumor cells showed reduced tumor growth and prolonged survival associated with high numbers of CD4⁺ and CD8⁺ T cells and an increased CD8⁺/Treg ratio detected in the tumor.

In summary, we demonstrated that tumor-infiltrating MO-MDSCs exerted key features to promote tumor progression. Increased expression of suppressive factors by MO-MDSC in the tumor tissue might directly downmodulate T cell responses, whereas chemokine secretion might

induce the accumulation of tumor-infiltrating regulatory T cells, resulting in additive immune suppression. Those findings defined a new regulatory role of MDSCs in recruiting Tregs, which might be clinically relevant in developing novel immunotherapeutic strategies for cancer patients.

3 INTRODUCTION

3.1 The immune system

The immune system represents a complex network of cells, tissues and organs that protects the host from foreign pathogens and tumors. The main function of the immune system is accomplished by the ability to recognize “non-self” and “altered-self” structures on infected or transformed cells. Molecules that can be recognized by the immune system are considered antigens. In vertebrates, the immune system is divided into two distinct components based on antigen specificity and kinetics of activation: the innate and the adaptive immunity.

3.1.1 The innate immune system

The innate immune system serves as the first line of host defence against pathogens and prevents the entrance and establishment of infectious agents. It is naturally present and does not require sensitization to antigens. The innate immune system is comprised of a variety of cells, including natural killer (NK) cells, monocytes/macrophages and dendritic cells (DCs) and several plasma proteins like the complement system.

Once an infectious agent penetrates physical and chemical barriers (e.g. epithelia), pattern recognition receptors (PRRs) of the innate immune system sense their molecular structures so called pathogen associated molecular patterns (PAMPs). Bacterial PAMPs often include cell wall components such as lipopolysaccharides (LPS), peptidoglycan and lipoteichoic acids. Additionally, fungal molecules (β -glycans) as well as viral proteins or unmethylated CpG motifs in bacterial and viral nucleic acids can be recognized. The best characterized PRRs are the Toll-like receptors (TLR), whose activation leads to pathogen uptake by phagocytic cells (including macrophages, dendritic cells, neutrophils). Beside pathogen destruction, pro-inflammatory cytokines and chemokines are secreted resulting in recruitment and activation of other immune cells [1]. One of the most potent effector cells of the innate immune system are DCs. They reside as immature cells in the tissue. Pathogen detection and uptake lead to their maturation and secretion of factors that support innate immune responses. Once matured, they migrate to the local lymph node, where they induce adaptive immune responses. Thus, DCs link the innate with the adaptive immune system by priming and enhancing further effector mechanisms.

3.1.2 The adaptive immune system

In contrast to innate immunity, the adaptive immune system shows delayed responses to pathogens. The two main cell populations of the adaptive immune system are T and B lymphocytes (T and B cells), which recognize a high diversity of antigens. Their receptors are random products of somatic gene rearrangement during maturation. The genes encoding these receptors are assembled from variable and constant fragments through the activity of enzymes called RAG-1 and RAG-2 (recombination activation gene) [2].

Defence against extracellular microbes and microbial toxin is mediated by B cells. They originate from bone marrow and their maturation is accompanied by the expression of membrane bound immunoglobulins, called B cell receptors (BCRs). Activation of B cells upon antigen encounter leads to their differentiation into either memory or antibody-secreting plasma cells. Antibodies are composed of different classes and therefore mediate a variety of specific responses including antigen neutralization, opsonization of pathogens or activation of the complement system.

While extracellular pathogens are recognized by B cells, intracellular microorganisms are detected by T lymphocytes via cell-mediated immune responses. T cells also arise in the bone marrow but, unlike B cells, migrate to the thymus to complete their maturation. Their receptors, T cell receptors (TCRs), recognize antigens only when displayed as peptides bound to self major histocompatibility complex (MHC). Based on the class of MHC molecules they bind to, T cells are divided into CD4⁺ (bind to MHC class II) or CD8⁺ subsets (bind to MHC class I). To fully activate T cells, additional costimulatory signals are necessary, which are displayed by antigen-presenting cells (APCs).

3.2 Tumor immunology

The ability of the immune system to identify and destroy tumor cells has been studied for many decades. In 1909, Paul Ehrlich proposed that the immune system could protect the host from neoplastic disease. Nearly 50 years later the concept of cancer immunosurveillance was introduced by Burnet and Thomas. Based on the better understanding of tumor biology, they predicted that lymphocytes were responsible for the elimination of continuously arising transformed cells [3]. Data supporting this hypothesis are derived from several studies carried out with immunodeficient mice. Moreover, clinical data have led to a growing appreciation that cancer immunosurveillance also occurred in humans (reviewed in [4]). Later on, Schreiber and colleagues proposed a more sophisticated theory implicating that immunity not only protects the host from tumor development but also promotes tumor growth by generating more aggressive tumors. The term “cancer immunoediting” has been used to describe this dual host protective and tumor promoting mechanism [5], [6].

3.2.1 Hallmarks of cancer

Cancers arise in a multistep process that reflects dysregulation of oncogenes, tumor suppression and pro-apoptotic signals. Genetic and epigenetic alterations lead to changes in cell growth, proliferation and differentiation and thus cause the development of tumors. As suggested by Hanahan and Weinberg, six essential alterations in cell physiology contribute to transform normal cells into malignant cancer cells: (a) self-sufficiency in growth signals, (b) insensitivity to anti-growth signals, (c) limitless replicative potential, (d) evasion of apoptosis, (e) sustained angiogenesis and (f) tissue invasion and metastasis [7].

a) Self-sufficiency in growth signals. Normal cells are dependent on growth signals to move into a proliferative state. Many cancer cells acquire the ability to generate their own growth factors, thereby reducing their dependence on stimulation from their normal tissue microenvironment. This creates a positive feedback loop that is known as autocrine stimulation.

b) Insensitivity to anti-growth signals. To maintain cellular quiescence and tissue homeostasis multiple anti-proliferative signals are established within a normal tissue. Such signals include soluble growth inhibitors like transforming growth factor- β (TGF- β), which prevents activation of transcription factors responsible for the cell cycle machinery. Many tumors disable components of the TGF- β -mediated signaling pathway to achieve insensitivity to those inhibitory signals.

c) Limitless replicative potential. In addition to avoiding anti-growth signals and generating positive growth signals, tumor cells also escape the normal limits of cell replication. Most malignant cells upregulate the expression of the enzyme telomerase (e.g. the subunit TERT; telomerase reverse transcriptase), which adds nucleotides to the ends of DNA. This in turn permits unlimited multiplication of descendant cells.

d) Evading apoptosis. Uncontrolled cell division can also be fueled by a cancer cell ability to evade programmed cell death (apoptosis). The apoptotic program can be carried out through two main pathways: surface receptors that bind survival or death factors (e.g. FAS receptor CD95), therefore monitoring the extracellular environment, and intracellular sensors that respond to abnormalities including DNA damage. Tumors can develop resistance to apoptosis-inducing effector mechanisms mediated by these pathways.

e) Sustained angiogenesis. The oxygen and nutrients supplied by the vasculature are crucial for cell function and survival. During tumor development incipient neoplasias display increased angiogenic ability in order to progress to a larger size. Secretion of augmented levels of the vascular endothelial growth factor (VEGF) to promote angiogenesis is one of the most common features of tumor cells.

f) Tissue invasion and metastasis. During tumor progression cancer cells escape the primary tumor mass and invade distant tissues. This invasion - metastasis - requires alterations of proteins involved in cell-cell adhesion (e.g. E-cadherin), as well as in the secretion of proteases like matrix metalloproteinases (MMPs) which degrade extracellular matrix proteins.

In the late 90s, “immuno evasion” has been proposed as an additional hallmark of tumors. In order to progress, tumors have to evolve strategies for evading immune responses. These mechanisms include production of immunosuppressive cytokines, apoptosis of activated T cells or loss of costimulatory and HLA class I molecules [8].

3.2.2 Cancer immunoediting

The concept of cancer immunoediting predicts that the immune system can recognize neoplastic cells. By eliminating high immunogenic tumor cells, new tumor cell variants with reduced immunogenicity may be selected and therefore favor the generation of tumors that show increased resistance to immune attack or that have acquired mechanisms that suppress immune effector functions. Taken together, cancer immunoediting comprises a dynamic process composed of three phases: elimination, equilibrium and escape (Figure 3.1). Elimination represents the classical concept of cancer immunosurveillance where immune cells fight arising tumors; equilibrium embodies the stage of immune-mediated latency after incomplete tumor destruction and escape refers to the final outgrowth of immune resistant tumors that are resistant to the immune system.

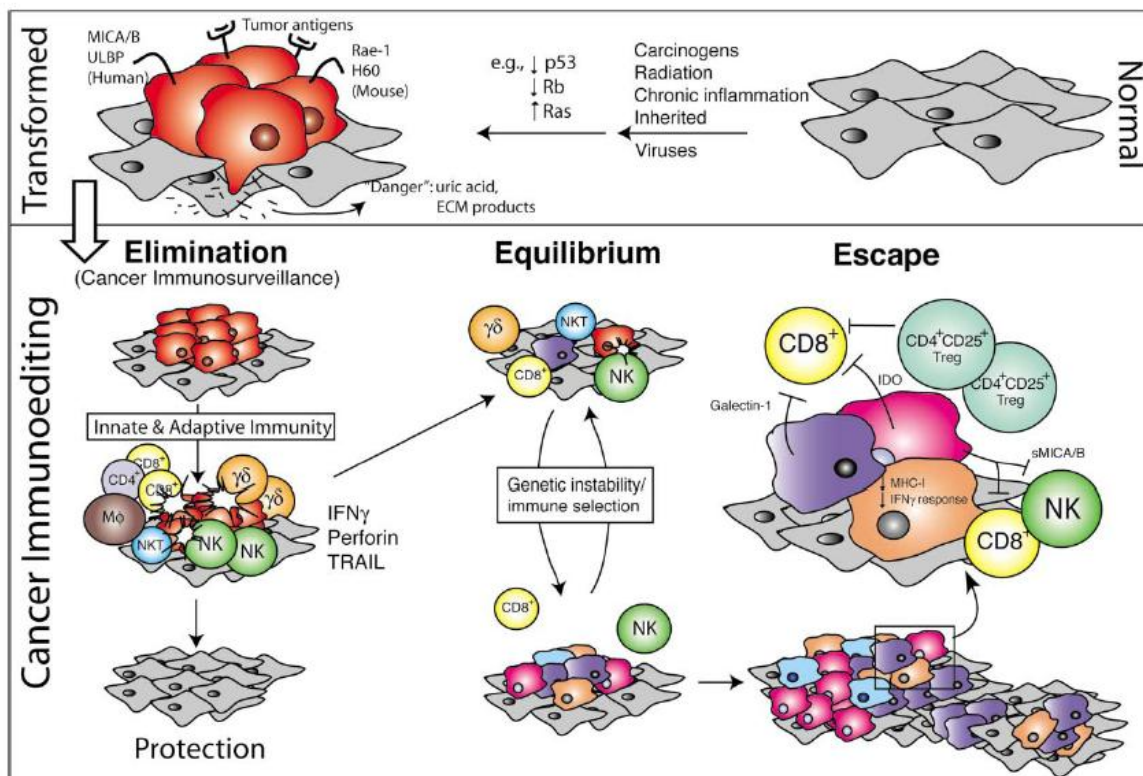


Figure 3.1: The three phases of the cancer immunoediting process

A variety of oncogenic stimuli transform normal cells into tumor cells (top). At early stages these cancer cells express distinct tumor-specific markers and initiate pro-inflammatory responses (bottom). In the elimination phase innate and adaptive immune cells recognize and kill tumor cells. During equilibrium tumor cells persist but are prevented from expanding by the immune system. However, less immunogenic tumor cells survive and escape resulting in tumor outgrowth. (Dunn *et al. Immunity* 2004; 21: 137-148)

3.2.2.1 Elimination phase: Anti-tumor immune responses

The elimination phase requires an integrated response involving both the innate and the adaptive arms of the immune system. Evidence was supported by tumors in mice lacking RAG-2, which cannot produce T cells, B cells and NKT cells. They develop tumors faster and with higher frequency than wild-type controls [9].

The initiation of the anti-tumor immune response occurs when cells of the innate immune system become alerted of the presence of the growing tumor. Local tissue disruption as a result of increased angiogenesis or tissue-invasive growth induces pro-inflammatory molecules (e.g. interleukin 1 (IL-1), tumor necrosis factor α (TNF- α), granulocyte-macrophage colony-stimulating factor (GM-CSF) or IL-15), leading to the recruitment of innate immune cells. Dendritic cells may act as sentinel cells sensing tissue stress, damage and transformation. Their ability to uptake heat shock proteins and products of extracellular matrix breakdown promotes differentiation and subsequent cross-talk between DCs and NK cells.

NK cells, macrophages, $\gamma\delta$ T cells and NKT cells are recruited to the site of “danger” and recognize molecules that can be induced on tumor cells upon cellular transformation, such as stress induced ligands for the activating receptor NKG2D [10]. In addition, MHC-tumor-associated peptide complexes or glycolipid-CD1 complexes expressed on developing tumor cells can be recognized by T cells and NKT cells, respectively [11]. These immune cells exert several effector mechanisms to eliminate tumor cells including the release of IFN- γ and perforin or the expression of death receptor ligands such as TRAIL. Secretion of IFN- γ controls tumor growth and amplifies immune responses through the production of chemokines. In return, chemokines attract more immune cells to the tumor site generating a positive feedback loop for tumor elimination.

In the next phase tumor antigens released during tumor cell killing drive the development of tumor-specific adaptive immune responses. Recruited immature DCs become activated through the tumor cytokine milieu and uptake of tumor antigens and migrate to the lymph nodes, where they induce the activation of naïve tumor-specific CD4⁺ and CD8⁺ T cells [12]. Once activated, tumor-specific T cells home to the tumor site to eliminate antigen-expressing tumor cells.

3.2.2.2 Equilibrium phase: Tumor persistence

In the equilibrium phase immune cells and tumor cells which survived the elimination phase enter a dynamic process where new tumor variants with increased resistance to the immune attack arise. Schreiber and colleagues hypothesized that equilibrium may be the longest of the three phases and may occur over a period of many years in humans [13]. During this period heterogeneity and genetic instability of remaining cancer cells may favor the generation of tumors that are either poorly recognized by the immune system or that have acquired mechanisms that suppress immune effector functions.

3.2.2.3 Escape phase: Tumor progression

In the escape phase, selective pressure of immune responses and further mutations in malignant cells lead to tumor progression. Most likely, tumors circumvent either one or both arms of the immune system by employing multiple immunoevasive strategies. Several studies documented that tumors can either directly (tumor intrinsic mechanism) or indirectly (tumor extrinsic mechanism) impede anti-tumor immune responses. Tumor intrinsic mechanisms include: (a) modified expression level of MHC class I/II and costimulatory molecules [14], (b) dysregulation of antigen processing [15] and (c) low levels of tumor antigen expression [16]. Indirect mechanisms are associated with: (a) tolerance of T cells to tumor-specific antigens resulting from energy [17], (b) suppression of immune effector cells via immunosuppressive cytokines such as TGF- β or IL-10 [18] or via regulatory cells [19] and (c) secretion of soluble ligands that block lymphocyte activation [20].

3.3 Monocyte and macrophage heterogeneity

Macrophages comprise an extremely heterogeneous population that originates from blood monocytes. They play an important role in the immune system with defined functions in both innate and adaptive immunity. In innate immunity they provide immediate defense against foreign pathogens through phagocytosis and subsequent degradation of apoptotic or possibly neoplastic cells. During the adaptive immune phase they interact with T and B cells by releasing cytokines, chemokines and reactive radicals. In cancer, macrophage activities can either prevent the establishment and spread of cancer (pro-inflammatory) or support tumor growth (anti-inflammatory). These polar phenotypes are not expressed simultaneously but are regulated through decisive functional programs in response to different micro-environmental signals [21].

3.3.1 Macrophage plasticity

Macrophages can be divided schematically into two main classes. M1 macrophages are classically activated macrophages induced by microbial products like LPS or cytokines like IFN- γ , TNF and GM-CSF. Alternative activation of M2 macrophages is regulated by IL-4, IL-13, IL-10 or glucocorticoids [22].

M1 and M2 polarized macrophages display a number of distinct features (Figure 3.2). Classical M1 macrophages are characterized by a high capacity to present antigens, they produce elevated levels of IL-12 and IL-23 and therefore activate type I T cell responses. Due to their high production of toxic intermediates (nitric oxide, NO; reactive oxxygen, intermediates ROI), M1 macrophages are potent effector cells that kill tumor cells and microorganisms. When exposed to

signals such as LPS and IFN- γ , they express opsonic receptors like Fc γ RIII (CD16) and produce pro-inflammatory cytokines in order to elicit adaptive immunity.

Alternatively activated M2 macrophages possess poor antigen presenting capacity, have an IL-12^{low}IL-10^{high} phenotype, secrete CCL17 and CCL22, suppress inflammatory responses and Th1 adaptive immunity, scavenge debris and promote wound healing, angiogenesis and tissue remodeling. They express surface markers like E-cadherin, CD163 and CD206 [23]. Instead of citrulline and NO production via iNOS as seen in M1 macrophages, the arginine metabolism of M2 macrophages is oriented towards ornithine and polyamine production [24], [25].

Mantovani and colleagues defined that various environmental signals further designate distinct M2 activation forms: M2a macrophages are activated by IL-4 and IL-13, M2b cells arise after exposure to immune complexes or agonists of TLR and IL-1R and M2c macrophages are predominantly induced by IL-10 [26].

Analogous to the M1/M2 paradigm, Geissmann *et al.* identified inflammatory and resident monocyte subsets. In mice, inflammatory monocytes exhibit a CX3CR1^{low}CCR2⁺Gr-1⁺ phenotype, are short-lived and recruited to inflamed tissue, whereas resident monocytes are characterized by a CX3CR1^{high}CCR2⁻Gr-1⁻ phenotype and are recruited to non-inflamed tissue [27].

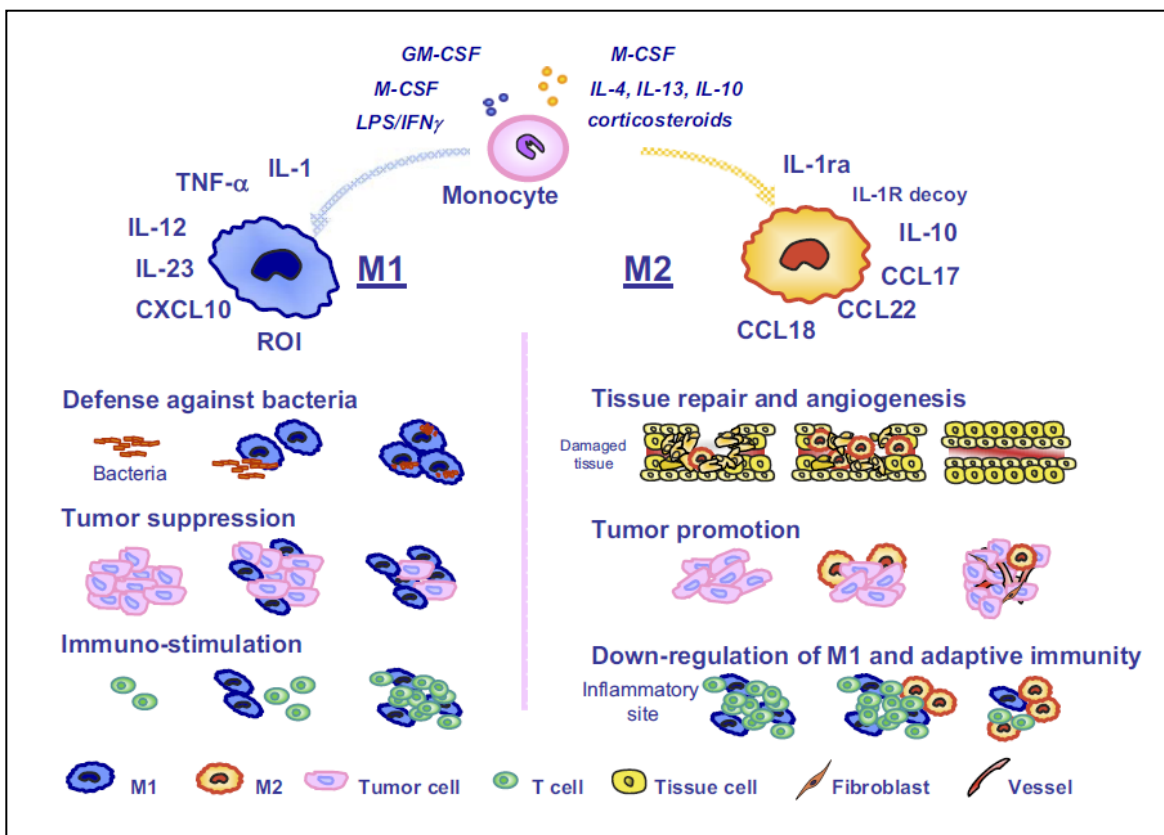


Figure 3.2: Polarization of macrophage function

Macrophages can be divided into two main classes: M1 and M2. Blood monocytes recruited from the circulation differentiate into mature macrophages within the tissue. In the presence of LPS/IFN- γ or GM-CSF polarization of M1 macrophages is induced. M1 macrophages produce high levels of IL-1, TNF- α , IL-12, IL-23, CXCL10 and ROI. They are characterized by cytotoxic activity against bacteria and neoplastic cells and by the capability of antigen presentation. Cytokines like IL-4, IL-13, IL-10 or glucocorticoids drive the M2 polarization. M2 macrophages secrete high amounts of IL-1ra, IL-10, CCL17, CCL18 and CCL22. They promote tissue repair, angiogenesis and tumor progression and additionally downregulate M1-mediated functions as well as adaptive immunity (Solinas *et al. Journal of Leukocyte Biology* 2009; 86: 1065-1073).

3.3.2 Molecular pathways of macrophage polarization

Macrophage phenotype and activation are regulated by three different pathways: (a) cytokine signaling pathway using Jak-STAT molecules, (b) microbial recognition receptors including TLRs and (c) immunoreceptors that signal via ITAM motifs (immunoreceptor tyrosine-based activation motif). M1 stimuli such as LPS and IFN- γ trigger TLR-4, IFN- α/β receptor or IFN- γ receptors. These signals result in activation of the transcription factors NF κ B, AP-1, IRF3 and STAT1 and further to the transcription of M1 genes. In contrast, M2 stimuli such as IL-4/13, signal through IL-4R α to activate STAT6, which regulates the expression of M2 genes. Immune complexes trigger the Fc γ R, an ITAM-containing receptor, leading to activation of kinases (e.g. Syk and PI3K) and the expression of molecules like prostaglandin E and IL-10 [28].

3.4 Tumor-associated macrophages

Solid tumors are constituted of different cell types including neoplastic cells, fibroblasts, endothelial and immune-competent cells, the latter mainly consists of macrophages and lymphocytes. Macrophages infiltrating the tumor, so called tumor-associated macrophages (TAM), are usually the most abundant immune population in the tumor and represent up to 50% of the tumor mass [29].

Pollard and colleagues have been proposed that macrophages in tumors confer several properties that enhance progression and metastasis, where each function is affected by a particular macrophage subpopulation ([30]; Figure 3.3).

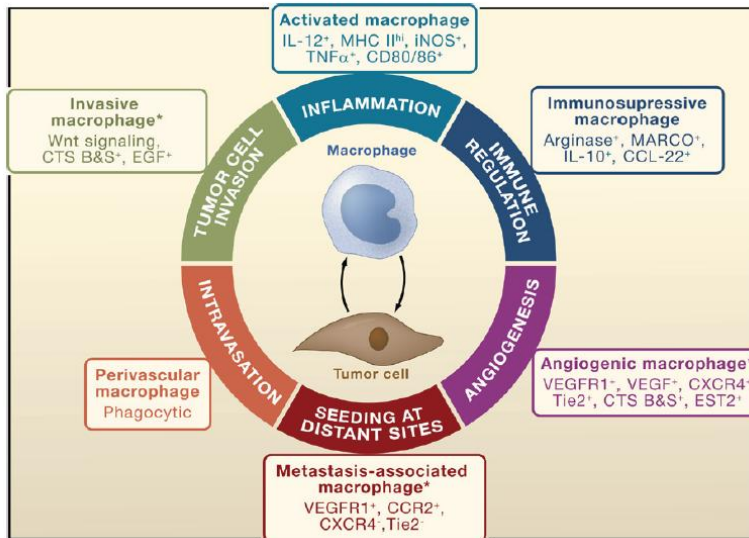


Figure 3.3: Macrophage subpopulations during tumorigenesis

Macrophages promote cancer progression. Shown are six macrophage functions that support tumor growth. Each function can be ascribed to a unique macrophage subpopulation

(Qian *et al Cell* 2010; 141: 39-51).

TAMs originate from blood monocytes that are recruited to the tumor site by several factors including macrophage colony-stimulating factor (M-CSF), GM-CSF, IL-3 and chemokines like CCL2. Experimental and clinical studies in thyroid, lung and hepatocellular cancers demonstrated that high levels of tumor-infiltrating macrophages were often correlated with poor prognosis [31], [32]. One of the key players of macrophage regulation is M-CSF, which overexpression was also associated with poor prognosis in several cancer types [33], [34]. In the breast cancer model polyoma middle T (PyMT) genetic ablation of M-CSF reduced macrophage infiltration as well as tumor progression and metastasis [33]. Similar effect could be achieved with antibody treatment that inhibits M-CSF or its receptor [35]. On the other hand, overexpression of M-CSF in wild-type tumors resulted in macrophage recruitment and increased tumor progression and metastasis.

TAMs resemble a modified M2 phenotype and their functional polarization is a result of the absence of M1 signals in the tumor like IFN- γ or bacterial components. Furthermore, M2 polarizing factors are highly presented and support their differentiation towards an IL-12^{low} IL-10^{high} phenotype. IL-10 secretion by TAMs promotes monocyte differentiation into macrophages and therefore avoids a differentiation to DCs [36]. An established gradient of IL-10 also influence incoming monocytes by their localization within the tumor. In breast cancer TAMs were equally distributed throughout the tissue whereas DCs were only present in the periphery [37]. Sica *et al.* observed that murine TAMs displayed a defective NF κ B activation in response to M1 signals confirming their low production of inflammatory cytokines (IL-12, IL-1 β , TNF- α and IL-6) [38]. Moreover, TAMs were poor producers of NO due to their low expression iNOS and secrete only low levels of reactive oxygen species (ROS) [39]. Genetic profiling of TAMs revealed an upregulation of several M2-associated genes such as CD162, Fc fragment of IgG, C-type lectin domains and heat shock proteins, therefore supporting their role as M2 macrophages [40].

3.4.1 Functions of TAMs

According to the M2 phenotype, TAMs have several pro-tumoral functions contributing to tissue remodeling and repair, promotion of angiogenesis and skewing inflammatory responses and adaptive immunity (Figure 3.4).

Angiogenesis. TAMs contribute to angiogenesis by producing multiple pro-angiogenic factors like TGF- β , VEGF, platelet derived growth factor (PDGF) and members of the fibroblast growth factor (FGF) family. In human cervical cancer, TAMs favor lymphoangiogenesis and formation of lymphatic metastasis through the release of VEGF [41]. In lung cancer, PDGF production by TAMs was proposed to support tumor progression [42]. Another feature of TAMs that promote angiogenesis is the production of various chemokines. Several studies indicated that secretion of CXCL12, CCL2, CXCL8, CXCL1, CXCL13 and CCL5 was involved in angiogenic processes including neo-vascularization [43], [44]. Production of these pro-angiogenic factors was further supported by the ability of TAMs to preferentially accumulate in hypoxic regions characterized by low oxygen levels. Hypoxia triggers a pro-angiogenic program which is mainly regulated by the transcription factors HIF-1 and HIF-2 (hypoxia-inducible factor-1/2). They induce expression of several pro-angiogenic factors such as VEGF, FGF, CXCL8 and CXCL12, which in turn amplify angiogenic responses [45].

Matrix remodeling and metastasis. TAMs support tumor invasion and metastasis by producing factors that can cleave the extracellular matrix and disrupt basal membrane. These factors include enzymes like MMP2 and MMP9. In several tumors MMP2 and MMP9 expression was highly increased, which was correlated with increased metastatic potential [46]. Moreover, chemokines like CCL5 or factors such as TNF- α , IL-1 β and VEGF can further increase the expression of MMPs resulting in an enhanced invasiveness of malignant cells [47], [48].

Suppression of adaptive immunity. The third feature of TAMs is to suppress adaptive immune responses directly through the secretion of immunosuppressive cytokines and indirectly through the release of chemokines. Due to the high activity of IL-10 and defective NF κ B pathway, low levels of immune stimulatory cytokines like TNF- α , IL-1 and IL-12 are produced resulting in decreased anti-tumor immune responses [38]. Mantovani and colleagues demonstrated that TAMs were poor antigen presenting cells but showed high potential to suppress T cell activation and proliferation via TGF- β and IL-10 [49], [23]. In addition, TAMs abrogate immune responses by their release of chemokines. In ovarian cancer it was shown that CCL18 attracted naïve T cells that became anergic in the tumor environment [50]. Moreover, by attracting Tregs to the tumor through the secretion of TAM-derived CCL17 and CCL22, anti-tumoral T cell responses were abolished [51].

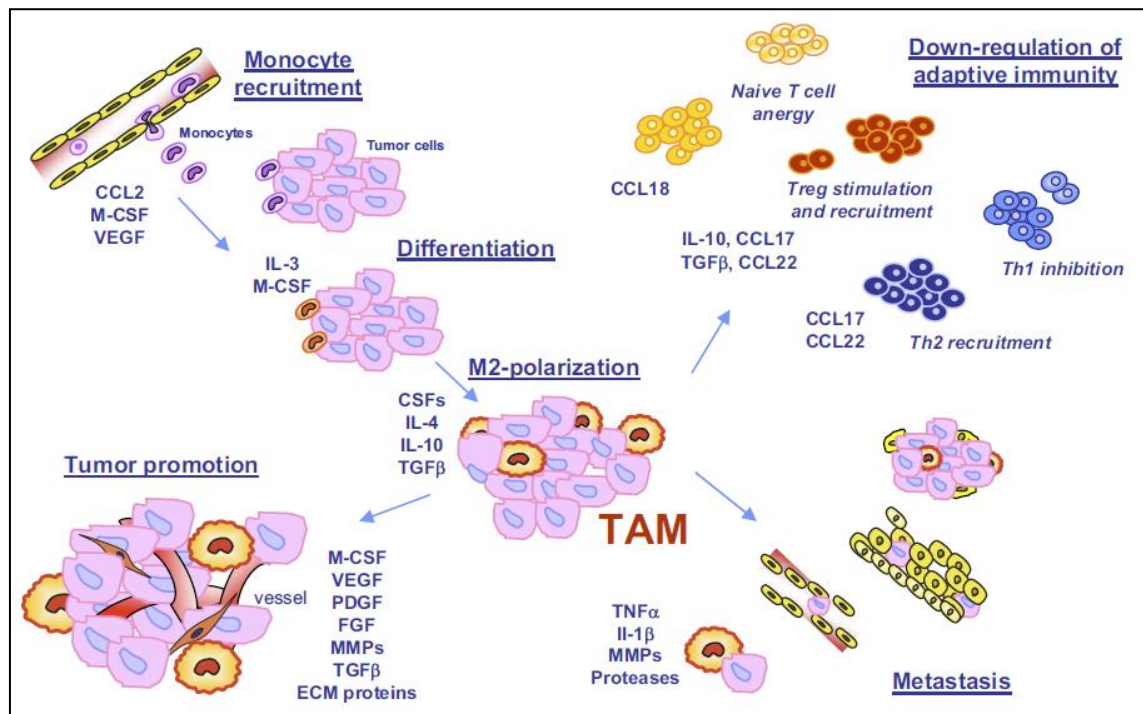


Figure 3.4: Origin and function of tumor-associated macrophages

Monocytes are recruited through the blood stream to the tumor site via CCL2, M-CSF and VEGF where they differentiate into TAMs. TAMs resemble M2 macrophages and support tumor growth and metastasis and downregulate adaptive immunity (Solinas *et al. Journal of Leukocyte Biology* 2009; 86: 1065-1073).

3.4.2 Therapeutic targeting of TAMs

Since TAMs support tumor growth and represent up to 50% of the tumor mass, therapeutic targeting of these cells might be an attractive approach for immunotherapy. Up to date three different strategies exist: (a) inhibition of TAM recruitment to tumor site, (b) blocking their pro-angiogenic functions and (c) reversal of their suppressive phenotype towards pro-inflammatory macrophages.

Recruitment. Recently it has been reported that Trabectedin, a natural product derived from the marine organism *Ecteinascidia turbinata*, exhibited anti-tumor activity with cytotoxic effect on monocytes and macrophages, including TAMs. While sparing the lymphoid population, Trabectedin reduced the production of CCL2 and IL-6 both in TAMs and tumor cells [52]. In the murine breast cancer model 410.4, it was shown that tumor cells recruited macrophages via CCL5. Treatment with Met-CCL5, a receptor antagonist for CCR5, decreased the level of TAMs along with reduced tumor size [53].

Angiogenesis and metastasis. VEGF plays an important role in monocyte recruitment to the tumor but also in neo-vascularization of tumors. Therefore, blocking of VEGF and its receptor

seemed to be a promising strategy. Anti-VEGF neutralizing antibody therapies could decrease metastasis whereas specific inhibition of VEGFR reduced macrophage infiltration into the tumor [54]. Another molecule, zoledronic acid, inhibits efficiently MMPs. Zoledronic acid treatment in murine cervical cancer suppressed MMP9 expression by infiltrating macrophages and blocked its activity, therefore reducing premalignant lesions and tumor growth [55].

Suppression. Shifting the M1-M2 balance towards M1 phenotype is the third strategy to circumvent pro-tumoral features of TAMs. Multiple studies indicated that the activation of Toll-like receptors like TLR9 stimulated M1 polarization of macrophages by inducing an inflammatory program [56]. Indeed, combination therapy of CpG, the ligand of TLR9, and anti-IL-10R antibody shifted infiltrating macrophages towards M1 phenotype and resulted in triggering innate immune responses [57].

3.5 Myeloid-derived suppressor cells

Myeloid-derived suppressor cells (MDSCs) represent a heterogeneous population of myeloid cells comprising macrophages, granulocytes, dendritic cells and other myeloid cells at different stages of differentiation. During tumor progression MDSCs accumulate in blood, lymph nodes, bone marrow and tumor site in cancer patients and tumor-bearing mice. These cells are potent suppressors of various T cell functions and their suppressive function is highly correlated with increased production of reactive oxygen and nitrogen species as well as elevated levels of arginase-1.

3.5.1 Historical overview

Studies in 1970s identified a formerly unknown cell population with suppressive features. These cells accumulated in bone marrow and spleen of tumor-bearing mice and were capable of suppressing T cell responses *in vitro* and *in vivo* [58], [59]. The term “natural suppressor cells” has been embossed and further characterization revealed their involvement in tolerance induction by inhibiting different effector functions of the immune system [60]. Subsequent studies described these cells as immature myeloid cells that were precursors of DCs, macrophages and granulocytes. Additional terms like “immature myeloid cells” (IMCs) or “myeloid suppressor cells” (MSCs) were used to specify their features. In 2007 the name “myeloid-derived suppressor cells” (MDSCs) was suggested [61].

3.5.2 Origin of MDSCs

In the bone marrow of healthy individuals hematopoietic stem cells give rise to common myeloid precursor cells, which generate immature myeloid cells without suppressive function. Under normal conditions, these cells are released into the peripheral blood and migrate to peripheral lymphoid organs. In the periphery, they differentiate into mature macrophages, DCs or neutrophils. Several pathologic processes like infection, trauma, inflammation or cancer can block the differentiation of IMCs and thereby expanding this immature population and abrogating the development of functional effector cells. During tumor development or infection these cells can be activated in response to tumor- or pathogen-derived factors. As a result, IMCs differentiate into MDSCs and produce factors like arginase-1 or and iNOS to suppress immune functions.

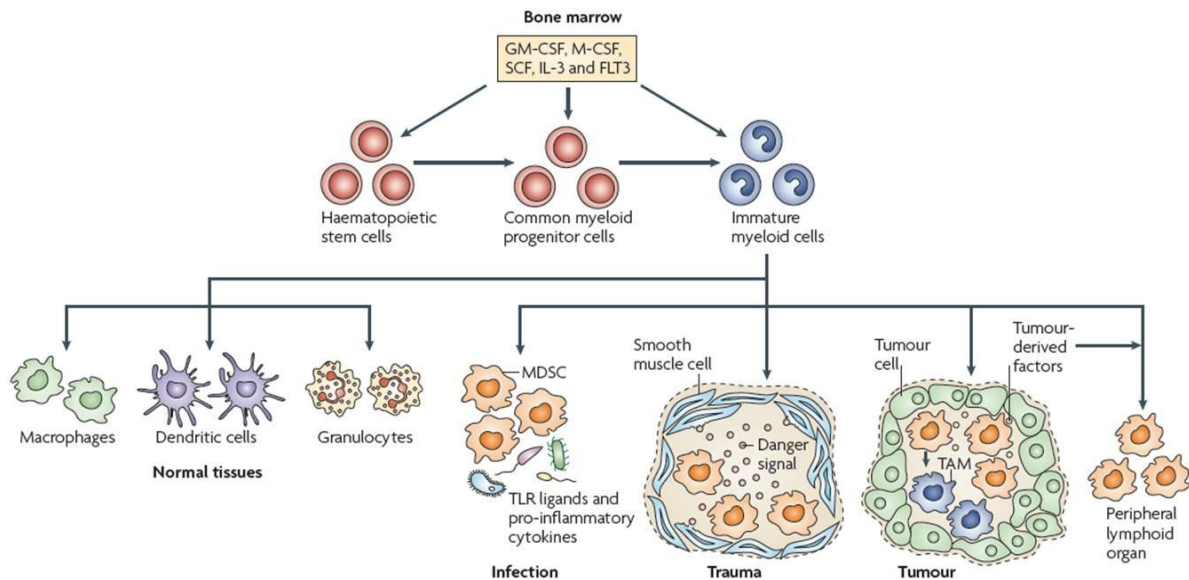


Figure 3.5: The origin of MDSCs

Myelopoiesis of immature myeloid cells (IMC) is controlled by soluble factors including GM-CSF, M-CSF, SCF, IL-3 and FLT3. Under healthy conditions, IMCs migrate to peripheral organs and differentiate into macrophages, DCs and granulocytes. Infection, trauma or tumor environment promote the accumulation of IMCs, prevent their differentiation and induce their activation to MDSC. (Gabrilovich *et al. Nature Reviews Immunology* 2009; 9: 162-174).

3.5.3 Mouse MDSC subset definition

MDSCs comprise a phenotypically heterogeneous population of myeloid cells, which are in mice characterized by the co-expression of the myeloid cell differentiation antigen Gr-1 and CD11b (α M-integrin) [62], [19]. In healthy mice, these cells display 20-30 % of bone marrow cells, 2-4 % of splenocytes and are absent from the lymph nodes. Recently, two morphological and functional distinct MDSC subpopulations were described based on their expression of Gr-1 (see 3.5.6). The

Gr-1 antigen includes the macrophage and neutrophil markers Ly6C and Ly6G, which can be separately detected by antibodies specific for their distinct epitopes. The Ly6 family displays a group of low molecular weight molecules (12-20 kDa) that are phosphatidylinositol-anchored cell surface glycoproteins. Their triggering leads to a signal transduction resulting in T cell activation [63]. Using Ly6G and Ly6C markers, two MDSC subsets were identified: CD11b⁺Ly6G⁺Ly6C^{low} MDSCs morphologically resembling polymorphonuclear granulocytes (PMN-MDSCs) and CD11b⁺Ly6G⁻Ly6C^{high} MDSCs with monocytic phenotype (MO-MDSCs) [64]. Analysis of different tumor models showed that during tumor growth both subpopulations expanded, but in most cases the accumulation of PMN-MDSC was more prominent [65].

Novel studies defined an additional subset according to the Gr-1 staining intensities. CD11b⁺ splenocytes from different tumor models could be divided into Gr-1^{high}, Gr-1^{int} and Gr-1^{low} cells. Gr-1^{high} cells represented the PMN-MDSC subset, which exerted weak or no suppression on CD8⁺ T cells. While Gr-1^{low} cells resembled MO-MDSCs with strong suppressive potential, the Gr-1^{int} subset displayed moderate suppression [66].

Further studies have identified additional phenotypic markers: including CD80 (B7.1) [67], CD115 (M-CSF receptor) [68] and CD124 (IL-4 receptor α) [69]. However, the involvement of CD124 and CD115 in T cell suppression remains controversial. Bronte and colleagues proposed that the suppressive activity of MDSCs was exclusively restricted to CD124⁺ cells, whereas Youn *et al.* showed that MDSCs had the same ability to suppress T cell proliferation independent on CD115 and CD124 [65], [69]. Overall, these studies suggested that MDSCs were not a defined subset of cells but rather a group of heterogeneous myeloid cells that share the common biological activity to suppress T cells.

3.5.4 Human MDSCs

The lack of a Gr-1 homologue in humans makes it difficult to identify human MDSCs. Since there are no specific markers known yet, human MDSCs are even less well defined than in mice. Several different combinations of surface molecules have been used to describe MDSCs in cancer patients based on their suppressive capacities. First reports characterized MDSCs as Lin⁻HLA-DR-CD33⁺ or CD14⁻CD11b⁺CD33⁺ cells [70], [71]. More recently, new markers have been associated with their function. In melanoma patients, the monocytic fraction expressing CD14⁺CD11b⁺HLA-DR^{-/low} was identified to mediate immune suppression via TGF- β [72]. Similarly, monocytic CD14⁺ MDSCs with high arginase activity from hepatocellular carcinoma were observed to suppress autologous T cell proliferation and induced the expansion of IL-10 secreting regulatory T cells [73]. Similar to mice, several reports suggested CD124 as a MDSC marker in humans. Patients with non-small cell lung cancer showed an increased level of MDSCs expressing CD124, which were able to downregulate the expression of CD3 ζ chain on CD8⁺ T cells [74]. Moreover, studies in melanoma patients revealed that the upregulation of CD124 correlated with an immunosuppressive phenotype of MO-MDSCs [75]. Rodriguez *et al.* proposed CD66b, a member of the carcinoembryonic antigen (CEA)-like glycoprotein family, as a marker for the granulocytic MDSC subpopulation in patients

with renal cell carcinoma [76]. Due to the heterogeneity of human MDSC populations the identification in cancer patient is challenging and further investigations are required to identify new and potentially unique markers.

3.5.5 Expansion and activation of MDSCs

Various findings indicated that tumor-derived factors (TDF) promoted not only MDSC expansion but also their activation toward an immunosuppressive phenotype. Table 3.1 summarizes factors, which influence MDSC expansion and their activation in mouse models and human cancers.

FACTORS	TUMOR MODEL (mouse)	TYPE OF CANCER (human)
MDSC Expansion		
Prostaglandins	Mammary carcinoma, lung cancer, renal and colon cancer	ND
Stem cell factor (SCF)	Colon carcinoma	ND
M-CSF	Sarcoma and mammary carcinoma	Human renal carcinoma cell lines
IL-6	Mammary carcinoma	ND
GM-CSF	Lewis lung carcinoma, colon carcinoma, mammary adenocarcinoma	Melanoma
G-CSF	Lewis lung carcinoma, methA sarcoma, melanoma	ND
VEGF	Breast cancer, sarcoma, melanoma, lymphoma, lung carcinoma	Breast cancer, renal cell cancer, pancreatic cancer
S100A8 and S100A9	Colon carcinoma, lymphoma, fibrosarcoma, mammary carcinoma	ND
MDSC Activation		
IFN- γ	Mammary adenocarcinoma, fibrosarcoma, colon carcinoma, lymphoma	ND
IL-4/IL-13	Colon carcinoma, fibrosarcoma, mammary adenocarcinoma, lymphoma	ND
TGF- β	Colon carcinoma, fibrosarcoma, mammary adenocarcinoma	Head and neck cancer
IL-1 β	Fibrosarcoma, mammary carcinoma	ND
CCL2	Lewis lung carcinoma, methA sarcoma, melanoma, lymphoma	ND

Table 3.1: Factors involved in MDSC expansion and activation

Table adapted from Gaborilovich *et al. Nature Reviews Immunology* 2009; 9: 162-174

Mechanisms of MDSC expansion. Prostaglandins, stem cell factor (SCF), M-CSF, IL-6, GM-CSF and VEGF belong to the well studied factors that can induce MDSC expansion. In myeloid cells many of them are involved in the triggering of Janus kinase (JAK) and signaling transducer and activator of transcription 3 (STAT3) signaling pathways, which results in the expression of B cell lymphoma XL (Bcl-XL), cyclin D1, MYC and survivin (Figure 3.6). Subsequently, survival and proliferation of myeloid progenitor cells are increased [77]. Nefedova *et al.* observed that MDSCs from tumor-bearing mice had elevated levels of phosphorylated STAT3 compared to healthy mice. Constitutive STAT3 activity prevented maturation of DCs and thereby promoted expansion of MDSCs [78]. Ablation of STAT3 in conditional knock-out mice impaired MDSC expansion and abolished suppressive activity of MDSCs in tumor-bearing mice [79]. Downstream of STAT3 signaling the expression of calcium-binding pro-inflammatory proteins S100A8 and S100A9 is induced, whose receptors are expressed on MDSCs [80]. *In vitro* studies revealed that STAT3-dependent upregulation of S100A8/A9 in hematopoietic progenitor cells inhibited DC and macrophage differentiation and promoted MDSC accumulation. Tumor-bearing mice lacking S100A9 showed a reduced level of MDSCs accompanied by tumor regression [81]. Sinha *et al.* reported that S100A8/A9 contributed to the recruitment of MDSCs to tumor sites through NF κ B-dependent pathways [82]. Moreover, accumulation of MDSCs in spleen was abrogated in mice deficient of the transcription factor C/EBP- β , which was controlled by STAT3 [83].

Mechanisms of MDSC activation. Gabrilovich and colleagues have proposed that factors responsible for MDSC expansion were not sufficient to generate MDSC activity [84]. MDSCs seem to require a second activating signal to upregulate suppressive factors including arginase, NO and immune suppressive cytokines. The second signal is provided by activated T cells, tumor stromal cells and infected cells, which secrete IFN- γ , ligands for TLRs, IL-4, IL-13, and TGF- β resulting in STAT1 and STAT6 signaling (Figure 3.6). Similar to STAT3 in MDSC expansion, STAT1 and STAT6 play a central role in MDSC activation. STAT1 is the main transcription factor activated by IFN- γ and IL-1 β . STAT1 deficient MDSCs failed to inhibit T cell proliferation due to the inability to upregulate arginase or iNOS [85]. Activation of STAT6 by CD124 signaling results in the expression of arginase-1 and TGF- β , which increases the suppressive activity of MDSCs [86], [87]. Studies in a polymicrobial sepsis model revealed MDSC accumulation in spleen, which was dependent on the TLR adaptor protein MyD88. However, experiments with TLR4 deficient mice with bacterially induced sepsis demonstrated that MDSCs could still accumulate indicating that they might be activated through other TLRs [88].

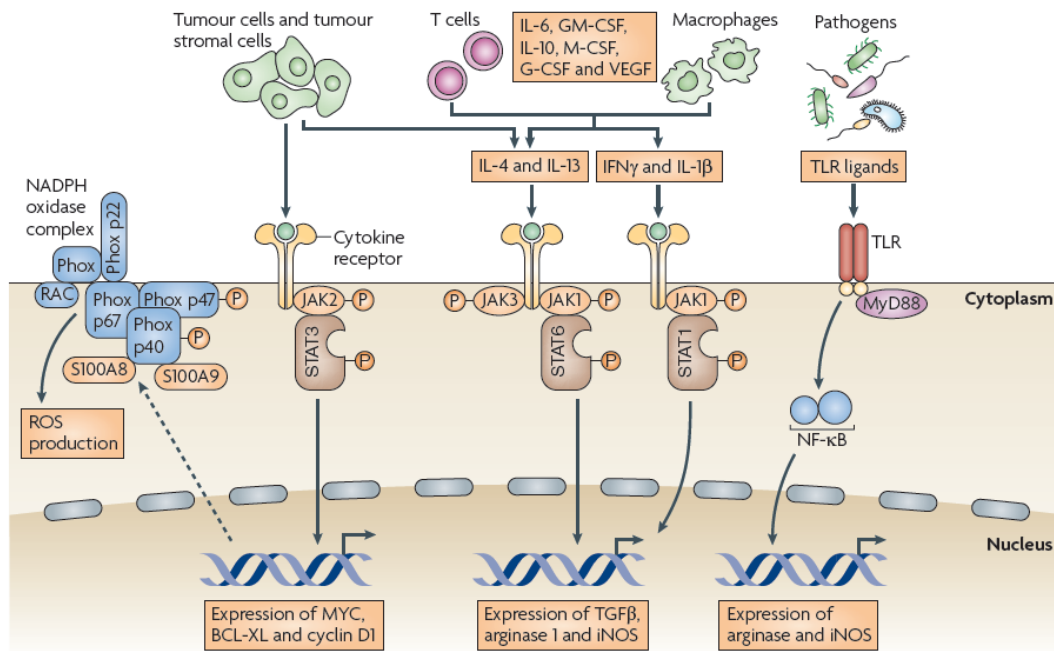


Figure 3.6: Signaling pathways involved in MDSC expansion and activation

MDSC expansion and activation is regulated by several factors secreted by tumor cells, tumor stromal cells, T cells, macrophages and pathogens. These factors trigger different pathways involving STAT3, STAT6, STAT1 and NF κ B. Once activated these transcription factors induce the expression of survival and cell cycle genes like *myc*, *bcl-xl* and *cyclin D1* or genes like TGF- β , *arginase-1* and *iNOS*, which are involved in T cell suppression. In addition, STAT3 triggers an alternative pathway leading to the expression of the pro-inflammatory proteins S100A8 and S100A9 and upregulation of reactive oxygen species (Gabrilovich *et al. Nature Reviews Immunology* 2009; 9: 162-174)

3.5.6 MDSC-mediated suppression

MDSCs suppress immunity by interfering with both innate and adaptive immune responses. First studies in mice demonstrated that MDSCs inhibited T cell responses by blocking their activation (IFN- γ production) and proliferation [62]. Subsequent reports showed that MDSC activity required cell-cell contact and could be antigen-specific or non-specific, dependent on the MDSC subpopulation [65]. The role of MDSCs suppressing NK cells is controversial. Some studies observed that they abrogated NK cell cytotoxicity against tumor cells and inhibited IFN- γ production by NK cells [89], [90]. On the contrary, it has been reported that monocytic MDSC expressing Rae-1, the ligand for NKG2D, activated NK cells to produce IFN- γ [91]. Moreover, cross-talks between MDSCs and macrophages have been reported. High production of IL-10 by MDSCs converted macrophages to M2 phenotype, which resulted in downregulation of the macrophage type I cytokine IL-12 [92]. The following paragraph summarizes mechanisms that have been implicated in MDSC-mediated suppression.

L-arginine metabolism. Initial studies associated the suppressive activity of MDSCs with the L-arginine metabolism. L-arginine is used for biosynthesis of the proteins creatine and agmatine and is mainly metabolized by the enzymes arginase and NOS to produce urea and L-ornithine, and NO and L-citrulline, respectively (Fig. 3.7) [93].

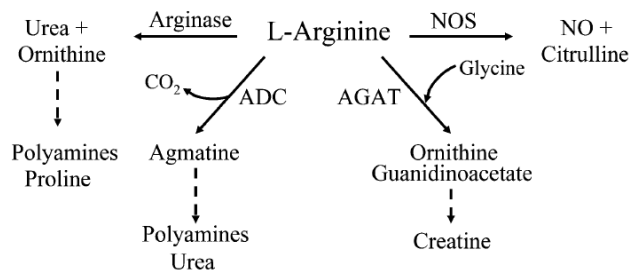


Figure 3.7: L-arginine metabolism

L-arginine is metabolized by arginase into urea and ornithine, which is used as a substrate for polyamine and proline synthesis. In addition L-arginine is degraded by NOS into NO and citrulline to produce creatine. (Rodriguez *et al. Immunological Reviews* 2008; 222: 180-191)

Two arginase isoforms (Arg-1 and Arg-2) have been identified in mammals, which share 58% sequence identity at the amino-acid level. The liver-type arginase, Arg-1, is located in the cytoplasm of hepatocytes and is an important component of the urea cycle. Exposure to IL-4, IL-13, IL-10 or TGF- β upregulates Arg-1 via the transcription factor STAT6. The kidney-type Arg-2 is located in the mitochondria of renal cells, neurons and macrophages and is involved in L-proline synthesis [94]. In addition, three distinct isoforms of NOS have been described so far: nNOS (NOS1, in neuronal tissue), iNOS (NOS2, inducible in various cells of the immune system) and eNOS (NOS3, in endothelial cells). iNOS expression has been reported in macrophages, granulocytes, DCs and NK cells and can be induced by IFN- γ , LPS, IL-1, TNF and type I IFNs. These cytokines activate the transcription factors NF κ B, AP1 and STAT1 [95].

It was shown that MDSCs express Arg-1 and iNOS, either separately or in combination to inhibit immune responses. Rodriguez *et al.* observed that MDSCs expressing Arg-1 can take up L-arginine from the extracellular environment, which inhibits the re-expression of the CD3 ζ chain after internalization by antigen-stimulated T cells [96]. CD3 ζ is the main signal-transduction component of the TCR and is required for correct assembly of the receptor complex. Depletion of L-arginine and high production of urea alter the translation of mRNA in T cells resulting in repression of CD3 ζ (Figure 3.9a). NO produced by iNOS mediates T cell suppression via mechanisms associated with the IL-2 signaling cascade. Uptake of NO by T cells leads to nitrosylation of crucial cysteine residues or to the activation of cyclic-GMP-dependent kinase [97]. These changes interfere with the IL-2 receptor signaling pathway by blocking the phosphorylation of kinases or by altering the IL-2 mRNA stability (Figure 3.8b).

Reactive oxygen and nitrogen species. When both enzymes Arg-1 and iNOS are activated, the production of reactive oxygen and nitrogen species is initiated (e.g. superoxide O_2^- , peroxynitrites $ONOO^-$, hydrogen peroxide H_2O_2). $ONOO^-$ is a product of the chemical reaction between O_2^- and NO and represents a highly reactive oxidizing agent. In the cytoplasm of T cells it can induce post-translational protein modifications by nitrating tyrosine, cysteine, methionine and tryptophan residues of proteins and thereby influencing enzyme activity, cell proliferation and survival [98]. H_2O_2 is induced by the interaction of O_2^- with hydrogen protons (H^+) from H_2O . It is stable, diffuses

across membranes and can interfere the expression of B cell lymphoma 2 (Bcl2), CD95 ligand (CD95L) and CD3 ζ . As a result, T cell dysfunction and apoptosis is initiated (Fig 3.8c) [99].

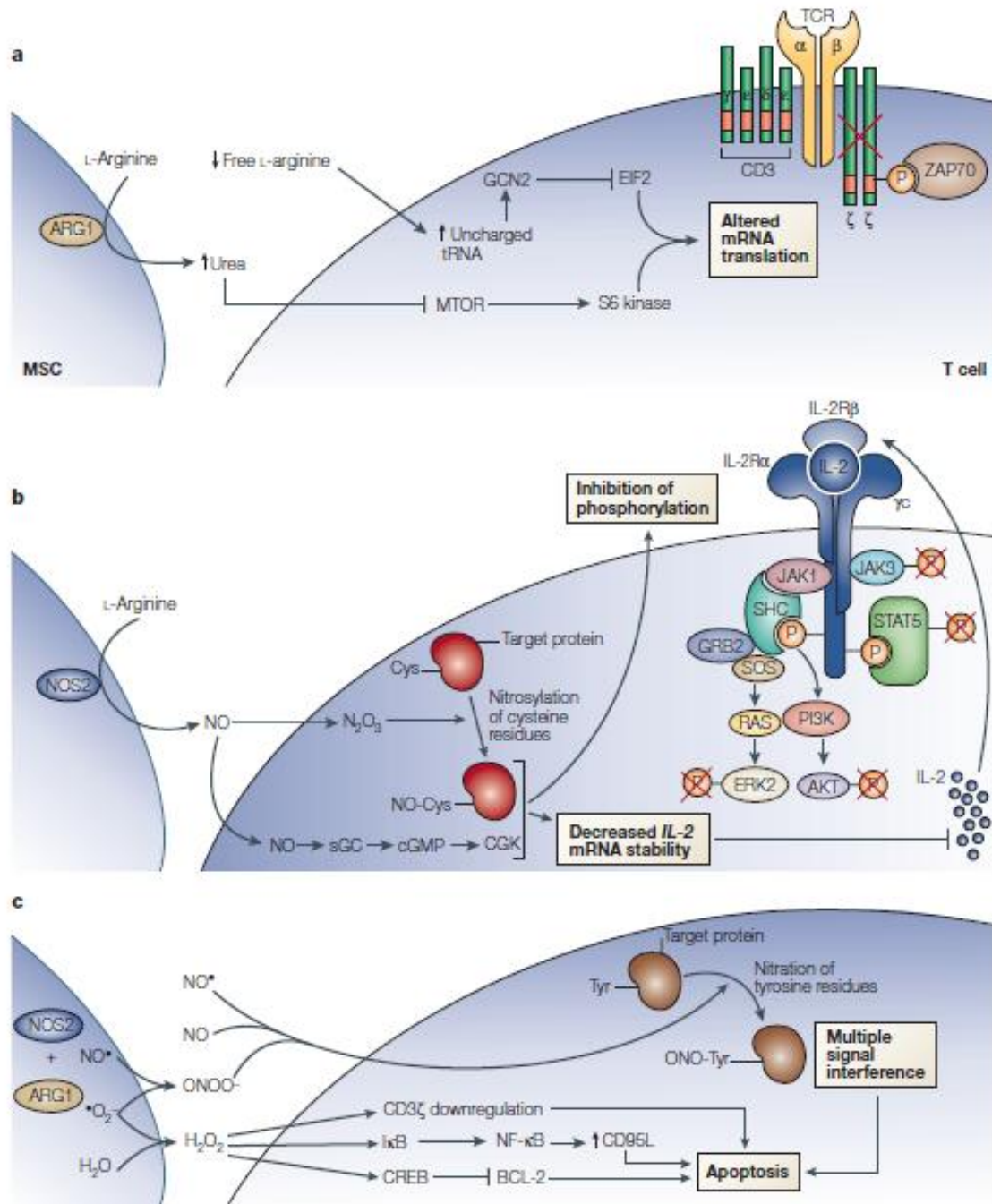


Figure 3.8: Arg-1 and iNOS activity involved in MDSC suppression

MDSC-induced immune subversion is associated with the activity of Arg-1 and iNOS. **a)** Arg-1 activity increases urea and decreases L-arginine concentration from the microenvironment, which causes translational blockade of CD3 ζ via the kinases mammalian target of rapamycin (MTOR) and kinase general control non-depressible 2 (GCN2). **b)** iNOS produces NO, which nitrosylates cysteine residues in proteins and activates cyclic GMP resulting in the blockade of IL-2 receptor signalling. **c)** Both enzymes together shift the NO production towards peroxynitrite (ONOO⁻) and hydrogen peroxide (H₂O₂), which leads to nitration of tyrosine residues and changes in Bcl-2 and CD95L activity resulting in T cell apoptosis (Bronte *et al. Nature Reviews Immunology* 2005; 5: 641-654)

Cysteine. Cysteine is an essential amino acid for T cells to synthesize proteins. In general, cells either produce cysteine from their intracellular pool of methionine using the enzyme cystathionase or they import cystine, the oxidized form of cysteine, via xc-transporter to reduce it intracellularly to cysteine. Since T cells lack cystathionase and xc-transporter, they depend on APCs to provide cysteine during antigen processing and presentation. In addition, APCs secrete thioredoxin which reduces extracellular cystine to cysteine (Fig 3.9) [100]. Srivastava *et al.* observed that MDSCs interfered with T cell activation by inhibiting cysteine uptake. By increasing extracellular cysteine levels they demonstrated that MDSC-induced T cell suppression could be reverted. Furthermore, they showed that MDSCs consumed cysteine but did not return it to their microenvironment due to the lack of the ASC transporter, which exports cysteine. Therefore, MDSC block T cell response by depriving cysteine from the surroundings [101].

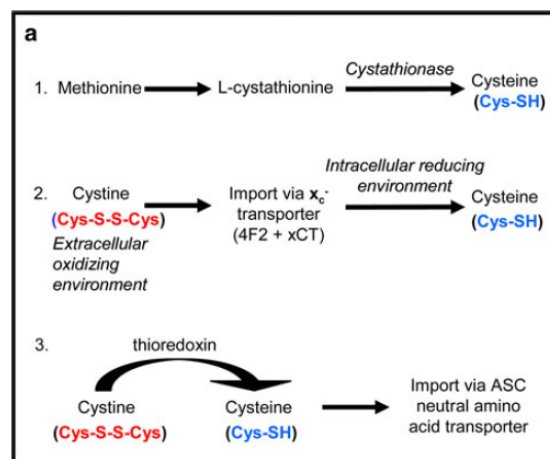


Figure 3.9: Three ways of cysteine production by immune cells

Ostrand-Rosenberg *Cancer Immunology Immunotherapy* 2010; 59(10): 1593-1600

L-selectin. Naïve T cells migrate through the blood stream to draining lymph nodes where they become activated by antigen presenting cells. High expression of L-selectin (CD62L) on the surface directs T cells to their destined locations. L-selectin mediates extravasation of leukocytes from blood to lymph nodes but also to the tumor tissue. Recent studies demonstrated that reduced expression of L-selectin on T cells inversely correlated with MDSC levels in both cancer patients and tumor-bearing mice. This downregulation was caused by proteolytic cleavage and shedding of the L-selectin ectodomain by ADAM17 (a disintegrin and metalloproteinase domain 17). MDSCs constitutively express ADAM17 and thereby prevent T cell homing to lymph nodes or tumor sites [102].

Induction of regulatory T cells. MDSCs also indirectly inhibit T cell responses by inducing Tregs, which in turn block T cell activation. In murine colon carcinoma, MDSCs promote the development of Tregs from adoptively transferred CD25⁺CD4⁺ T cells in the presence of IL-10 and IFN- γ [68]. In other reports, MDSCs act as APCs to present tumor specific antigens to Tregs that expanded in an Arg-1-dependent and TGF- β -independent manner [87]. Yang *et al.* further observed a CTLA4-dependent (cytotoxic lymphocyte antigen 4, CD152) activation of Tregs by MDSCs. MDSCs express CD80, the ligand for CTLA4, and after deletion or blockage of CD80 the suppressive function of Treg was significantly downregulated [67]. Moreover, it has been demonstrated that the expression of the immune stimulatory receptor CD40 on MDSCs was required to induce T cell tolerance and Treg accumulation [103].

3.5.7 Therapeutic targeting of MDSCs

Since MDSCs are one of the main suppressive factors in cancer, several pharmacological approaches are currently under investigation that involves either their elimination or modulation. Such MDSC inhibitors can be divided into 4 groups according to their ability to control: (a) MDSC maturation from precursors, (b) MDSC differentiation into mature cells, (c) MDSC accumulation and (d) MDSC function.

MDSC maturation. To block MDSC maturation from hematopoietic precursors this group of inhibitors has been developed with the ability to neutralize factors involved in MDSC expansion. As summarized in table 3.1, these factors are comprised of: prostaglandins, SCF, M-SCF, IL-6, GM-CSF, G-CSF and VEGF. Since most of these factors trigger signaling pathways that activate STAT3, this transcription factor seems to be a promising therapeutic target. Collaborations of the National Cancer Institute, Merck, Sigma Aldrich and Ryan databases identified via *in silico* screening of chemical libraries two small molecules, STA-21 and S31-201, which are able to inhibit STAT3 [104]. Another strategy to inhibit STAT3 is using the platinum complex, CPA-7, which possesses anti-tumoral activity due to DNA cross-linking. CPA-7 treatment leads to the reduction of phosphorylated STAT3 levels in tumor-infiltrating DCs in line with increased NK response against tumor [79]. Recently, it was reported that sunitinib, a tyrosine kinase inhibitor, might target STAT3 in MDSCs from renal cell carcinoma. Receptor tyrosine kinases are surface molecules that transduce extracellular signals to the cytoplasm to activate Ras/Raf, STAT3 and protein kinase C pathways. Sunitinib is a broad inhibitor blocking VEGF receptor (VEGFR), platelet derived growth factor receptor (PDGFR), stem cell factor receptor (c-kit), Flt3 and M-CSF receptor. Sunitinib therapy of metastatic renal cell carcinoma patients correlated with a reduction of MDSCs, increased DC expansion [105], increased Th1 and reduced Th2 response together with diminished Treg populations [106].

MDSC differentiation. Promising approaches to target MDSCs is promoting their differentiation into mature cells in order to circumvent their suppressive features. It is known that vitamin A induces the differentiation of myeloid progenitor cells into DCs and macrophages. Studies using all-*trans* retinoic acid (ATRA), a derivate of vitamin A, demonstrated that administration of ATRA favored the differentiation of MDSCs into mature cells [107]. The main mechanism of ATRA-mediated differentiation includes the upregulation of glutathione synthesis (GSS) and the reduction of ROS levels in MDSCs. In addition, reduced levels of MDSCs due to ATRA enhanced T cell responses against tumors [108]. Further, patients with head and neck cancer squamous cell carcinoma (HNSCC) were orally treated with vitamin D, which decreased the numbers of CD34⁺ suppressor cells and increased IFN- γ levels [109].

MDSC accumulation. Previous studies used an *in vivo* administration of the Gr-1 antibody to deplete Gr-1⁺ MDSCs, which reversed T cell tolerance and reduced tumor progression. Unfortunately, a rapid accumulation of MDSCs was observed when the antibody concentration was decreased or its application interrupted [110]. Therefore, administration of chemotherapeutic drugs, such as gemcitabine, has been preferred. Gemcitabine is a nucleoside analog of cytidine, which causes chain termination when incorporated into DNA during

replication. Tumor-bearing mice treated with gemcitabine showed reduced numbers of splenic MDSCs and an improvement of anti-tumor immune responses that was associated with accelerated apoptosis of MDSCs [111]. Another chemotherapeutic drug, 5-Fluorouracil (5-FU), functions as a pyrimidine analog and induces cell cycle arrest and apoptosis after incorporation into DNA and RNA. Like gemcitabine, *in vivo* treatment with 5-FU decreased splenic and tumor-infiltrating MDSCs but had no effect on tumor progression [112].

MDSC function. Another approach to inhibit MDSCs is to interfere with signaling pathways, which regulate the function of suppressive factors. ROS inhibitors like nitroaspirin had been shown to decrease MDSC-mediated immune suppression by downregulation of Arg-1 and iNOS in splenic MDSCs and by suppression of cancer cell proliferation. However, after end of administration no statistical difference in survival rates was observed between treated and untreated groups [113]. Another approach to block MDSC function is targeting phosphodiesterase 5 (PDE5). PDE5 reduces cGMP, which results in stabilizing the mRNA of Arg-1 and iNOS. Blockade of PDE5 with the PDE5 inhibitor sildenafil showed increased levels of cGMP in line with decreased expression of CD124 and diminished activity of Arg-1 and iNOS. Furthermore, recovery of T cell proliferation and an enhanced tumor infiltration of CD8⁺ T cells were detected [114]. Table 3.2 summarizes therapeutic approaches to inactivate MDSCs. Pharmacological MDSC inhibition seems to be a promising strategy to overcome tumor-induced immune suppression but therapeutic effects might be more efficient when used in combination with immunotherapy and not administered alone.

Differentiation		
(1) ATRA (all-trans-retinoic-acid)	Favours differentiation of myeloid progenitors to DCs and macrophages	
(2) Vitamin D3	In humans, reduces the number of CD34 ⁺ cells, increases HLA-DR expression in PBMCs, together with IL-12, IFN- γ ; improves T-cell blastogenesis	
Maturation		
(3) STAT 3 Inhibitors	Inhibition of several pathways, among which, suppression of anti-apoptotic, pro-proliferative, pro-angiogenic genes and ROS production	
(4) TK inhibitors	Sunitinib Inhibits VEGFR, PDGFR, c-KIT, Flt-3 and CSF-1 receptor signal pathway Decreases Treg cells (decreased FoxP3 and IL-10) Increases Th1 response	
(5) Bevacizumab	Decreases MDSC subsets (VEGFR ⁺ cells)	
(6) Anti-BV8 mAb	Reduces the number of tumor-associated CD11b ⁺ /Gr-1 ⁺ cells, regulating their mobilization and, potentially, their homing to the tumor site	
(7) Amino-Bisphosphonates	Reduce CD11b ⁺ /Gr-1 ⁺ /F4/80 ⁺ cells in tumor stroma	
(8) MMP9 Inhibitors	Reduce MDSC generation from HSC and their support to tumor stroma	
Accumulation		
(9) Gemcitabine	Reduces the number of CD11b ⁺ /Gr-1 ⁺ cells	
(10) 5-Fluorouracil (5-FU)	Reduces the number of CD11b ⁺ /Gr-1 ⁺ cells	
(11) CXCR2 and CXCR4 specific antagonists	Reduce MDSC accumulation	
Function		
(12) ROS scavengers	Reduce nitration of proteins in tumor microenvironment	
ARG and NOS inhibitors	(13) Nitroaspirin	Reduces nitration of proteins in tumor microenvironment Inhibits ARG and NOS
	(14) PDE-5 (phosphodiesterase-5)	Inhibits ARG and NOS Inhibits IL-4R α expression
	(15) COX2 inhibitors	Downregulate ARG and NOS expression
	(16) Biotechnological drugs	Interfere with IL-13/IL-4R α /STAT 6 pathway

Table 3.2: Therapeutic strategies to target MDSCs

Inhibitors to target MDSCs can be divided into four groups according to their ability to control: (a) MDSC differentiation into mature cells (b) MDSC maturation from precursors (c) MDSC accumulation in peripheral organs and (d) MDSC function. (Ugel *et al. Current Opinion in Pharmacology* 2009; 9: 470-481)

4 AIM OF THE STUDY

Myeloid-derived suppressor cells (MDSCs) have been characterized in cancer patients and tumor bearing mice based on their ability to suppress T cell responses. During tumor progression MDSCs accumulate in bone marrow, blood, peripheral lymphoid organs and in the tumor tissue. They represent a heterogeneous population of myeloid cells at different stages of differentiation. In mice these cells are characterized by the co-expression of the surface markers Gr-1 and CD11b. Within this population, two distinct MDSC subpopulations with clear morphological differences have been identified, comprising mononuclear cells (MO-MDSCs), which express Ly6C and the macrophage marker F4/80, and polymorphonuclear cells (PMN-MDSCs), which express Ly6G and do not display F4/80 surface expression.

Increasing numbers of experimental and clinical studies suggest that for effective anti-tumor responses, effector cells of both innate and adaptive immunity have to be efficiently activated at the tumor site. So far, most studies had been focused on the analysis of MDSCs that accumulate in blood and spleen. The aim of our study was the comprehensive analysis of tumor-infiltrating MDSCs in comparison to blood MDSCs including their subset distribution, phenotype and function. In order to identify molecules and pathways that might be involved in MDSC regulation, gene expression profiling of blood and tumor-infiltrating MDSC subpopulations was performed using whole genome microarrays. We demonstrate that tumor-infiltrating MO-MDSCs displayed increased expression of genes involved in suppression, inflammatory responses and chemotaxis compared to blood MDSCs. Furthermore, we showed that chemokines produced by MO-MDSCs within the tumor played an important role in tumor progression by attracting Tregs. Therefore, our study reveals a novel aspect of MDSC function by recruiting Treg that should be considered in current therapeutic protocols for cancer treatment.

5 MATERIALS AND METHODS

5.1 Materials

5.1.1 Mouse strains

C57BL/6 (WT) mice were purchased from Charles River Laboratories (Sulzfeld, Germany and Erembodegem, Belgium). CCR5^{-/-} mice and congenic C57BL/6-Ly5.1⁺ mice were purchased from Jackson Laboratory (Bar Harbor, Maine USA) and were bred in our animal facility. Congenic OT-I/Thy1.1 mice were kindly provided by Prof. G. Hämmerling. Mice were housed under specific pathogen-free condition and used in experiments at 7-19 weeks of age. All experiments were performed according to local animal experimental ethics committee guidelines.

5.1.2 Cell lines

Name	Cell type	Medium
B16	Mouse melanoma	DMEM
MCA205	Mouse fibrosarcoma	DMEM
RMA-S	TAP2-deficient variant of mouse T cell lymphoma RMA	RPMI
2.4G2	Anti-CD16/CD32 hybridoma	DMEM

5.1.3 Cell culture products

Product	Company	Catalog No.
Standard tissue culture flasks/filter screw caps – 25 cm ²	TPP	90026
Standard tissue culture flasks/filter screw caps – 75 cm ²	TPP	90076
Standard tissue culture flasks/filter screw caps – 150 cm ²	TPP	90151
Tissue culture flasks/filter screw caps – 182 cm ²	Greiner	660175
96-well flat-bottom with lid – Standard TC	BD	353972
96-well U-bottom with lid – Standard TC	BD	353077
24-well flat-bottom with lid – Standard TC	BD	353047
50 ml conical tubes Falcon™	BD	352070
15 ml conical tubes	Greiner	188271
5 ml round-bottom polypropylene test tubes	BD	352008
5 ml round-bottom polystyrene test tubes w/ cell strainer	BD	352235
Serological pipettes: 5, 10, 25 and 50 ml, sterile	Costar	4487-4490
40 µM cell strainer Falcon™	BD	352340
70 µM cell strainer Falcon™	BD	352350
Cryovial, 2 ml sterile	Roth	E309.1
Nalgene™ Freezing Container, “Mr. Frosty”	Nunc	5100-0001

Safe lock tubes: 0.5, 1.5 and 2 ml	Eppendorf	13625, 12682, 12776
Filter tips: 10, 20, 100, 200, 300 and 1000 µl	Biozym	770010,-50,-280,-300,-400
50 ml Reagent Reservoirs, sterile	Corning	4870

5.1.4 Cell culture media

Product	Company	Catalog No.
RPMI 1640 (1x) w/o L-Glutamine	GIBCO-Invitrogen	31870
DMEM (1x) (High Glucose) with L-Glutamine, 4500 mg/L D-Glucose, w/o Sodium Pyruvate	GIBCO-Invitrogen	41965
D-PBS (1x) w/o Ca, Mg, Sodium Bicarbonate	GIBCO-Invitrogen	14190
Fetal Bovine Serum, Origin: EU approved	GIBCO-Invitrogen	10270
Penicillin/Streptomycin-Solution: 10,000 U Penicillin, 10,000 µg/ml Straptomycin	GIBCO-Invitrogen	15140
L-Glutamine 200 mM (100x), 29.2 mg/ml	GIBCO-Invitrogen	25030
Non-essential amino acids (100x)	GIBCO-Invitrogen	11140035
Sodium Pyruvate MEM 100mM	GIBCO-Invitrogen	11360088
β-Mercaptoethanol 50 mM	GIBCO-Invitrogen	31350010
Trypsin-EDTA (1x) HBSS w/o Ca, Mg with EDTA	GIBCO-Invitrogen	25300
Dimethylsulphoxide Hybri Max (DMSO)	Sigma-Aldrich	D2650

5.1.5 Magnetic cell sorting (MACS)

Product	Company	Catalog No.
Anti-APC	Miltenyi Biotec	130-090-855
Anti-CD11b	Miltenyi Biotec	130-049-601
Anti-DX5	Miltenyi Biotech	130-052-501
Anti-Ly6G	Miltenyi Biotec	130-092-332
LD Columns	Miltenyi Biotec	130-042-901
LS Columns	Miltenyi Biotec	130-042-401
Pan-T-cell Isolation Kit	Miltenyi Biotec	130-090-861

5.1.6 Kits

Product	Company	Catalog No.
BCA™ Protein Assay Kit	Pierce	23227
Bioplex cytokine reagent kit	Biorad	171-304000
Bioplex cell lysis kit	Biorad	171-304011

Bioplex mouse MIP-1alpha assay	Biorad	171-G5020M
Bioplex mouse MIP-1beta assay	Biorad	171-G5021M
Bioplex mouse RANTES assay	Biorad	171-G5022M
Bioplex mouse MIG assay	Biorad	171-G6005M
Bioplex mouse MIP-2 assay	Biorad	171-G6006M
Bioplex mouse IL-13 assay	Biorad	171-G5012M
DCFDA	Invitrogen	D399
FITC BrdU Flow Kit	BD	557891
Foxp3 Staining Buffer Set	eBioscience	00-5523
Griess Reagent R1/R2	Biozol	780018/780020
Mouse Ref-6 v2	Illumina	BD-202-0202
Mouse CCL3 DuoSet	R&D	DY450
Mouse CCL4 DuoSet	R&D	DY451
Mouse CCL5 DuoSet	R&D	DY478
Mouse IFN- γ OptEIA™ Set	BD	555138
OptEIA™ Reagent Set B	BD	550534
QuantiChrom Arginase Assay Kit	BioAssay Systems	DARG-200
RNeasy Mini Kit	Qiagen	74124
TURBO DNA-free™	Ambion	AM1907

5.1.7 Antibodies

Primary antibodies	Clone	Company	Catalog No.
BrdU FITC	PRB-1	eBioscience	11607142
CD115 PE	AFS98	eBioscience	12-1152
CD11b FITC	M1/70	BD	557396
CD11b PE	M1/70	Biolegend	101208
CD124 PE	mIL4R-M1	BD	552509
CD14 PE	Sa14-2	Biolegend	123310
CD3 APC	145-2C11	Biolegend	100312
CD31 FITC	MEC13.3	BD	553372
CD4 PerCP-Cy5.5	RM4-5	Biolegend	100540
CD40 PE	3/23	BD	553791
CD43 FITC	S7	BD	553270
CD49b PE	DX5	BD	553858
CD54 Alexa647	YN1/1.7.4	Biolegend	116114
CD62L PE	MEL-14	Biolegend	104407
CD68 Alexa647	FA-11	Biolegend	137004
CD8 FITC	53-6.7	Biolegend	100706
CD80 FITC	16-10A1	Biolegend	104706
CD86 PE	GL1	BD	553692
Dectin-2 PE	D2.11E4	AbD Serotec	MCA2415PE
F4/80 Alexa488	BM8	Caltag	MF48020
F4/80 APC	BM8	Caltag	MF48005
Foxp3 PE	FJK-16s	eBioscience	125773

Gr-1 APC	RB6-8C5	Biolegend	108412
Gr-1 PerCP-Cy5.5	RB6-8C5	Biolegend	108428
H-2D ^b PE	KH96	BD	553574
H-2K ^b PE	AF6-88.5	BD	553570
I-A/I-E PE	M5/114.15.2	BD	557000
Ly6C bio	HK1.4	Biolegend	128004
Ly6G FITC	1A8	BD	551460
NK1.1 PE	PK136	Biolegend	108708
panRae-1 PE	186107	R&D systems	FAB17582P
PD-L1 PE	10F.9G2	Biolegend	124308
PD-L2 PE	TY25	BD	557796
TLR-4 bio	UT41	eBioscience	13-9041-80

Isotype controls	Clone	Company	Catalog No.
armenian hamster FITC	HTK888	Biolegend	400906
mouse IgG2b PE	133303	R&D systems	IC0041P
ratIgG2a FITC	RTK2758	Biolegend	400506
ratIgG2a PE	RTK2758	Biolegend	400508
ratIgG2b Alexa647	RTK4530	Biolegend	400626
ratIgG2b PE	eB149/10H5	eBioscience	12403183

Secondary antibodies	Clone	Company	Catalog No.
SAv PE	Streptavidin	Biolegend	405204
SAv PerCP-Cy5.5	Streptavidin	Biolegend	405214

5.1.8 Chemicals and biological reagents

Product	Company	Catalog No.
7-AAD	BD	559925
All- <i>trans</i> retinoic acid (ATRA), 5 mg pellets	Innovative Research of America	V-111
CCL3, recombinant mouse	Peprtech	250-09-100
CCL4, recombinant mouse	Peprtech	250-32-100
CCL5, recombinant mouse	Peprtech	250-07-100
Carboxyfluorescein succinimidyl ester (CFSE)	Sigma-Fluka	21888
Concavalin A	Sigma	C5275
DNase I	Sigma-Aldrich	DN25
Eosin Y	Roth	7089.2
Hematoxylin	Roth	T865.3
Heparin-Sodium, 25,000 Units	Braun	1708.00.00
Hyaluronidase type V	Sigma-Aldrich	H6-254
Isofluran B	Braun	6724123.00.00
Linear polyacrylamide (LPA)	Ambion	AM9520

Lipopolysaccharide (LPS)	Sigma-Fluka	L4391
Lympholite M	Cedarline	CL5035
[methyl- ³ H] Thymidine	Amersham	TRK637-5MCI
Propidium Iodide (PI)	Biolegend	421301
RNA storage solution	Ambion	AM70000
Triton X-100	Sigma-Fluka	T9284

5.1.9 Solutions

Solution	Ingredients
ACK lysis buffer	0.829 g NH ₄ Cl 0.1 g KHCO ₃ 0.38 mg EDTA 100 ml ddH ₂ O pH 7.3
FACS buffer	1x PBS 0.02 % (v/v) NaN ₃ in PBS 1 % FCS 0.5 mM EDTA
Freezing medium	1x FCS 10% DMSO
MACS buffer	1x PBS 1 % FCS 0.5 mM EDTA
Primary cell culture medium	1x RPMI 10 % FCS 2 mM L-glutamine 100 U/ml Penicillin, 100 µg/ml Streptomycin 1 mM Sodium pyruvate 1x Non-essential amino acids 0.25 mM β-mercaptoethanol
10 x PBS	1.37 M NaCl 27 mM KCl 100 mM Na ₂ HPO ₄ (anhydrous) 20 mM KH ₂ PO ₄

5.1.10 Laboratory equipment

Equipment	Name	Company
Anesthesia machine	Vapor 19.1	Drägerwerk AG
Analytical scales	AE163	Mettler Toledo
Beta-counter	MicroBeta TriLux 1450 LSC	Perkin Elmer
Bioplex array system	Luminex 100	Biorad
Cell culture incubator	Heraeus BBD 6220 (CO ₂)	Kendro
Centrifuge	5415 R (table)	Eppendorf
	5417 R (table)	Eppendorf

	Zytopin 2	Shandon
	Heraeus Biofuge Pico	Kendro
	Heraeus Multifuge 4 K-R/3 S-R	Kendro
ELISA microplate reader	Multiscan Fc	Thermo Fischer
Flow cytometer	FACS™ Calibur	BD
	FACS™ Diva	BD
	Influx	BD
Flow hood	Heraeus Hera Safe BBD 6220	Kendro
	LabGuard NU-437-600E	IBS Integra
Freezer -20°C	Premium, Comfort, Profi line	Liebherr
Freezer -86°C	VIP series	Sanyo
Fridge	Premium, Profi line	Liebherr
Harvester	96-well automated, TOMTEC	PerkinElmer
Ice machine		Hoshizaki
Magnetic stirrer	MR3001 K	Heidolph
Microscope	Wllovert	Hund Wetzlar
	BX51	Olympus
N ₂ tank	Cryosystem 6000	MVE
pH meter	pH211	Hanna Instruments
photometer	NanoPhotometer	Implen
Pump	Econo Pump	Biorad
Thermomixer	Compact, Comfort	Eppendorf
Vortexer	VortexGenie 2	VWR/Scientific Industries
Water bath	Heraeus Julabo TW20	Kendro

5.2 Methods

5.2.1 Cell culture methods

Thawing cells

Frozen cryovials were shortly submerged in a 37°C water bath until 90 % of the cell suspension was thawed. The suspension was immediately diluted into 10 ml of appropriate medium and centrifuged (1200 rpm, 10 min, RT). Cells were resuspended in medium and cultured at 37°C, 5 % CO₂.

Splitting of adherent cells

Adherent cells were washed once in PBS and pre-warmed Trypsin-EDTA was added in sufficient amounts to cover the cell layer. Cells were incubated at 37°C until complete detachment from the flask was observed under the microscope. After resuspending in culture medium, cells were collected in Falcon tubes and centrifuged (1200 rpm, 10 min, RT). Cells were subsequently diluted at different ratios into new flasks or used in experiments.

Splitting of suspension cells

Cells in suspension reaching an optimal density were split in ratios ranging from 1:5 up to 1:20 by adding the appropriate volume of medium.

Determination of cell numbers

An aliquot of cell suspension was diluted 1:1 with trypan blue solution (0.05 % w/v) to distinguish dead from live cells. Cells were counted with a Neubauer counting chamber (0.1 mm depth). The number of live cells per ml cell suspension was calculated as the following:

Average cell number/chamber square (0.1 mm³) x dilution factor x 10⁴.

Freezing of cells

For cell freezing, cell suspensions were centrifuged (1200 rpm, 10 min, RT) and the pellet was resuspended in freezing medium at a concentration of 5 x 10⁶ cells/ml. 1.8 ml of cell suspension was aliquoted in cryovials and placed in freezing containers. After 24 h at -80°C vials were transferred to liquid nitrogen for long term storage.

5.2.2 Mouse tumor models

Tumor cell lines were harvested in the exponential growth phase and washed three times with PBS (1200 rpm, 10 min, 4°C). For RMA-S and MCA205 the cell concentration was adjusted to

1×10^7 cell/ml or 5×10^6 cells/ml for B16, respectively. Mice were injected subcutaneously into the right flank with 100 μ l of tumor cell suspension. Every second day tumor growth was assessed with a caliper measuring along the perpendicular axes of the tumor and expressed as the product of the two (surface) or three (volume) diameters. In survival studies mice were sacrificed when the tumor surface exceeded 4 cm².

5.2.3 *In vivo* treatment of mice

***In vivo* BrdU staining of proliferating MDSC**

RMA-S tumor-bearing mice were injected with 2 mg BrdU i.p. on day 19 after tumor cell inoculation. After 16 h mice were sacrificed and bone marrow, blood, spleen and tumor suspensions were prepared. MDSC subpopulations were analyzed for BrdU incorporation using the BD FITC BrdU Flow Kit according to manufacturer's instructions.

***In vivo* application of chemokines**

For tumor infiltration experiments, 1 μ g recombinant chemokine were co-injected with the tumor cells. Chemokines (1 μ g in 100 μ l PBS) were re-injected intratumorally every third day.

ATRA pellet implantation

ATRA pellets (21-day release, 5 mg) or placebo pellets were implanted s.c. in the neck of RMA-S tumor-bearing mice on day 7 after tumor cell inoculation. Mice were sacrificed two weeks later and tumor infiltrates were analyzed.

5.2.4 Organ dissection and preparation of single cell suspensions

Blood

Mice were sacrificed by asphyxiation with CO₂ and blood was obtained by heart puncture or by puncture of the orbital vein. Per mouse 0.7-1 ml blood was collected and subsequently mixed with 40 μ l heparin. To obtain cell lysis, blood was treated with 30 ml of ACK buffer and further washed with PBS (1500 rpm, 10 min, 4°C).

Spleen

Animals were sacrificed by dislocation of the neck. The spleen was excised using sterile forceps and kept in ice-cold PBS. Single cell suspensions were obtained by mincing the spleen through a 70 μ m cell strainer followed by washing with PBS (1500 rpm, 10 min, 4°C). For the erythrocyte lysis, splenocytes were treated with 1.5 ml ACK buffer per spleen and washed with PBS.

Tumor

Tumor bearing mice were sacrificed by dislocation of the neck and tumor was excised using sterile forceps. Subsequently, tumors were cut into small pieces and digested in 10 ml digestion buffer (0.5 mg/ml hyaluronidase type V, 0.5 mg/ml DNase I) for 30 min at 37°C. Single cell suspension was obtained by mincing the digested tumor through a 70 µm-pore cell strainer. Cells were collected in a 50 ml Falcon tube and washed with PBS (1500 rpm, 10 min, 4°C). Pellet was resuspended in 8 ml of PBS and filtered through a 40 µm-pore strainer. Live cells were enriched by centrifugation (1500 g, 20 min, RT) of cell suspension loaded on 7 ml Lympholite M gradient and subsequent collection of the interphase. Cells were washed with PBS (1500 rpm, 10 min, 4°C).

Bone marrow

Animals were sacrificed by dislocation of the neck and the hind legs were dissected. Under sterile conditions bones were freed from all sinews and muscle tissue. Femur and tibiae were separated by breaking the knee and the heel, washed briefly in 80 % ethanol and placed in PBS. To rinse out the bone marrow cells, the ends of the bones were cut and rinsed out with 5-10 ml PBS using a 27G needle. The isolated bone marrow was filtered through a 70 µm-pore cell strainer followed by washing with PBS (1500 rpm, 10 min, 4°C). To remove erythrocytes, cells were subsequently treated with ACK buffer und washed one more time.

5.2.5 Cell staining**Surface staining**

1×10^6 cells from culture or primary cells from organs were washed and resuspended in 100 µl FACS buffer. To block Fc receptors, 10 % 2.4G2 supernatant was used and incubated for 15 min at 4°C. Appropriate antibodies were added and cells were further incubated for 30 min at 4°C in the dark. When biotinylated antibodies were used, cells were washed with FACS buffer and incubated with conjugated streptavidin for an additional 30 min at 4°C. After staining, all samples were washed in FACS buffer to remove unbound antibodies. Samples were acquired FACSCalibur® flow cytometer and data was analyzed using CellQuest software.

Intracellular staining

Like surface staining, cells were collected and stained for surface markers. At the end of the staining procedure, samples were washed with FACS buffer and fixed using Fixation/Permeabilization Buffer (eBioscience) according to manufacturer's instruction. Cells were further permeabilized with Permeabilization buffer (eBioscience) and incubated with 20 % 2.4G2 supernatant for 30 min at 4°C in 100 µl total volume of Permeabilization Buffer. Intracellular molecules were stained with the appropriate antibody for 45 min at 4°C. Samples were washed in Permeabilization Buffer to remove unbound antibodies and resuspended in FACS buffer for analysis.

Hematoxylin & Eosin staining (H&E)

Sorted cells were washed once with PBS and resuspended at a final concentration of 1×10^6 cells/ml. 100 μ l cell suspension was brought onto poly-L-lysine-coated microscopic glass slides (Sigma-Aldrich) by centrifugation using a cytospin instrumentation (800 rpm, 5 min, RT). Cells on the slides were fixed in 4 % PFA in PBS for 10 min and washed in PBS. Nuclei were stained with Mayer's Hematoxylin (Dako Cytomation) for 5 min at RT. Excess Hematoxylin was removed by washing extensively with running water for 10 min. Subsequently, cytosol was counter-stained with 10 % Eosin Y (Applichem) for 5 min. Excess Eosin was removed by washing with running water for 10 min. Cells were dehydrated with an ethanol range starting with 70 % ethanol for 3 min, 96 % ethanol for 3 min and finally with 100 % ethanol for another 3 min. Cells were then washed twice with xylol for 3 min and cells were mounted with coverslips using Vitro-Clud.

5.2.6 Cell separation

5.2.6.1 Magnetic cell sorting (MACS)

MDSC subpopulations

Single cell suspensions prepared from blood were resuspended in PBS at a concentration of 5×10^8 cells/ml and treated with 10 % 2.G42 supernatant for 15 min at 4°C. PMN-MDSCs were positively selected using Ly6G magnetic beads (Miltenyi Biotech) according to the manufacturer's instructions. To isolate MO-MDSCs, the negative fraction of the Ly6G MAC sort was further used and 1×10^8 cells/ml were stained with 5 μ l anti-Gr-1-APC antibody per 10^7 cells for 15 min at 4°C. MO-MDSCs were then isolated via positive selection with anti-APC beads (Miltenyi Biotech) according to the manufacturer's instructions.

T cells

Single cell suspensions prepared from naïve spleens were washed with MACS Buffer and resuspended at 1×10^8 cells/ml. Cells were treated with 10 % 2.4G2 supernatant for 15 min at 4°C. T cells were isolated via negative selection with pan T cell isolation kit (Miltenyi Biotech) according to the manufacturer's instructions.

NK cells

Single cell suspensions prepared from naïve spleens were washed with MACS Buffer and resuspended at 1×10^8 cells/ml. To block Fc receptors, splenocytes were incubated in 10 % 2.4G2 supernatant for 15 min at 4°C and positively selected for DX5⁺ cells using DX5 magnetic beads (Miltenyi Biotech).

5.2.6.2 Fluorescence activated cell sorting (FACS)

Blood MDSCs

Single cell suspensions prepared from blood were resuspended in PBS at a concentration of 5×10^8 cells/ml and treated with 10 % 2.G42 supernatant for 15 min at 4°C. MDSC subpopulations were pre-separated using Ly6G magnetic beads (Miltenyi Biotech) according to the manufacturer's instructions. Ly6G⁺ fraction containing PMN-MDSCs and the negative fraction containing MO-MDSCs were subsequently stained with fluorochrome labeled anti-Gr-1 and anti-F4/80 antibody for 30 min at 4°. After washing (1500 rpm, 10 min, 4°C) cells were resuspended in PBS at a concentration of 5×10^7 cells/ml and filtered through a 30 µm cell mesh. Propidium iodide (PI) was added to the cell suspension 10 min prior sort to label dead cells. PI⁻Gr-1⁺F4/80⁻ PMN-MDSCs and PI⁻Gr-1⁺F4/80⁺ MO-MDSCs were sorted using FACSDiva® or FACSInflux® cell sorter instruments.

Tumor-infiltrating MDSCs

Single cell suspensions prepared from tumors were enriched via anti-Gr-1-APC and anti-APC beads according to the manufacturer's instructions. The positive fraction was washed with PBS and resuspended at 5×10^7 cells/ml. MDSCs were subsequently stained with a fluorochrome labeled anti-F4/80 antibody for 30 min at 4°C. After washing cells were filtered through a 30 µm cell mesh and PI was added to the cell suspension 10 min prior sort to label dead cells. PI⁻Gr-1⁺F4/80⁻ PMN-MDSCs and PI⁻Gr-1⁺F4/80⁺ MO-MDSCs were sorted using FACSDiva® or FACSInflux® cell sorter instruments.

Tumor-associated macrophages

Single cell suspensions prepared from tumors were enriched via CD11b beads (Miltenyi Biotech) according to the manufacturer's instructions. The positive fraction was washed with PBS and resuspended at 5×10^7 cells/ml. TAMs were subsequently stained with fluorochrome labeled anti-F4/80, anti-CD11b and anti-Gr-1 antibodies for 30 min at 4°C. After washing cells were filtered through a 30 µm cell mesh and PI was added to the cell suspension 10 min prior sort to label dead cells. PI⁻CD11b⁺F4/80⁺Gr-1⁻ TAMs were sorted using FACSDiva® or FACSInflux® cell sorter instruments.

5.2.7 Functional assays

5.2.7.1 Proliferation assays

³H-Thymidine incorporation

PMN- or MO-MDSCs were sorted by flow cytometry and co-cultured with 1×10^5 splenocytes from naïve mice at different effector/target ratios. To stimulate T cell proliferation either 2 µg/ml ConA (Sigma) was added or pre-coated plates with 1 µg/ml anti-CD3/CD28 antibodies were used. Cells were cultured for 72 h and 1 µCi of ³H-Thymidine was added for the final 18 h of culture. After incubation cells were harvested and ³H-Thymidine incorporation was measured using MicroBeta TriLux Counter (Perkin Elmer).

CFSE dilution

Naïve T cells from C57BL/6-Ly5.1 mice were enriched via pan T cell isolation kit (Miltenyi) and 1×10^7 cells/ml were labeled with 1 µM CFSE. Cells were cultured for 10 min at 37°C and washed twice with primary cell culture medium. 1×10^5 T cells were co-cultured with FACS sorted MDSC subsets at different effector/target ratios. T cell proliferation was induced using either 2 µg/ml ConA (Sigma) or pre-coated plates with 1 µg/ml anti-CD3/CD28 antibodies. After 3-4 days cells were harvested and T cells were stained with fluorochrome labeled anti-CD45.1, anti-CD4 and anti-CD8 antibodies. T cell proliferation (CFSE dilution) was analyzed by flow cytometry.

5.2.7.2 Suppressive activity of MDSC subsets

Arginase activity

MDSC subpopulations were FACS sorted and 6×10^5 cells were washed in PBS. Pellets were resuspended in 100 µl lysis buffer (0.4 % TritonX-100 with 10mM Tris-HCl and protease inhibitors) for 30 min at 4°C. Samples were centrifugated (20000g, 10 min, 4°C) and supernatants were used for arginase assay. Arginase activity was measured using the QuantiChrom arginase assay kit (BioAssay Systems).

Nitrite/NO production

MDSC subpopulations were FACS sorted and 5×10^5 cells were cultured in 200 µl primary cell medium with and without 1 µg/ml LPS. Supernatants were collected after 24h and 100 µl were mixed with 0.5 volume Griess Reagent R1 and 0.5 volume Griess Reagent R2. After 10 min of incubation the absorbance at 540 nm was measured. Nitrite concentrations were determined by comparing the absorbance values for the test samples to a standard curve generated by serial dilution of 0.25mM sodium nitrite.

ROS production

Oxidative sensitive dye DCFDA (Invitrogen) was used to measure ROS production by MDSC subsets. Single cell suspensions from blood and tumors were incubated at 37°C in PBS containing 2.5 μ M DCFDA for 30 min. For induced activation, cells were simultaneously cultured with 30 ng/ml PMA. After incubation cells were labeled with anti-Gr-1 and anti-F4/80 antibodies and PI was added to exclude dead cells. Analysis was conducted by flow cytometry (FACSCalibur®).

5.2.8 Quantification of chemokines and cytokines

Enzyme-linked immunosorbent assay (ELISA)

To quantify IFN- γ production by T cells or NK cells, 10^5 cells were cultured alone or co-cultured with sorted MDSCs at different effector/target ratios in primary cell culture medium supplemented with the appropriate stimuli for 12-96 h. Protein levels were measured by IFN- γ ELISA (BD) according to the manufacturer's instructions.

To determine chemokine levels, FACS sorted MDSC subpopulations were cultured in primary cell culture medium for 24 h. Supernatants were analyzed using the murine CCL3, CCL4 and CCL5 ELISA (R&D) according to the manufacturer's instructions.

Bioplex protein array

For the determination of cytokine and chemokine production by MDSCs, subpopulations of naïve and blood and tumor from tumor-bearing mice were FACS sorted. 5×10^4 cells were cultured in 100 μ l primary cell culture medium for 24h. Supernatants were collected and further diluted 1:1 with Bioplex Sample Diluent (Biorad). Cytokine and chemokine release was determined with the Bioplex Protein Array according to the manufacturer's instructions.

5.2.9 Gene expression profile analysis

Experimental setup

Groups of 30 mice were injected subcutaneously with PBS (naïve controls) or groups of 25 mice were subcutaneously injected with 10^6 RMA-S cells resuspended in 100 μ l PBS. Mice were sacrificed on day 20 post-injection. Single cell suspensions were prepared from blood and tumor. PMN- and MO-MDSCs were isolated from the pooled blood and tumor samples as described in 5.2.6.2. Sorted cells showed a purity of ≥ 98 %. Biological triplicates were collected for each group (naïve, tumor-bearing), each organ (blood, tumor) and each subpopulation (PMN-, MO-MDSC).

RNA isolation

RNA was isolated from MDSC subpopulations using RNeasy Mini Kit (Qiagen). Cells were lysed in RLT buffer according to manufacturer's instructions and lysates were stored at -80°C until continuing isolation. Obtained RNA was treated with DNase using TURBO DNA-free kit (Ambion) in order to remove any possible genomic DNA contamination.

RNA precipitation

20 $\mu\text{g}/\text{ml}$ linear polyacrylamide (LPA), 0.1 volume 3 M NaAc pH 5.2 and 4 volumes 100 % ethanol was added to 50 μl RNA solution and incubated for 30 min at -80°C . RNA was pelleted (16000g, 30 min, 4°C) and washed twice with ice-cold 75 % ethanol. Pellets were dried to remove any remaining ethanol for max. 2 min and resuspended in RNA Storage Solution (Ambion). Quantity and quality of obtained RNA was analyzed using RNA Pico Assay performed on the Bioanalyzer 2100 Lab-on-a-Chip system. High quality RNA samples were chosen for microarray experiment.

Microarray experiment

Gene expression was detected using Mouse Ref-8 v2 array from Illumina. Six experimental groups were examined, with triplicates for each group. cDNA and cRNA synthesis, and hybridization to arrays were performed according to the manufacturer's instructions.

Microarray data analysis

Raw microarray data were processed using BeadStudio v9. Briefly, raw values were quantile normalized, background subtracted and \log_2 -transformed. Statistical and cluster analysis was performed using software package MeV v4.6 (MultiExperiment Viewer) from TM4 Microarray Software Suite. Statistical Analysis of Microarrays (SAM) was used to identify significantly regulated genes among groups under study. Unless otherwise stated a false discovery rate (FDR) of 5 % was utilized as a cutoff for determination of significance. Only genes, which showed a fold change ≥ 1.5 .were analyzed,

Microarray pathway analysis

To identify pathways that are likely to be affected by differential expression, an ORA approach using Fisher's exact test was performed. Analyzed pathways were collected from the KEGG database (Kyoto Encyclopedia of Genes and Genomes).

5.2.10 Statistical analysis

Differences between groups were calculated using unpaired Student's *t*-test. Differences in survival between groups of mice were calculated using log-rank test. Values of $P < 0.05$ were considered to be statistically significant.

6 RESULTS

6.1 Characterization of tumor-infiltrating MDSC subpopulations

6.1.1 Tumor-infiltrating MDSCs consist of a mononuclear and polymorphonuclear fraction

So far, most studies had been focused on MDSCs that accumulate in spleens of different tumor models [115], [64], [65]. Movahedi *et al.* demonstrated that splenic Gr-1⁺CD11b⁺MDSCs consisted of a Ly6G⁺SSC^{high} polymorphonuclear (PMN) and a Ly6G⁻SSC^{low} mononuclear (MO) fraction. MO-MDSCs express the macrophage marker F4/80 whereas it is absent on the PMN-MDSC subset [64]. The goal of our study was to characterize MDSC subsets, which infiltrated the tumor with regards to their phenotype and function. In our experiments, we used the TAP2-deficient mouse lymphoma model RMA-S derived from C57BL/6. Subcutaneous injection of the RMA-S cell line resulted in continuous tumor growth and expansion of Gr-1⁺CD11b⁺ MDSCs in blood, spleen and tumor after three weeks of tumor progression (Figure 6.1A). Blood from naïve mice contained 10.7 %, whereas the naïve spleen showed up to 4.8 % of Gr-1⁺CD11b⁺ cells. A significant increase in the proportion of MDSCs (blood 20.8 %; spleen 8.2 %) as well as 1.2 % of tumor-infiltrating Gr-1⁺CD11b⁺ cells were observed in mice bearing RMA-S tumors after 19 days of tumor cell inoculation.

In concordance to previous reports, Gr-1⁺CD11b⁺ cells in tumor-bearing mice consisted of two major subfractions based on differential expression of F4/80 (Figure 6.1B left panel). To further investigate the characteristics of these MDSC subpopulations, surface stainings for the Ly6G and Ly6C epitopes were performed. Gr-1⁺CD11b⁺F4/80⁻ MDSCs from blood and tumor expressed both Ly6G and Ly6C (Figure 1B middle panel). While Gr-1⁺CD11b⁺F4/80⁺ MDSCs lacked the Ly6G epitope, they expressed Ly6C at high levels (Figure 1B right panel). Blood and tumor-infiltrating MDSCs did not differ in their expression of Ly6G and Ly6C.

To address the question whether the two subpopulations display different morphologies, the nuclei of FACS sorted MDSC subsets from blood and tumor were analyzed (Figure 6.1C). Both Gr-1⁺CD11b⁺F4/80⁻ MDSCs from blood and tumor showed a polymorphonuclear morphology (these cells will be termed PMN-MDSCs), whereas Gr-1⁺CD11b⁺F4/80⁺ MDSCs were mononuclear (these cells will be termed MO-MDSCs)

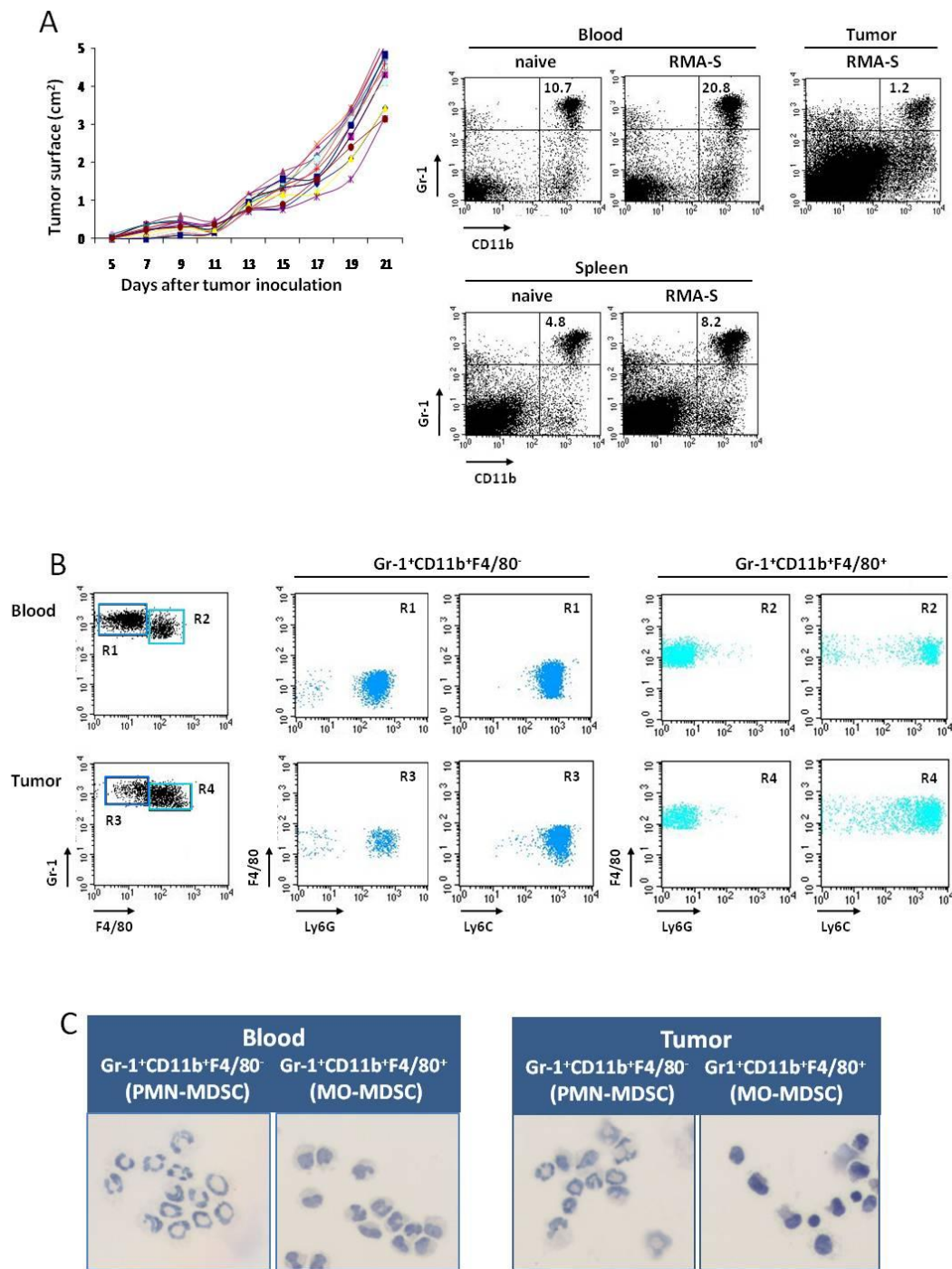


Figure 6.1: MDSCs in tumor-bearing mice consist of a polymorphonuclear and mononuclear subpopulation

Mice were subcutaneously injected with 10^6 RMA-S cells. MDSCs were analyzed on day 19 after tumor cell inoculation. **A)** *Left* Tumor growth was measured in regular time intervals. *Right* Blood, spleens and tumors were collected from RMA-S tumor-bearing mice or untreated naïve mice. Cell suspensions were stained for Gr-1 and CD11b expression. The percentages of Gr-1⁺CD11b⁺ MDSCs are indicated. **B)** Gr-1⁺CD11b⁺ were stained for their F4/80 expression (left panel). Both subpopulations were further analyzed for Ly6G and Ly6C expression (middle and right panel). **C)** Gr-1⁺CD11b⁺F4/80⁻ and Gr-1⁺CD11b⁺F4/80⁺ MDSC subsets were purified as described in “Methods” and subjected to hematoxylin and eosin staining. Magnification 200 x. Data are representative of three (A,B) and two experiments (C).

6.1.2 Phenotypic analysis of tumor-infiltrating MDSC subsets

To gain further insight in the lineage commitment and potential function of MDSC subpopulations in blood and tumor, the expression of different surface markers, as described earlier [64], was analyzed (Figure 2). The IL-4 receptor α (CD124) was expressed on both subsets from blood and on MO-MDSCs from the tumor. However, tumor-infiltrating PMN-MDSCs displayed only low surface expression of CD124. The macrophage marker CD115 (M-CSF receptor) was absent on blood PMN-MDSCs, slightly expressed on MO-MDSCs and highly expressed on tumor-infiltrating MDSCs. CD68 (macrosialin), which is associated with a monocytic/macrophage phenotype, was predominantly expressed by the MO-MDSC subpopulation. The adhesion molecules CD54, CD43, CD31, CD49b and CD62L showed differential expression patterns. Whereas CD54 was absent on PMN-MDSCs from blood and hardly detectable on PMN-MDSCs from the tumor, it was highly expressed on the monocytic counterpart. PMN-MDSCs from blood exhibited high levels of CD43 expression compared to the other subsets. CD49b was detected only on MDSCs from blood, whereas CD62L and CD31 were expressed on all subsets in all organs. In addition, we screened for surface markers, which are involved in antigen presentation. Although MHC class I molecules and CD86 were highly expressed on all MDSC subsets, only tumor-infiltrating MDSCs showed high expression of MHC class II and CD40 suggesting a higher potential for antigen presentation to CD4⁺ T cells. Also molecules involved in interaction with T cell were detected. CD80 was slightly expressed on all subsets, whereas PD-L1 expression was detected on an elevated surface level. Furthermore, the NKG2D ligand Rae-1, reported earlier as an additional marker for the monocytic subset [91], was highly expressed on tumor-infiltrating MO-MDSCs.

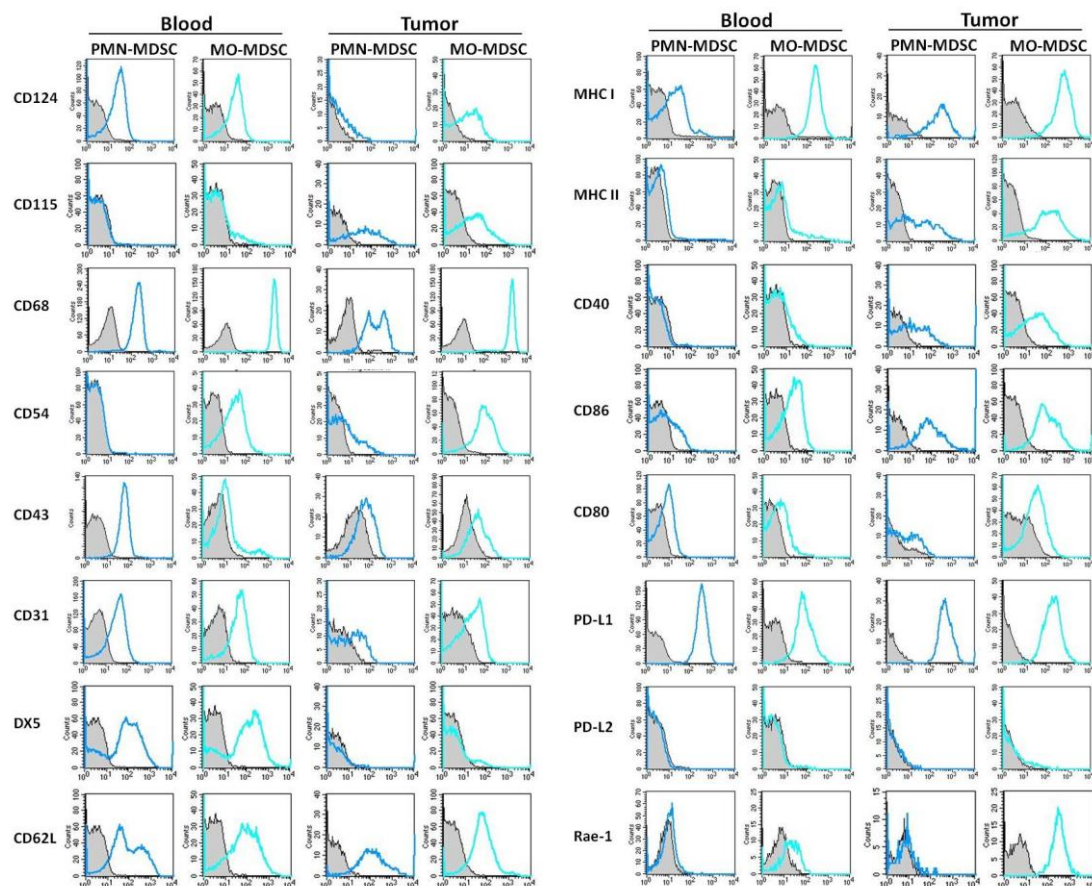
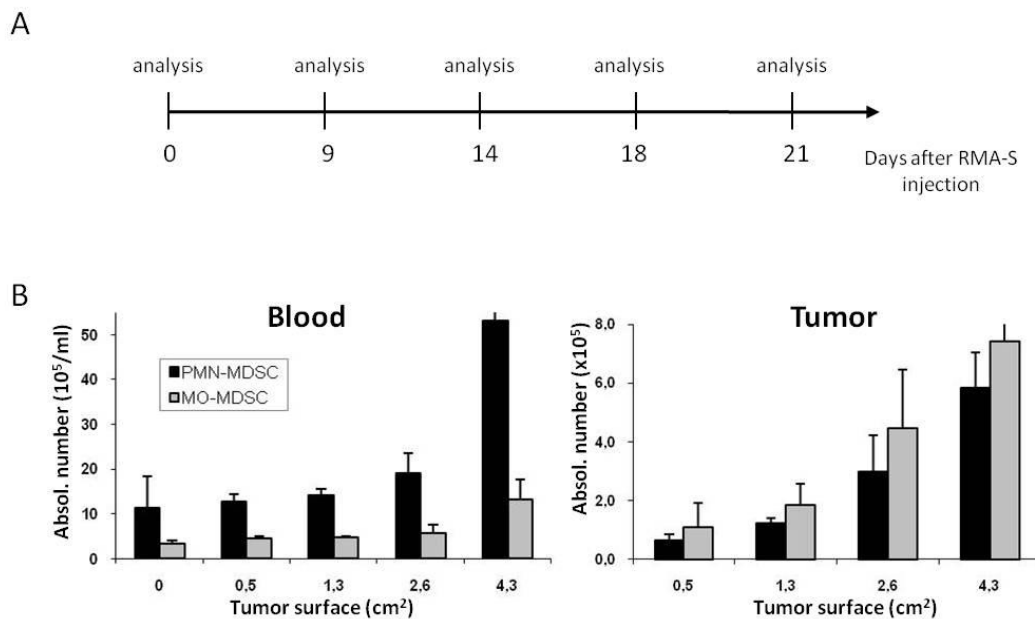


Figure 6.2: Phenotype of MDSC subsets

Mice were subcutaneously injected with 10^6 RMA-S cells. MDSCs were analyzed on day 19 after tumor cell inoculation. Subsets from blood and tumor were characterized for the expression of various surface markers (PMN-MDSC gated on Gr-1⁺CD11b⁺F4/80⁻; MO-MDSC gated on Gr-1⁺FCD11b⁺F4/80⁺). Stainings are representative of a pool of 2-3 mice.

6.1.3 Accumulation of MDSC subsets in the RMA-S tumor model

To determine the kinetics of PMN- and MO-MDSC accumulation, the total cell number of the two subsets in blood and tumor was measured at various time points after tumor cell inoculation (Figure 6.3A). In blood, both subpopulations were induced during tumor progression. However, PMN-MDSCs were the more prominent subpopulation. Tumor-infiltrating subsets accumulated with similar kinetics (Figure 6.3B).

**Figure 6.3: Kinetics of tumor-induced MDSC subset accumulation**

The accumulation of PMN- and MO-MDSCs was analyzed during tumor progression. **A**) 10^6 RMA-S cells were injected subcutaneously into 20 C57BL/6 mice and accumulation of MDSC subsets was analyzed in regular time intervals. Days indicate time points of MDSC subset analysis. **B**) The absolute cell number of blood and tumor PMN-MDSCs (Gr-1⁺CD11b⁺F4/80⁻) and MO-MDSCs (Gr-1⁺CD11b⁺F4/80⁺) was determined by flow cytometry analysis. Values represent the mean \pm SD (n=3-4).

6.1.4 MO-MDSCs show a high proliferation rate

Several studies observed that tumor progression stimulated hematopoiesis in spleen [116], [117]. To address the origin and dynamics of tumor-infiltrating MDSCs, we analyzed the turnover of PMN- and MO-MDSCs by BrdU incorporation. After 16 hours of *in vivo* labeling, 1 % of PMN-MDSCs and 13 % of MO-MDSCs in the bone marrow were BrdU positive. Less than 1 % PMN-MDSCs in blood, spleen and tumor showed BrdU incorporation, suggesting that precursors of PMN-MDSCs in the peripheral tissue extravasated at these sites after expansion and mobilization from the bone marrow. Moreover, up to 8 % of MO-MDSCs in spleen and tumor exhibited BrdU labeling compared to 1 % in blood. Thus, MO-MDSCs proliferate more rapidly than PMN-MDSCs (Figure 6.4).

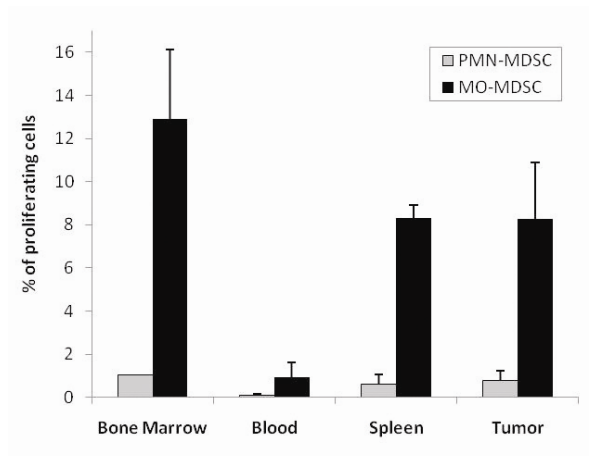


Figure 6.4: Turnover of MDSC subpopulations
RMA-S tumor-bearing mice were systemically injected with BrdU on day 19 after tumor cell inoculation. After 16 h BrdU uptake by PMN- and MO-MDSCs from bone marrow, blood, spleen and tumor was analyzed by flow cytometry. Data are representative of two experiments. All values represent the mean \pm SD (n=2).

6.2 Gene expression profile of tumor-infiltrating MDSC subsets

So far, most studies had been focused on the analysis of MDSCs that accumulated in blood and spleen. Therefore, the aim of our study was the comprehensive analysis of tumor-infiltrating MDSCs including their subset distribution, phenotype and function. We performed a global gene expression profiling of tumor-infiltrating MDSC subpopulations from RMA-S tumor-bearing mice. In order to identify molecules and pathways that might be involved in functional regulation of MDSCs, additional blood MDSC subsets from naïve and tumor-bearing mice were included in our experimental setup (Figure 6.5A). PMN- and MO-MDSCs were isolated from blood of naïve mice and from blood and tumor of tumor-bearing mice on day 19 after tumor cell inoculation. To obtain highly purified MDSC subsets ($\geq 96\%$), cells were sorted by flow cytometry. Subsequently, total RNA was isolated from sorted cells and tested for its quantity and quality (Figure 6.5B). High quality RNA was labeled and hybridized with mouse whole genome microarrays. Each experimental group comprised biological triplicates.

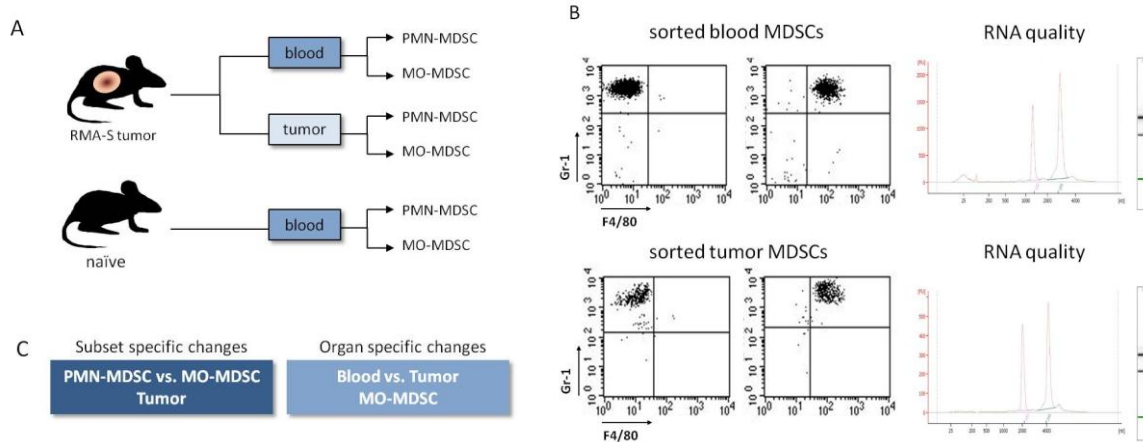


Figure 6.5: Experimental setup of the gene expression analysis

A) 30 mice per group were subcutaneously injected with 10^6 RMA-S cells or with PBS (naïve controls). On day 19 after tumor cell inoculation PMN-MDSCs and MO-MDSCs were isolated from blood and tumor tissue. Each group was represented by biological triplicates. **B)** Highly purified MDSC subsets were obtained by flow cytometry sorting (left). Samples with purity $\geq 96\%$ were selected for RNA isolation. Total RNA was analyzed for quantity and quality using RNA 6000 Pico Assay performed on the Bioanalyzer 2100 Lab-on-a-Chip system (right). RNA of similar high quality was labelled and hybridized with Mouse Ref-6 v2 Illumina microarray chips. **C)** Comparisons of differently regulated genes were performed on tumor-infiltrating MDSC subsets (PMN-MDSC vs MO-MDSC) or on MO-MDSC from different organs (blood vs tumor).

The dataset of the mouseWG-6 v2.0 expression bead chip contained expression levels for 45.200 transcripts. Based on the Complete Linkage method and the Pearson's correlation coefficient as a measure of similarity in the Chipster software, hierarchical cluster analysis was performed to group the samples according to the degree of similarity present in the gene expression data. In the resulting dendrogram five distinct clusters were detected (Figure 6.6). Due to the high similarity of PMN-MDSCs from naïve and tumor-bearing blood, these groups formed one cluster (red). One replicate of the MO-MDSC group (purple) from tumor-bearing mice had to be excluded, since this sample did not cluster with its dedicated group. In the dendrogram shown below, MO-MDSCs from naïve (blue) and tumor-bearing blood (purple) were the most similar and formed the first node, followed by tumor-infiltrating MO-MDSCs (green). The last two clusters (PMN-MDSCs from tumor = yellow; PMN-MDSCs from blood = red) joined latest, showing the largest difference to the MO-MDSC clusters.

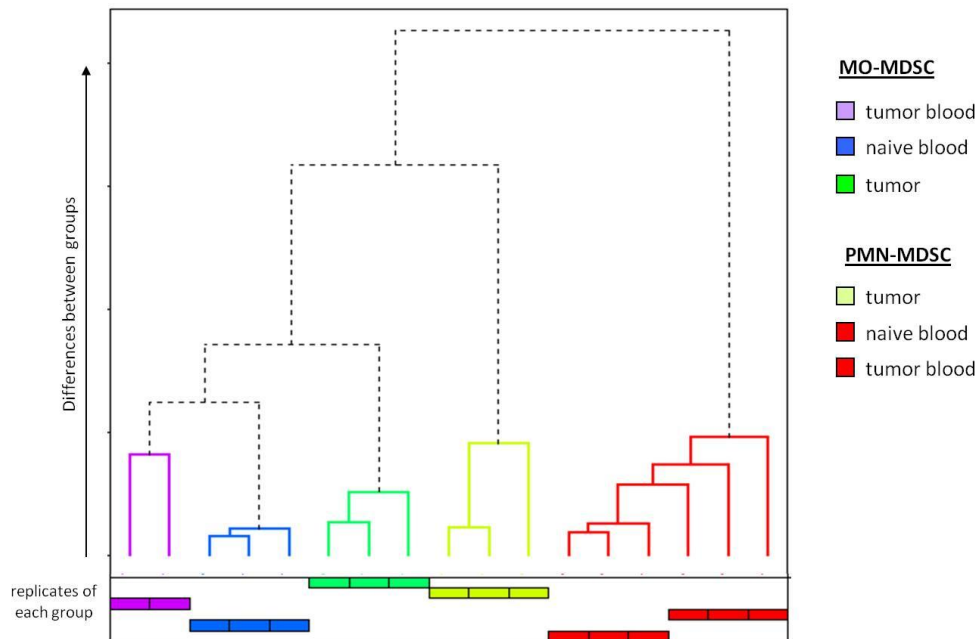


Figure 6.6: Hierarchical cluster analysis of MDSC subsets

The schematized dendrogram reflects the process of clustering microarray samples according to the similarity in their gene expression profiles as measured by the Pearson correlation coefficient. Distances between the array sample clusters are approximated by the vertical axis. Along the x axis of the dendrogram the microarray replicates are listed

Functional classification of differently expressed genes between blood and tumor-infiltrating MDSCs revealed their involvement in the control of immune responses (Table 6.1). Most significantly affected pathways in tumor-infiltrating MDSCs included the MAPK signaling pathway (MO-MDSC) and unexpectedly, the T cell receptor signaling pathway (PMN-MDSC). The MAPK signaling pathway comprised upregulated genes like CD14, Jun, Hras1, Raf1, Akt2 and IL-1 β , which are involved in the regulation of cell proliferation, differentiation and inflammation. The T cell receptor signaling exhibited genes like CD3 ϵ , ZAP70, Itk, NFAT as well as CD28, PI3K, Akt and Gsk3b, suggesting effector functions typically triggered upon CD3 ϵ and CD28 engagement. Of note, CD3 ϵ protein expression on MDSCs was detected by flow cytometry (data not shown).

Pathway	Affected subset	Hits	Percentage	Significance
MAPK signaling	MO-MDSC	20	4.1	0.0044
Toll-like receptor signaling	MO-MDSC	9	1.8	0.11
Renal cell carcinoma	MO-MDSC	10	2.0	0.0025
T cell receptor	PMN-MDSC	11	2.4	0.0044
Apoptosis	PMN-MDSC	9	2.0	0.0098
DNA replication	PMN-MDSC	6	1.3	0.013
VEGF signaling	PMN-MDSC	8	1.8	0.02
Nucleotide excision repair	PMN-MDSC	6	1.3	0.032

Table 6.1: Signaling pathways affected by differential gene expression in tumor-infiltrating MDSCs

To identify pathways that are likely affected in tumor-infiltrating MDSCs from RMA-S injected mice, an ORA (overrepresentation analysis) approach using Fisher's exact test was performed. Pathways were analyzed using the DAVID software according to the KEGG (Kyoto Encyclopedia of Genes and Genomes) database.

In the second analysis, comparisons between tumor-infiltrating PMN-MDSCs and MO-MDSCs were made. MO-MDSCs within the tumor significantly upregulated genes of the lysosome pathway, including lysosomal acid hydrolases (cathepsins A/B/C/H/Z; Lamp1; neuraminidase-1) and CD68, suggesting a high activity in phagocytosis. In addition, several genes involved in antigen processing and presentation were detected, such as MHC class I, MHC class II and CD74. This finding indicates that tumor-infiltrating MO-MDSCs might play an important role in cross-talks with T cells and NK cells.

Pathway (MO-MDSCs)	Hits	Percentage	Significance
Lysosome	24	4	0.0000
Systemic lupus erythematosus	12	2.0	0.017
Antigen processing and presentation	11	1.8	0.022
Sphingolipid metabolism	7	1.2	0.047
Cell adhesion molecules	14	2.3	0.055

Table 6.2: Signaling pathways affected by differential gene expression subsets of tumor-infiltrating MDSCs

To identify pathways that are likely affected between tumor-infiltrating PMN-MDSCs and MO-MDSCs, an ORA approach using Fisher's exact test was performed. Pathways were analyzed using the DAVID software according to the KEGG database.

Moreover, when we focused on the tumor-infiltrating MO-MDSC subpopulation, the pan-genomic analysis revealed a cluster of more than 400 genes, which were explicitly upregulated in MO-MDSCs from the tumor tissue compared to all other samples (Figure 6.7). Within this cluster, we found genes that have been associated with suppression (e.g. arginase-1), inflammation (e.g. CD14, Dectin-2) and chemotaxis (e.g. CCL3/4/7/24). The following paragraphs will focus on the three selected groups.

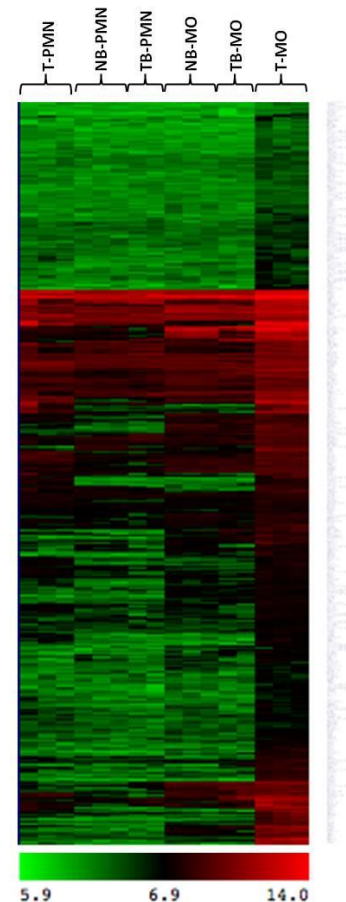


Figure 6.7: Genes upregulated in tumor-infiltrating MO-MDSCs

Differently expressed genes were identified and clustered according to their upregulation in tumor-infiltrating MO-MDSC subset using the MeV (MultiExperimentViewer) analysis software. Genes were sorted corresponding to their log₂ value of 5.9 to 14.0. *NB* = naïve blood; *TB* = blood from tumor-bearing mice; *T* = tumor; *MO* = MO-MDSC; *PMN* = PMN-MDSC

6.2.1 Tumor-infiltrating MO-MDSCs upregulate expression of genes involved in suppression

MDSCs are potent suppressors of various T cell functions. Their suppressive activity is highly correlated with increased production of reactive oxygen and nitrogen species as well as elevated levels of arginase-1 [118]. Several studies have suggested that the mononuclear subset rather than the polymorphonuclear fraction is responsible for T cells suppression through iNOS and arginase-1 [119] [118]. Consistent with previous findings showing that arginase-1 was mainly expressed in MO-MDSCs, its transcript was highly increased in the tumor-infiltrating MO-MDSCs compared to all other subsets from all organs in our experiment (Figure 6.8A). Next, we analyzed the arginase-1 activity to validate significant changes on protein levels. MDSC subpopulations from blood and tumor of RMA-S injected mice were FACS sorted and their arginase-1 activity measured. In addition to the transcriptional level, the arginase-1 activity of tumor-infiltrating MO-MDSCs was highly increased, whereas comparably low levels were measured in the PMN-MDSC subsets.

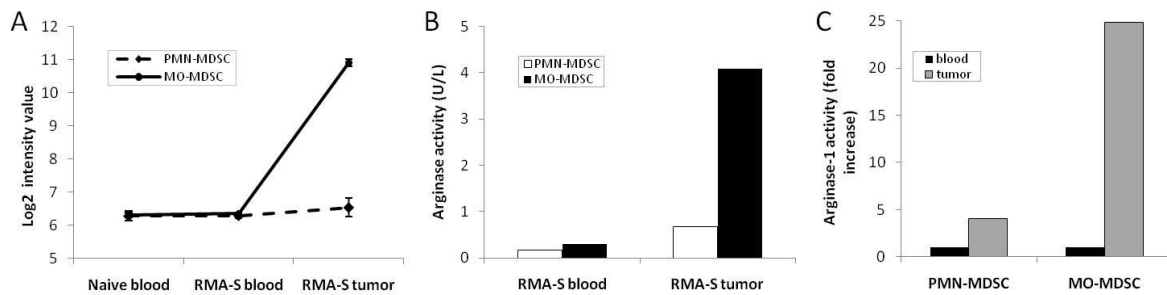


Figure 6.8: Tumor-infiltrating MO-MDSC upregulated arginase-1

The arginase-1 expression profile of MDSC subpopulations from naïve blood, RMA-S blood and from RMA-S tumors was analyzed. **A)** Relative expression levels of the arginase-1 gene in different MDSC subsets are expressed as the Log₂ intensity value. Values represent the mean \pm SD (n=3). **B+C)** MDSC subpopulations from blood and tumor of RMA-S injected mice were sorted and their arginase-1 activity was measured as described in “Methods”. **B)** Total levels of arginase-1 activity. **C)** Fold increase of arginase-1 activity in tumor-bearing MDSC subsets compared to blood MDSCs. Arginase-1 activity of blood MDSCs was set to 1.

In addition to arginase-1, also other factors are involved in T cell suppression. We asked, whether tumor-infiltrating MDSC subsets might display higher levels of iNOS or ROS. Although neither the iNOS gene nor genes involved in ROS production were upregulated on transcriptional levels (data not shown), iNOS activity via NO secretion and the production of ROS were evaluated. In response to stimulation with LPS, monocytic MDSCs produce significantly higher levels of NO than their granulocytic counterpart (Figure 6.9A). In contrast, PMN-MDSCs from blood of tumor-bearing mice displayed significantly higher levels of ROS production than PMN-MDSCs from the tumor (Figure 6.9B). The MO-MDSC subset showed lower absolute values in ROS production.

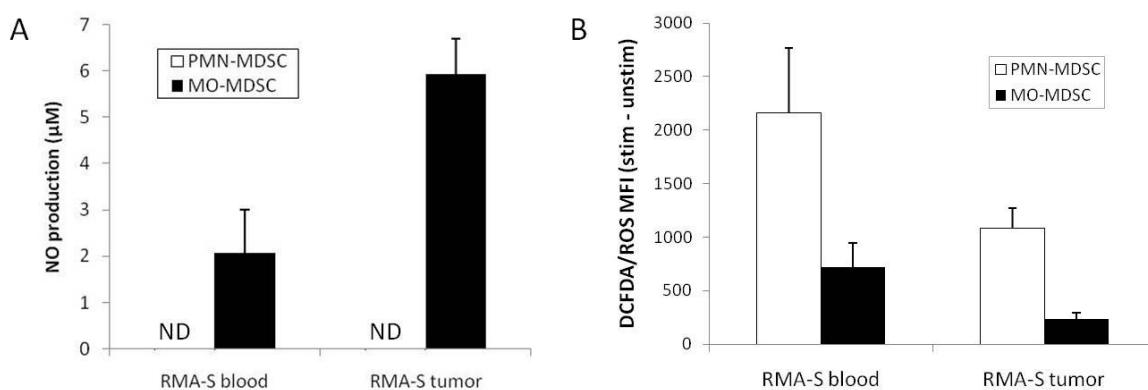


Figure 6.9: Suppressive activity by MDSC subpopulations

A) Sorted population of MDSCs were stimulated with 1 μ g/ml LPS for 24 h, supernatants were collected and the nitrite/NO concentration was measured as described in “Methods”. *ND*, not detected **B)** MDSCs from blood and tumor cell suspensions were pre-gated on Gr-1⁺CD11b⁺F4/80⁻ (PMN) and Gr-1⁺CD11b⁺F4/80⁺ (MO) and their ROS production was determined via mean fluorescence intensity of DCFDA before and after 30 min of PMA stimulation. Data are representative of two experiments. All values represent the mean \pm SD.

Together, these experiments showed that MO-MDSCs from tumor tissue exhibited high arginase-1 and iNOS activity compared to their blood counterpart. These findings suggested a potential role of tumor-infiltrating MO-MDSCs in T cell suppression. In contrast to MO-MDSCs, PMN-MDSCs displayed high ROS levels in blood, whereas in the tumor, a reduction in ROS was detected.

6.2.2 Tumor-infiltrating MDSCs upregulate the expression of pro-inflammatory genes

It has been shown that MDSCs accumulate in response to pro-inflammatory mediators that induce a variety of suppressive mechanisms to block both innate and adaptive anti-tumor immunity [120-121]. In addition to responding to pro-inflammatory signals, MDSCs also contribute to the inflammatory tumor microenvironment by secreting factors like IL-6 or S100A8/A9 [82]. We asked whether the tumor-infiltrating MO-MDSC subset display an inflammatory phenotype and thereby, might contribute to tumor progression.

We found that the CD14 gene expression was significantly upregulated in tumor-infiltrating MO-MDSCs, whereas it was downregulated in the polymorphonuclear subset compared to blood (Figure 6.10A). At protein level we confirmed increased expression of CD14 on tumor-infiltrating MO-MDSCs. Interestingly, although transcript levels of CD14 was decreased in tumor-infiltrating PMN-MDSCs, CD14 expression at protein level was increased compared to blood PMN-MDSCs (Figure 6.10B).

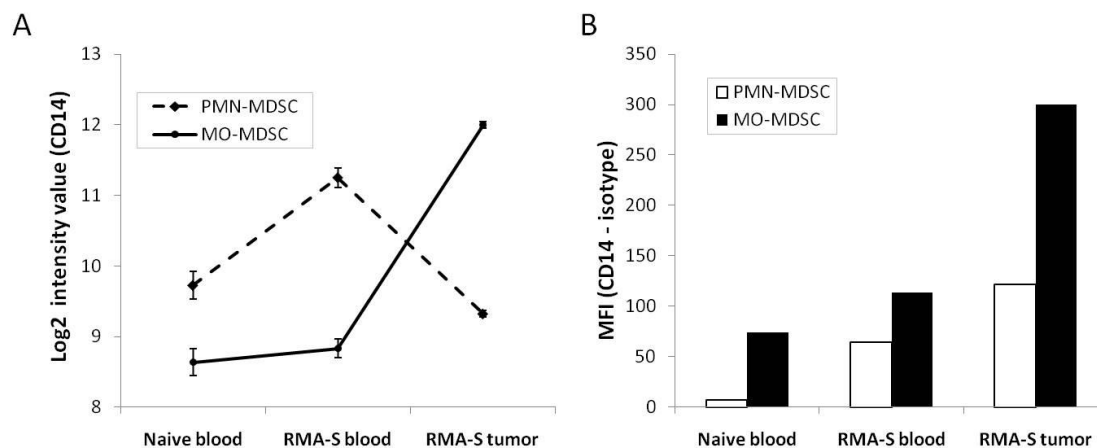


Figure 6.10: Upregulation of CD14 on tumor-infiltrating MO-MDSCs

The CD14 expression profile of MDSC subpopulations from naïve blood, RMA-S blood and from RMA-S tumors was analyzed **A)** Relative expression levels of the CD14 gene in different MDSC subsets are expressed as the Log2 intensity value. **B)** Different MDSC subpopulations from blood and tumor of RMA-S injected mice as well as from naïve blood were stained for CD14 surface expression. Graph indicates the mean fluorescence intensity (MFI) of the different experimental groups containing a pool of three animals. Data are representative of one (A) and two (B) experiments.

The CD14 molecule acts as a co-receptor, and together with TLR-4, binds bacterial compounds like LPS [122] or pro-inflammatory molecules such as S100A8/A9 [123]. Triggering of the CD14/TLR-4 complex leads to the activation of two distinct signaling pathways. One pathway is activated by the adaptor protein MyD88 (myeloid differentiation primary response gene 88), which results in induction of the pro-inflammatory cytokines TNF- α and IL-1, IL-6 and IL-10. The second pathway functions via the adaptor TRIF (TIR-domain-containing adapter-inducing interferon- β) leading to the induction of type I interferons IFN- α and IFN- β [124].

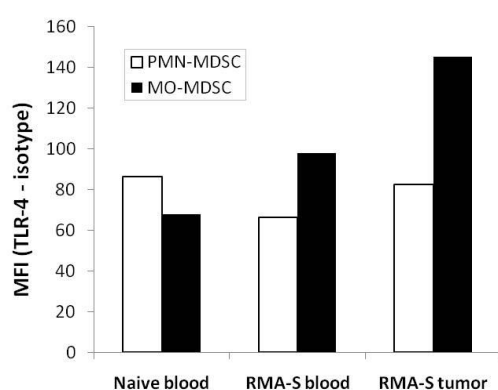


Figure 6.11: Expression of TLR-4 on different MDSC subpopulations

Different MDSC subsets from blood and tumor of RMA-S injected mice as well as from naïve blood were stained for TLR-4 surface expression. Graph indicates the mean fluorescence intensity (MFI) of the different experimental groups containing a pool of three animals. Data are representative of two experiments.

To evaluate the protein level of the co-receptor TLR-4, MDSC subpopulations from blood and tumors were stained for TLR-4 surface expression. Like CD14, tumor-infiltrating MO-MDSCs exhibited an increased expression of TLR-4, whereas no changes were detected on the PMN-MDSC subset (Figure 6.11). These data indicate that elevated levels of the CD14/TLR-4 complex might result in an increased activation of the TLR-4 signaling cascade. Therefore, we focused on target genes which were upregulated in tumor-infiltrating MO-MDSCs. Using the DAVID software according to the KEGG database we found several potential target genes of TLR-4 induced transcription factors, which were significantly upregulated in our microarray analysis (Table 6.3).

	Gene name	Gene symbol	Fold change
Inflammatory cytokines	Tumor necrosis factor	tnf	3.06
	Chemokine (C-C motif) ligand 3	ccl3	10.12
	Chemokine (C-C motif) ligand 4	ccl4	9.58
	Chemokine (C-X-C motif) ligand 10	cxcl10	1.26
	Chemokine (C-X-C motif) ligand 9	cxcl9	3.22
Co-stimulatory molecules	CD 40 antigen	cd40	2.25
	CD86 antigen	cd86	1.73

Table 6.3: Target genes of TLR-4 induced transcription factors

To identify potential target genes that might be upregulated in the tumor-infiltrating MO-MDSC subset, KEGG pathway analysis for TLR-4 signaling was performed. The fold change of differently expressed target genes compared to all other subsets is shown.

In addition to CD14 and TLR-4, Dectin-2 (dendritic cell-associated C-type lectin-2) was significantly upregulated in the tumor-infiltrating MO-MDSC subpopulation. Dectin-2 belongs to the C-type lectin family, a protein group which was originally defined by their ability to recognize carbohydrate structures [125]. The receptor is mainly expressed on tissue macrophages, DCs and peripheral blood monocytes, where expression levels are transiently increased upon induction of inflammation [126]. Via its CRD domain (carbohydrate recognition domain), Dectin-2 recognizes zymosan, numerous pathogens and mannose [127], [128]. So far, the only endogenous ligand was detected on Tregs upon UV irradiation [129]. Dectin-2 has a short cytoplasmic domain which lacks signaling motifs and thereby, associates with FcR γ to transduce signals. Triggering of the receptor leads to the activation of the transcription factor NF κ B and production of TNF- α and IL-1 receptor antagonists [128]. So far, the role of Dectin-2 in the tumor microenvironment is unclear.

We found that the Dectin-2 gene *clec4n* was significantly upregulated in tumor-infiltrating MO-MDSCs, whereas it was downregulated in the polymorphonuclear subset compared to blood (Figure 6.12A). In addition, we confirmed that Dectin-2 is highly expressed on the cell surface of tumor-infiltrating MO-MDSCs. Despite the reduction of mRNA levels discovered by the microarray analysis, slightly increased surface levels of Dectin-2 on tumor-infiltrating PMN-MDSCs were detected compared to the subset in blood (Figure 6.12B).

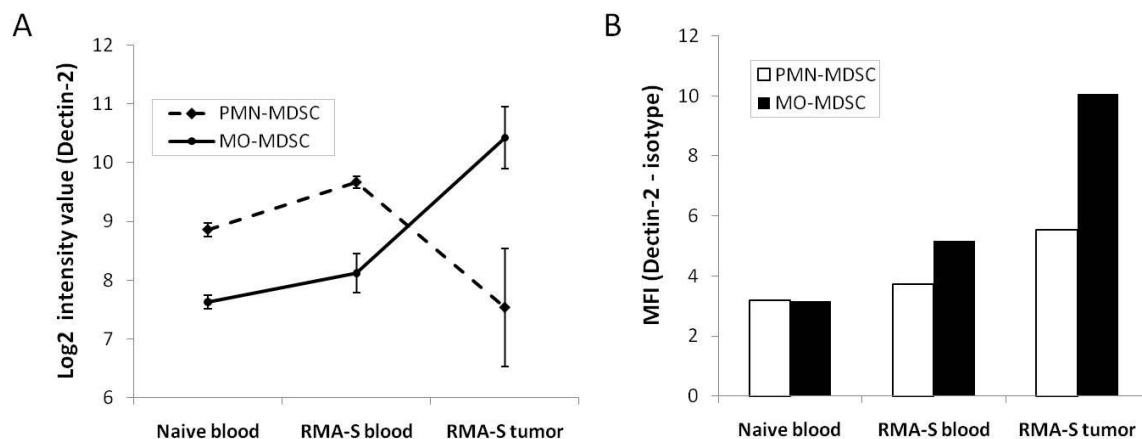


Figure 6.12: Upregulation of Dectin-2 on tumor-infiltrating MO-MDSCs

The Dectin-2 expression profile of MDSC subpopulations from naïve blood, RMA-S blood and from RMA-S tumors was analyzed **A)** Relative expression levels of the Dectin-2 gene in different MDSC subsets are expressed as the Log2 intensity value. **B)** Different MDSC subpopulations from blood and tumor of RMA-S injected mice as well as from naïve blood were stained for Dectin-2 surface expression. Graph indicates the mean fluorescence intensity (MFI) of the different experimental groups containing a pool of three animals. Data are representative of one (A) and two (B) experiments.

So far, we showed that the inflammatory molecules CD14, TLR-4 and Dectin-2 were highly upregulated on both RNA and protein levels in tumor-infiltrating MO-MDSCs from RMA-S tumors. To confirm that this expression profile is not restricted to lymphoma tumors, we analyzed MDSC subpopulations from tumors of different origin. Like in lymphoma, in B16 melanoma and MCA205

fibrosarcoma MO-MDSCs exhibited the same pattern of CD14 and Dectin-2 expression (Figure 6.13). Compared to RMA-S and MCA205 tumors, tumor-infiltrating PMN-MDSCs from B16 melanoma completely downregulated the expression of CD14 and TLR-4 on the cell surface.

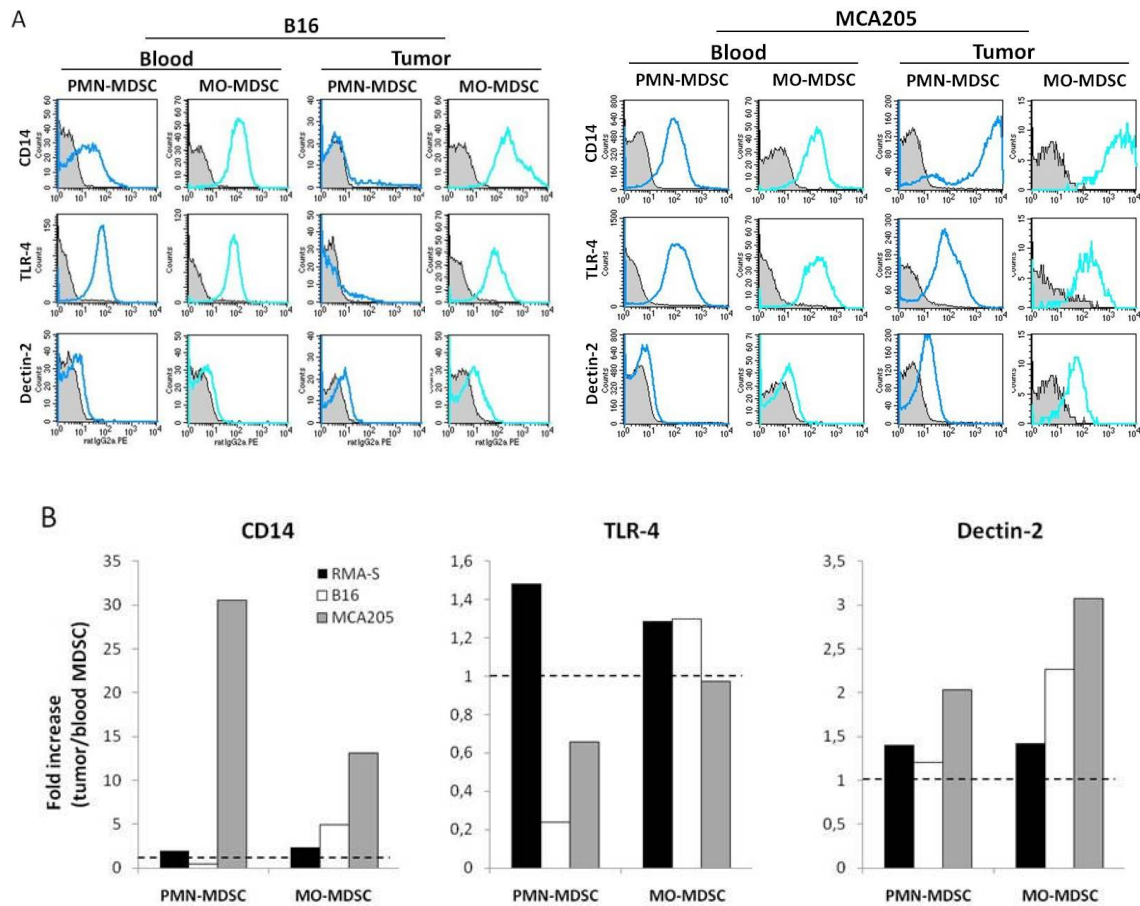


Figure 6.13: Expression of inflammatory molecules on MDSC subsets from tumors of different origin

Mice were subcutaneously injected with 5×10^5 B16 melanoma and 10^6 MCA205 fibrosarcoma cells. MDSCs were analyzed on day 15 (B16) and on day 25 (MCA205) after tumor cell inoculation and subsets from blood and tumor were characterized for the expression of the inflammatory surface markers CD14, TLR-4 and Dectin-2 by flow cytometry. **A)** Histograms indicate the expression levels of the different experimental groups containing a pool of three animals. **B)** Values show fold increase of expressed proteins from (A) in tumor-infiltrating MDSCs compared to blood. Data are representative of two experiments.

In summary, our data demonstrated that tumor-infiltrating MO-MDSCs exhibited an inflammatory phenotype by expressing high levels of CD14, TLR-4 and Dectin-2. Triggering of these receptors might result in the production of pro-inflammatory cytokines TNF- α , IL-1, IL-6 or IL-10 and thereby further contribute to a pro-inflammatory tumor microenvironment.

6.2.3 Tumor-infiltrating MO-MDSCs upregulate the expression of chemokines

Chemokines play an important role in tumor growth and dissemination. They are not only key mediators in homing of cancer cells to metastatic sites but also in the recruitment of different cell types to the tumor microenvironment. Chemokines are classified based on the presence of conserved cysteine motifs in the protein sequence. The first group, CC subfamily (juxtaposition of the first two cysteines), comprises 28 members, whereas the CXC group (single variable amino acid between the first two cysteines) is composed of 17 members. In addition two smaller subgroups, CX3C and XC, are defined [130].

It has been shown that the migration of MDSCs to the tumor is mediated by CCL2. MDSCs ubiquitously express the CCL2 receptor CCR2 and blockade of this interaction resulted in reduced recruitment and decreased tumor growth [131], [132]. However, chemokine secretion by MDSCs and their influence on cell recruitment and tumor growth has not been described so far. Our data demonstrated that several chemokine genes were significantly upregulated in tumor-infiltrating MO-MDSCs compared to other subsets (Figure 6.14). CCL3, CCL4, CXCL2, CXCL9, CCL7 and CCL24 are all inflammatory chemokines supporting further an inflammatory role of MO-MDSCs during tumor progression.

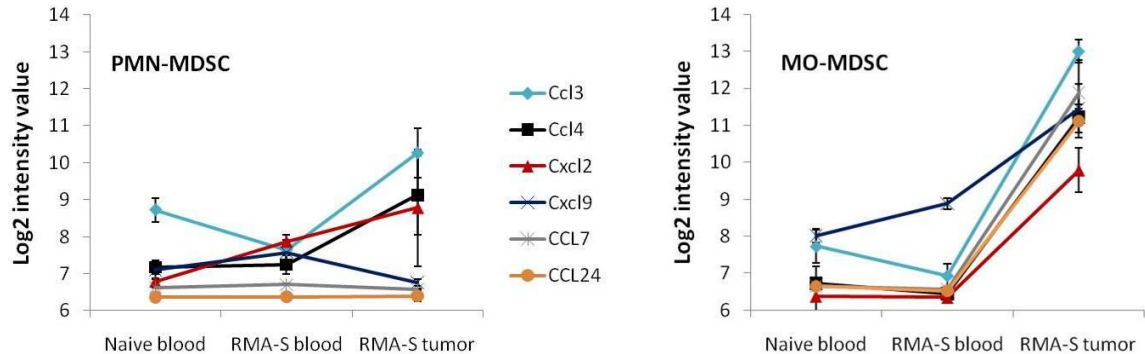


Figure 6.14: Upregulation of chemokines in tumor-infiltrating MO-MDSCs

The chemokine expression profile of MDSC subpopulations from naïve blood, RMA-S blood and from RMA-S tumors was analyzed. Shown are the Log2 intensity values of chemokine gene expression for Ccl3, Ccl4, Cxcl2, Cxcl9, Ccl7 and Ccl24 in different MDSC subsets.

Figure 6.15 summarizes all chemokines, which were upregulated in tumor-infiltrating MO-MDSCs. Shown are their dedicated receptors and the expression pattern of the chemokine receptors.

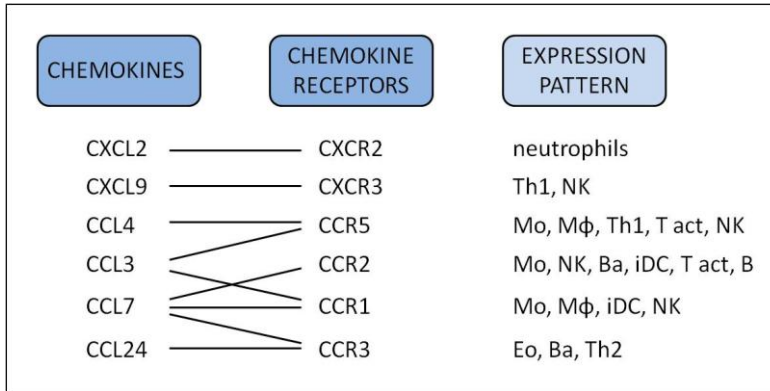


Figure 6.15: The chemokine system involved in tumor-infiltrating MO-MDSCs

Chemokines, their receptors and expression patterns are shown. Th1, T helper 1 cell; NK, NK cell; Mo, monocyte; M ϕ , macrophage; Tact, activated T cell; Ba, basophil; iDC, immature DC; B, B cell; Eo, eosinophil; Th2, T helper 2 cell.

In order to validate the chemokine profile, MDSC subpopulations were freshly isolated from blood and tumor of RMA-S tumor-bearing mice as well as from naïve blood. In addition, sorted TAMs and the tumor cell line RMA-S were included in our study. The production of CCL3, CCL4, CXCL2 and CXCL9 was assessed after 24 h of culture in medium. CCL7 and CCL24 were excluded, since reagents for CCL7 and CCL24 could not be provided by the manufacturer, whereas the chemokine CCL5 was further included. The results demonstrated consistently higher chemokine levels produced by tumor-infiltrating MO-MDSC compared to other subsets. Moreover, lower levels of all five chemokines were observed in cultures of TAMs, suggesting that these cells might also contribute to the chemokine milieu of the tumor tissue (Figure 6.16).

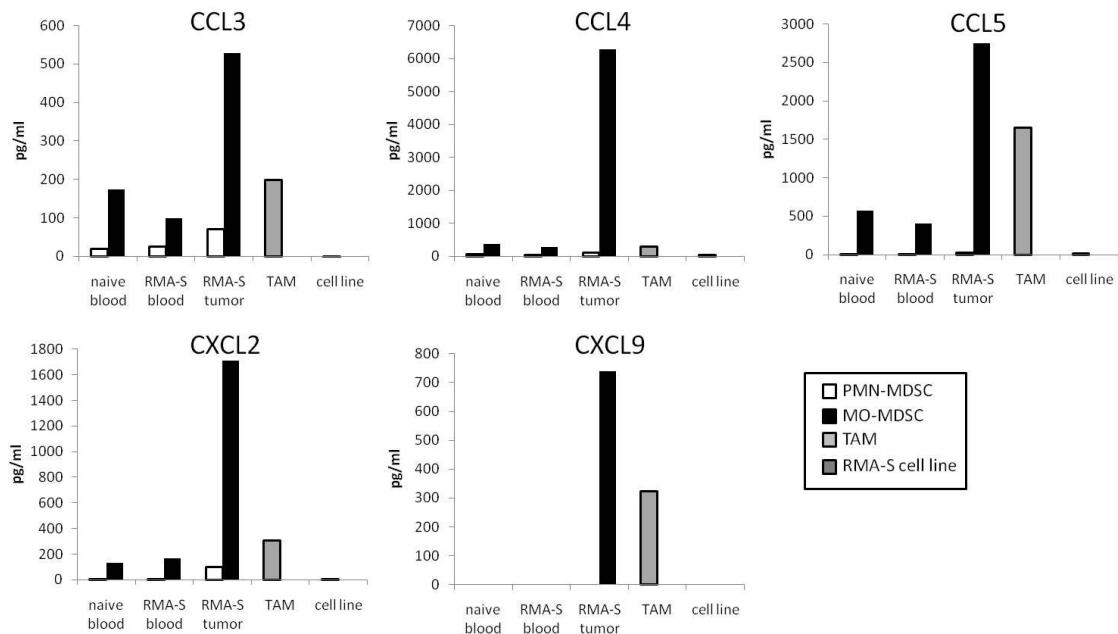


Figure 6.16: Increased chemokine production by tumor-infiltrating MO-MDSCs

C57BL/6 mice were subcutaneously injected with 10^6 RMA-S cells. 19 days after tumor cell inoculation MDSC subsets and TAMs (CD11b⁺F4/80⁺Gr-1⁻) were purified and cultured *in vitro* with medium for 24 h. The RMA-S cell line was cultured as a control. Supernatants were analyzed for chemokine production by Bioplex as described in "Methods". Data are representative of two experiments.

To confirm that this expression profile was not restricted to lymphoma tumors, the same approach was performed using the melanoma tumor B16. Like in lymphoma, MDSCs in B16 melanoma displayed similar chemokine productions (Figure 6.17). The tumor-infiltrating MO-MDSC subset was the most potent producer of CCL4, CXCL2 and CXCL9, while CCL3 and CCL5 were also secreted at high levels by B16 tumor cells.

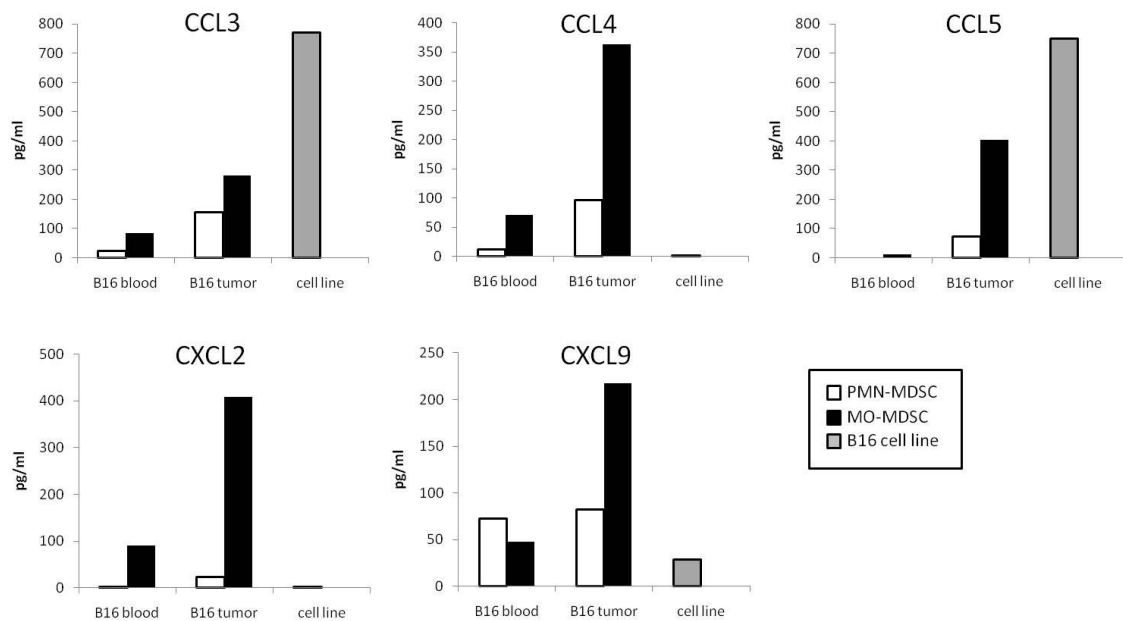


Figure 6.17: Increased chemokine production by tumor-infiltrating MO-MDSCs from B16 tumor model
C57BL/6 mice were subcutaneously injected with 5×10^5 B16 cells. 15 days after tumor cell inoculation MDSC subsets were purified and cultured *in vitro* with medium for 24 h. The B16 cell line was cultured as a control. Supernatants were analyzed for chemokine production by Bioplex as described in “Methods”.

6.3 Interaction of tumor-infiltrating MDSC subpopulations with immune cells

MDSCs suppress immunity by inhibiting both innate and adaptive immune responses. Previous studies demonstrated that MDSCs could block the activation and proliferation of $CD8^+$ and $CD4^+$ T cells. The suppressive activity requires cell-cell contact and is either antigen-specific or non-specific [133]. Tumor immunity is also impacted by the interaction of MDSCs and NK cells. Dependent on the tumor model MDSCs inhibit NK cell cytotoxicity against tumor cells and block $IFN-\gamma$ production or activate NK cells due to Rae-1, that interacted with NKG2D on NK cells [90], [91]. Here we analyzed the interaction of tumor-infiltrating MDSC subpopulations with T cells and NK cells.

6.3.1 Functional properties of tumor-infiltrating MDSCs cultured with T cells

Since high levels of arginase-1 and iNOS activity was detected in MO-MDSCs from the tumor, we examined whether tumor-infiltrating MDSC subsets from RMA-S tumor-bearing mice suppress the proliferation of T cells. MDSC subpopulations from the tumor were isolated and sorted by flow cytometry. Highly purified subsets were cultured in the absence or presence of CFSE-labeled pan T cells from naïve C57BL/6-Ly5.1 congenic mice at indicated ratio together with ConA. After four days, T cell proliferation via CFSE dilution was determined. Unexpectedly, we detected an increased T cell proliferation when co-cultured with MO-MDSCs or PMN-MDSCs compared to T cells alone (Figure 6.18A). A dose-dependent effect of MDSCs on T cell proliferation was detected, when T cells were cultured with different MDSC ratios (6.18B). In summary, despite the fact that tumor-infiltrating MO-MDSCs showed increased levels of arginase-1 and iNOS activity (as shown in Figure 6.8A and 6.9B), they did not suppress T cell proliferation.

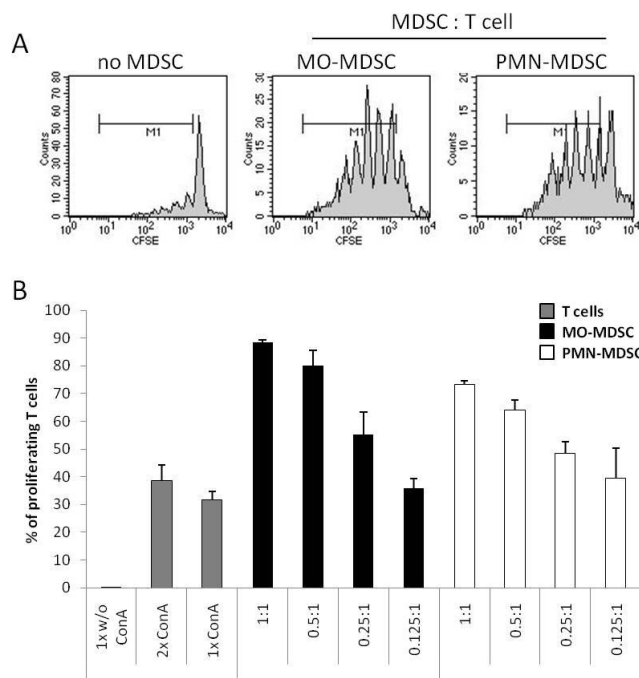


Figure 6.18: Tumor-infiltrating MDSCs induce T cell proliferation

C57BL/6 mice were subcutaneously injected with 10^6 RMA-S cells. On day 19 after tumor cell inoculation tumor-infiltrating MDSC subsets were purified and co-cultured with CFSE-labeled pan T cells from naïve C57BL/6-Ly5.1 congenic mice at different ratios in the presence of ConA. **A)** Proliferation was assessed by CFSE dilution on day 4. Shown are histograms with T cells alone (no MDSC) and 1:1 ratios with MO-MDSCs or PMN-MDSCs gated on $CD45.1^+7AAD^-$ T cells. **B)** Graph indicates the percentage of proliferating T cells within different ratios of the co-cultures. Data show the mean of triplicate cultures \pm SD and are representative of three experiments.

6.3.2 Effect of tumor-infiltrating MDSCs on NK cell function

In our previous study we showed that MO-MDSCs from blood and spleen of RMA-S tumor-bearing mice did not suppress NK cell proliferation but rather activated them to produce high levels of IFN- γ . This induction was partially mediated via the interaction with NKG2D on NK cells [91]. We asked whether the tumor-infiltrating MO-MDSC subset exhibits similar functional properties. As shown in Figure 6.2, tumor-infiltrating MO-MDSCs display elevated levels of Rae-1 compared to PMN-MDSCs. To determine the effect of MO-MDSCs on IFN- γ production, NK cells from naïve mice were cultured with IL-12 in the presence or absence of tumor-infiltrating MO-MDSCs. In

co-cultures with MO-MDSCs, IFN- γ production was highly increased compared to NK cells cultured alone (Figure 6.19). MO-MDSCs alone did not produce significant levels of IFN- γ . In summary our data indicated that tumor-infiltrating MO-MDSCs are potent inducers of IFN- γ production by NK cells.

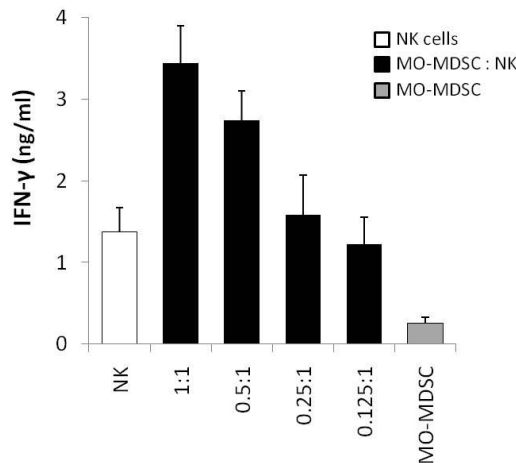


Figure 6.19: Tumor-infiltrating MO-MDSCs induce IFN- γ production by NK cells

C57BL/6 mice were subcutaneously injected with 10^6 RMA-S cells. On day 19 after tumor cell inoculation tumor-infiltrating MO-MDSC were purified and co-cultured with naïve NK cells in the presence of IL-12. Supernatants were harvested after 24 h and IFN- γ amounts were determined by ELISA. Data show mean of triplicate cultures \pm SD.

6.4 TLR-4 signaling in tumor-infiltrating MDSC subsets

As shown in Figure 6.10, gene expression profiling and flow cytometric analysis of blood and tumor-infiltrating MDSC subpopulations revealed profound changes of CD14 on the transcriptional as well as protein level. In addition, upregulation of TLR-4 was detected (Figure 6.11). Up to date, there are various ligands known to activate TLR-4 signaling, e.g. LPS [134], S100A8/A9 [135], and SAA3 [136]. To investigate the role of TLR-4 signaling in tumor-infiltrating MDSCs, we analyzed the effect of LPS stimulation *in vitro*.

Recently, Hamerman *et al.* demonstrated that murine peritoneal macrophages stimulated with LPS upregulated NKG2D ligands. We examined whether LPS stimulation of different MDSC subsets induced the expression of Rae-1. Blood and tumor MDSC subsets from RMA-S tumor-bearing mice were activated *in vitro* with LPS and after 24 h the cells were stained for Rae-1 surface expression. While low levels of Rae-1 were seen on unstimulated MO-MDSCs, an increase in staining was detected on LPS-activated MO-MDSCs from the tumor (Figure 6.20A). Rae-1 levels on MO-MDSCs from blood remained unchanged, whereas no effect was observed on PMN-MDSC subsets (data not shown). To test whether the induction of Rae-1 is associated with increased production of pro-inflammatory cytokines, supernatants of cultured tumor-infiltrating MDSCs were analyzed the presence of the pro-inflammatory cytokines/chemokines TNF- α , CXCL2 and IL-10. As shown in Figure 6.20B, LPS stimulation of tumor-infiltrating MDSCs resulted in increased production of TNF- α and CXCL2 and slight induction of IL-10. In summary, triggering of TLR-4 signaling in tumor-infiltrating MO-MDSCs led to the upregulation of Rae-1 expression and increased production of pro-inflammatory factors that might contribute to the modulation of innate immune responses, including NK cells.

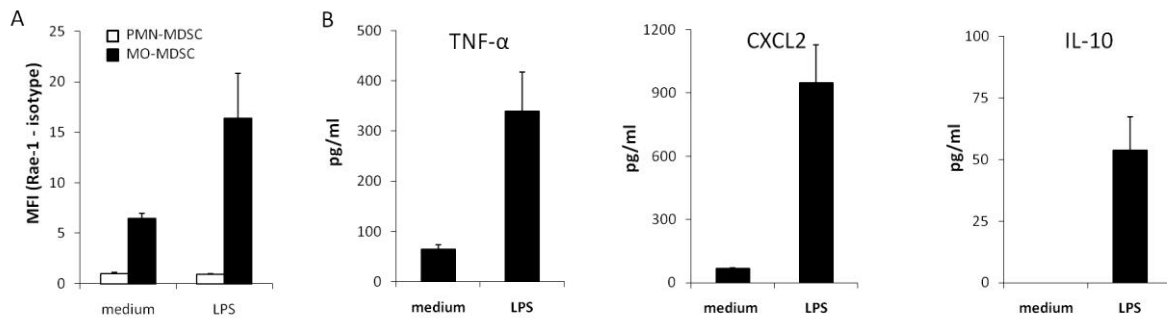


Figure 6.20: Tumor-infiltrating MO-MDSCs upregulate Rae-1 expression and production of pro-inflammatory molecules upon LPS stimulation

C57BL/6 mice were subcutaneously injected with 10^6 RMA-S cells. On day 19 after tumor cell inoculation Gr-1 enriched MDSCs from the tumor were stimulated for 24h with 200 $\mu\text{g/ml}$ LPS. **A)** Rae-1 surface expression on PMN-MDSC and MO-MDSC was determined by flow cytometry. **B)** Supernatants of tumor-infiltrating MDSCs were harvested and cytokine/chemokine amounts were measured by ELISA. Data are representative of three experiments. Values represent the mean \pm SD.

To test whether ligands other than LPS trigger TLR-4 signaling to upregulate Rae-1 expression, tumor-infiltrating MO-MDSCs were stimulated with S100A8, S100A9 and S100A8/A9 proteins. As shown in Figure 6.21, S100 proteins were more potent inducers of Rae-1 upregulation than LPS.

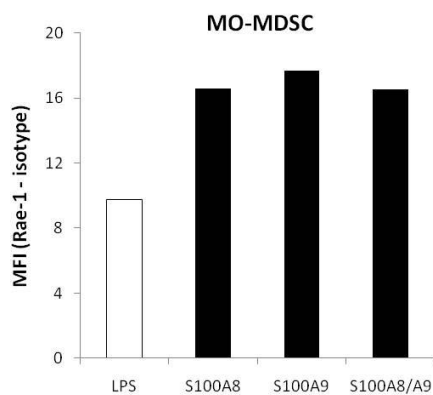


Figure 6.21: Tumor-infiltrating MO-MDSCs upregulate Rae-1 expression upon stimulation with S100 proteins

C57BL/6 mice were subcutaneously injected with 10^6 RMA-S cells. On day 19 after tumor cell inoculation Gr-1 enriched MDSCs from the tumor were stimulated for 24h with 200ng/ml LPS, 5 $\mu\text{g/ml}$ S100A8, S100A9 or the heterodimer S100A8/A9. Rae-1 surface expression on tumor-infiltrating MO-MDSC was determined by flow cytometry. Bars indicate the expression levels of the different groups containing a pool of three animals.

6.5 Tumor-infiltrating MO-MDSCs and their chemokine network

Chemokines levels determine chemoattraction of macrophages, neutrophils, and lymphocytes into tumor tissue. We demonstrated that the tumor-infiltrating MO-MDSC subset was a potent producer of certain chemokines. Among these, CCL3, CCL4 and CCL5 were the most abundant chemokines and they all share CCR5 as a common receptor. The role of CCR5 in cancer remains controversial. While CCR5 expression on tumor epithelia has been connected to tumorigenesis [137], some tumor therapies required a functional CCR5 signaling pathway [138]. Therefore, we investigated the impact of CCR5 and its ligands CCL3, CCL4 and CCL5 on RMA-S tumor progression using recombinant chemokines *in vivo* and CCR5 deficient mice.

6.5.1 Expression of the CCR5 receptor on immune cells

To evaluate the role of CCL3, CCL4 and CCL5 in chemotaxis, we studied the expression profile of their receptor CCR5 in tumor-bearing mice. Different immune cells from blood, spleen and tumor were stained for CCR5 surface expression to analyze, which cell populations might be recruited to the tumor site via CCR5. MDSCs and TAMs (defined as $CD11b^+F4/80^+Gr-1^-$) expressed no CCR5 in blood and spleen. However, when these cells infiltrated tumor tissue, CCR5 surface expression was detected (Figure 6.22). In addition, a subpopulation of Tregs in spleen expressed CCR5, whose expression was further increased in tumor-infiltrating Tregs. Splenic $CD8^+$ and $CD4^+$ effector T cells lacked CCR5 expression (data not shown). This finding suggested that Tregs might be preferentially recruited to the tumor by CCR5 ligands.

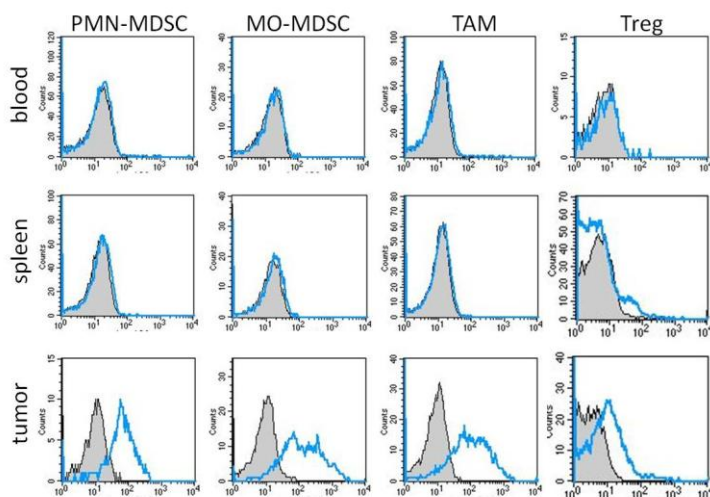


Figure 6.22: CCR5 expression by different immune cells.

C57BL/6 mice were subcutaneously injected with 10^6 RMA-S cells. On day 19 after tumor cell inoculation, MDSC subsets, TAMs and Tregs from blood, spleen and tumor were analyzed for CCR5 surface expression via flow cytometry. Histograms indicate the expression levels of the different experimental groups containing a pool of three animals. Data are representative of three experiments.

Cells are pre-gated as following: PMN-MDSCs: $Gr-1^+CD11b^+F4/80^-$; MO-MDSCs: $Gr-1^+CD11b^+F4/80^+$; TAMs: $CD11b^+F4/80^+Gr-1^-$; Tregs: $CD4^+Foxp3^+CD25^+$

6.5.2 Influence of exogenous CCR5 ligands on tumor progression

We investigated whether CCL3, CCL4 or CCL5 were able to chemoattract certain immune cells *in vivo* and thus potentially mediate increased infiltration of CCR5 expressing cells into the tumor. It was shown that these chemokines can recruit myeloid cells and Treg [139], [140]. Therefore, we injected recombinant CCL3, CCL4 or CCL5 together with RMA-S cells. Intra-tumoral chemokine injections were continued every third day and tumor growth and survival was assessed. We observed accelerated tumor growth (Figure 6.23A) and impaired survival (Figure 6.23B) of mice injected with CCL3, CCL4 or CCL5.

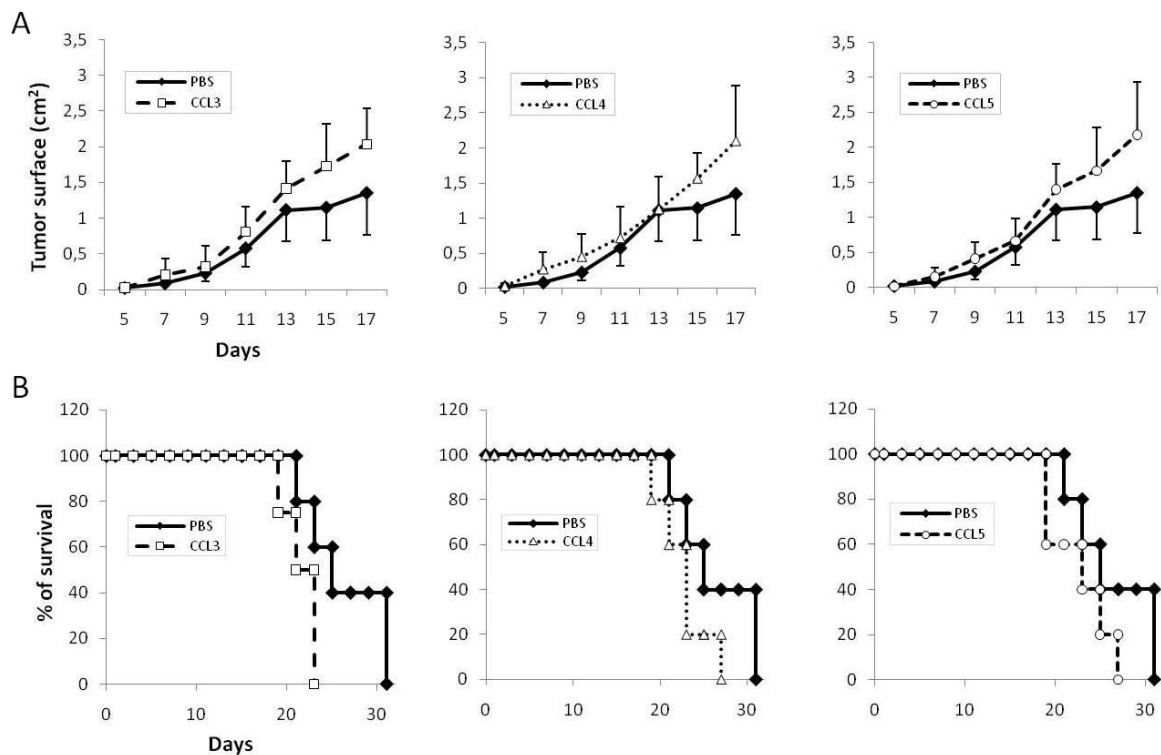


Figure 6.23: Acceleration of tumor growth and shortened survival mediated by recombinant CCR5 ligands

C57BL/6 mice (n=5) were subcutaneously injected with 10^6 RMA-S cells and intra-tumorally with 1 μ g recombinant CCL3, CCL4, CCL5 or PBS every third day. **A)** Tumor growth was monitored for 17 days. **B)** Survival was assessed for 31 days. Values represent the mean \pm SD of each group.

Next, we analyzed whether diverged levels of tumor infiltrates might cause these changes in tumor progression. C57BL/6 mice were injected with RMA-S cells and chemokines and the amount of tumor-infiltrating myeloid cells and T cells was determined. The distribution of PMN-MDSCs and TAMs among total tumor-infiltrating CD11b⁺ cells was not affected by chemokine injection. However, slight reduction of MO-MDSCs upon CCL3 and CCL4 injection was observed (Figure 6.24A). Moreover, CCL4 and CCL5 positively affected Treg accumulation resulting in decreased CD4/Treg and CD8/Treg ratios (Figure 6.24B). In summary, we concluded that intra-tumoral injection of CCL4 and CCL5 might accelerate tumor growth that correlated with increased levels of tumor-infiltrating Tregs.

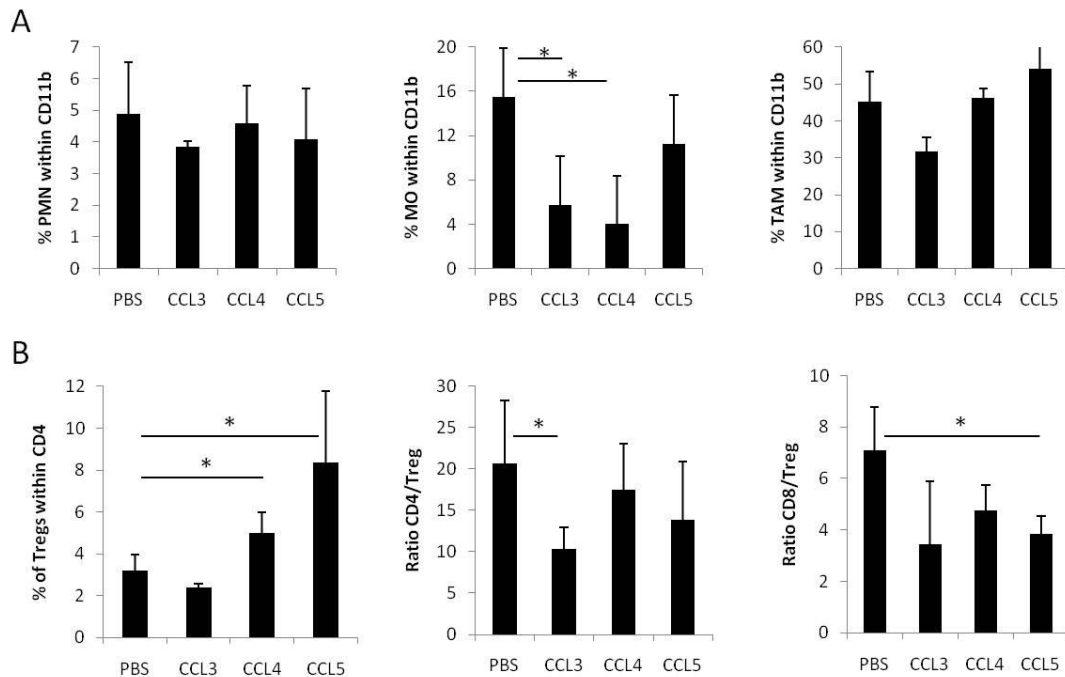


Figure 6.24: Distribution of tumor-infiltrating myeloid cells and Tregs upon chemokine injection

C57BL/6 mice (n=3) were subcutaneously injected with 10^6 RMA-S cells and intra-tumorally with 1 μ g recombinant CCL3, CCL4, CCL5 or PBS every third day. **A)** Percentage of myeloid cells was analyzed on day 13 after tumor cell inoculation. **B)** Percentage of Tregs, CD4/Treg and CD8/Treg ratios were assessed on day 13 after tumor cell inoculation. Values represent the mean \pm SD of each group. * $P < 0.05$

6.5.3 Influence of the CCR5 receptor on tumor progression

In the second approach, we sought to disrupt the CCR5-mediated chemotaxis by using CCR5 deficient mice. To investigate its impact on tumor progression, CCR5 knockout and wild type mice were injected with RMA-S cells and tumor growth and survival was monitored. We observed significant delay of tumor growth and prolonged survival in CCR5 deficient mice (Figure 6.25A). Analysis of tumor infiltrates on day 11 revealed increased levels of CD8⁺ and CD4⁺ T cells in CCR5 deficient mice, which was correlated with higher ratios of CD4/Treg and CD8/Treg (Figure 6.25B). Moreover, accumulation of TAMs was abrogated in CCR5 knockout mice compared to wild type mice (Figure 6.25C).

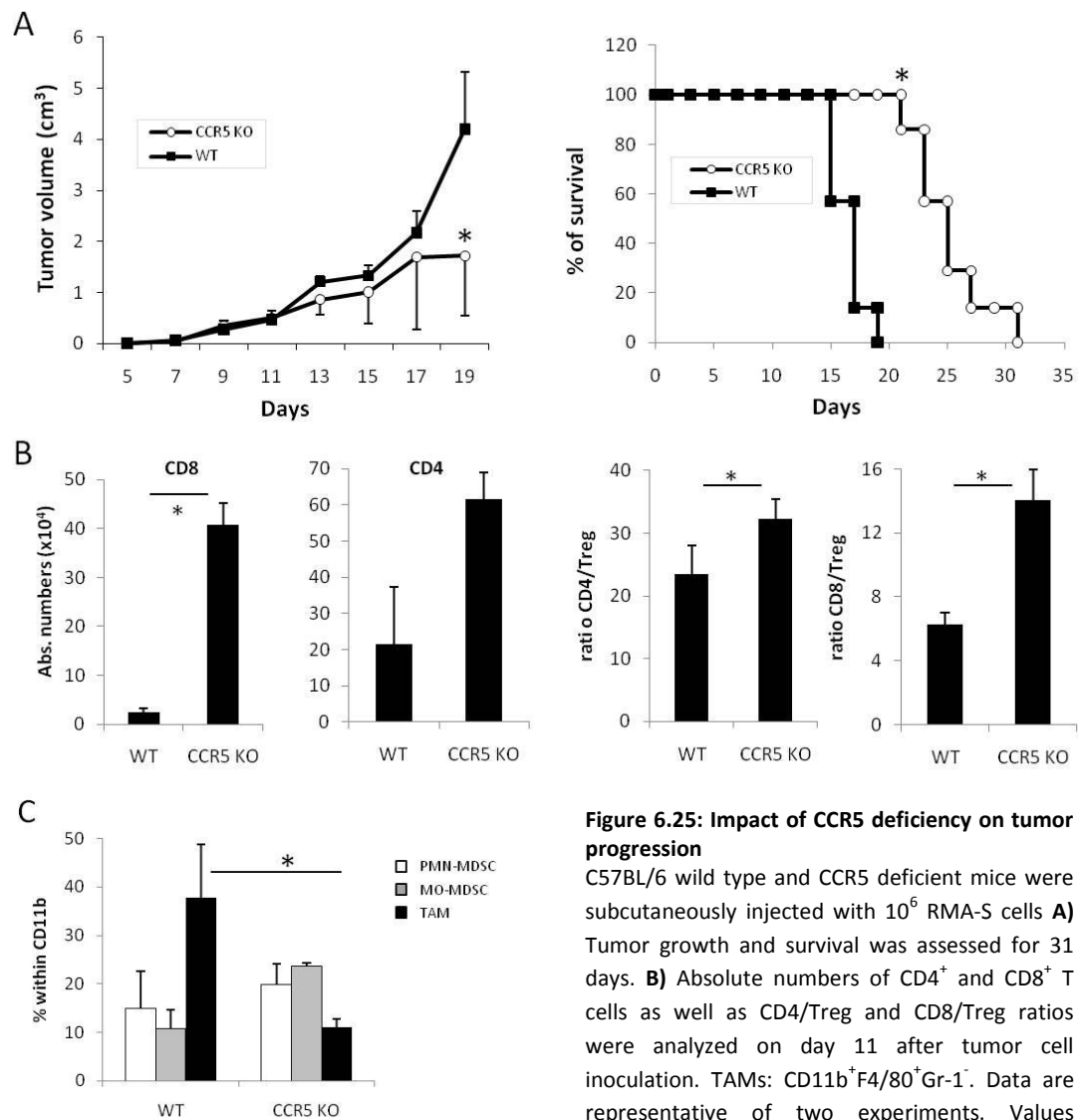


Figure 6.25: Impact of CCR5 deficiency on tumor progression

C57BL/6 wild type and CCR5 deficient mice were subcutaneously injected with 10^6 RMA-S cells **A**) Tumor growth and survival was assessed for 31 days. **B**) Absolute numbers of CD4⁺ and CD8⁺ T cells as well as CD4/Treg and CD8/Treg ratios were analyzed on day 11 after tumor cell inoculation. TAMs: CD11b⁺F4/80⁺Gr-1⁻. Data are representative of two experiments. Values represent the mean \pm SD of each group. * $P < 0.05$

6.6 Manipulation of MDSCs *in vivo*

Previously, we showed that tumor-infiltrating MO-MDSCs were potent producer of chemokines, resulting in increased level of tumor-infiltrating Tregs and reduced CD4/Treg and CD8/Treg ratios. To disrupt the CCR5-mediated chemotaxis, we aimed to manipulate MO-MDSCs *in vivo* in order to reduce chemokine levels in the tumor and thereby, improve anti-tumor immune responses. All-*trans* retinoic acid (ATRA) is a well known compound, which induces the differentiation of acute promyelocytic leukemia cells and has been successfully used in differentiation induction therapy in these patients [141], [142]. Recently, Kusmartsev and colleagues demonstrated that *in vivo* administration of ATRA reduced the amount of MDSCs in tumor-bearing mice by differentiating these cells into mature DCs, macrophages and granulocytes [107]. We implanted ATRA pellets subcutaneously into tumor-bearing mice to maintain its constant concentration in

the organism. As a control, mice were implanted with placebo pellets. Treatment with ATRA decreased the proportion of PMN- and MO-MDSCs in the tumor. Moreover, the percentage of CD11b⁺F4/80⁺Gr-1⁻ macrophages was significantly higher in ATRA-treated mice than in mice treated with placebo (Figure 6.26A). However, differentiation of MDSCs into macrophages did not result in delayed tumor growth (Figure 6.26B). To determine the chemokine levels of CCL3, CCL4 and CCL5 locally in the tumor tissue after ATRA treatment, tumor lysates were analyzed via ELISA. As shown in Figure 6.26C, the overall concentration of CCL3 was significantly reduced after ATRA treatment. However, no effect on CCL4 and CCL5 production was detected.

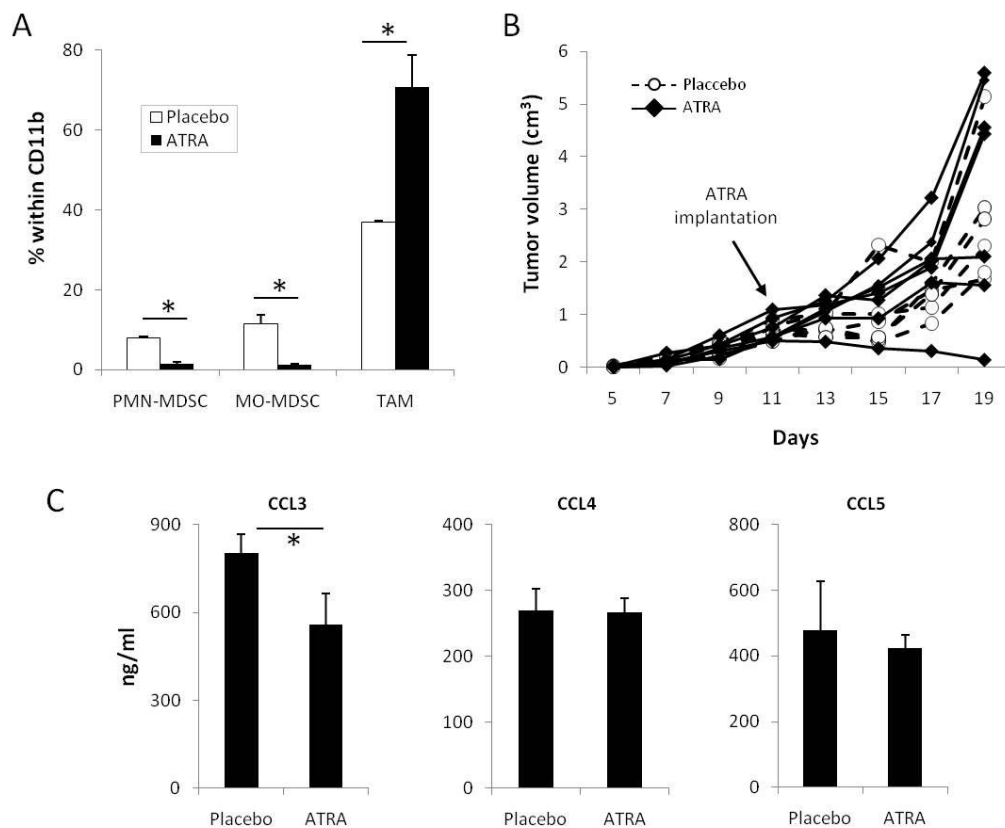


Figure 6.26: Differentiation of MDSCs *in vivo*

C57BL/6 mice (n=18) were subcutaneously injected with 10^6 RMA-S cells. 11 days (A+B) or 7 days (C) after tumor inoculation ATRA (5 mg) or placebo pellets (5 mg) were subcutaneously implanted **A)** Percentage of myeloid subsets was analyzed on day 19 after tumor cell inoculation. **B)** Tumor growth was monitored for 19 days. **C)** On day 19 tumor lysates were prepared and chemokine production was measured using ELISA. Data are representative of two (A, B) and one (C) experiments. Values represent the mean \pm SD of each group. * $P < 0.05$.

7 DISCUSSION

Established therapies currently used to treat cancer include surgery, local radiotherapy and chemotherapy. However, even when the primary tumor was initially removed, remaining micrometastases and cancer stem cells frequently lead to tumor relapse and therapeutic failure. Therefore, it became clear that is not sufficient to develop strategies only to eliminate cancer cells but also approaches are needed that stimulate anti-tumor immune responses. Dendritic cells pulsed with tumor antigens are broadly applied in cancer patients [143]. Adoptive cell therapy using autologous tumor-infiltrating T cells was an effective treatment for patients with metastatic melanoma [144]. However, a combination of immunotherapy and chemotherapy seems to be the most promising approach.

Researchers over the last decades observed that tumor-infiltrating cells play a dual role in cancer. They do not only suppress tumor growth by destroying cancer cells or inhibiting their outgrowth, they also promote tumor progression by inducing immune suppression. Understanding how these cells affect tumor development and progression is one of the most challenging questions in tumor immunology.

7.1 Tumor-infiltrating cells

Lymphocytes like T cells and NK cells were shown to infiltrate tumor tissues in mouse models and cancer patients [145], [146]. A high number of tumor-infiltrating lymphocytes is a useful prognostic marker in patients with melanoma [147], colorectal cancer [148] and pancreatic adenocarcinoma [149] and often correlates with an improved clinical outcome. Immune cells are involved in tumor immunosurveillance and elimination. *In vivo* studies revealed that mice deficient in NK or T cell function exhibit a more aggressive tumor growth and metastasis [150], [151]. Therefore, strategies resulting in increased infiltration of T cell and NK cells might be a promising approach in cancer immunotherapy.

Certain immune cells were shown to exhibit pro-tumoral features and thereby support tumor progression. These cells include Tregs, macrophages and MDSCs. They accumulate in blood and spleen, but are also found in the tumor tissue, where they are either induced by the tumor microenvironment or recruited by tumor-derived factors [30], [54]. Tregs inhibit anti-tumor immunity and promote tumor growth by suppressing host immune responses. Several studies reported elevated levels of Tregs in the tumor tissue including breast cancer [152], melanoma [153] and lymphoma [154]. Depletion of Tregs in many models led to the induction of anti-tumor immune responses [155]. In addition to Tregs, TAMs and MDSCs exhibit pro-tumoral features by suppressing effector functions of T cells and NK cells [69], [89]. Blocking their recruitment to the tumor tissue and abrogating their suppressive functions are approaches for immunotherapy that are currently under investigation (discussed in section 3.4.2 and 3.5.7). Further knowledge about the exact nature of immunosuppressive cell populations within the tumor microenvironment,

including their phenotypical and functional properties, might improve therapeutic strategies to overcome immune suppression within the tumor tissue.

In this study, we phenotypically and functionally characterized tumor-infiltrating MDSC subpopulations from RMA-S lymphoma. We showed that the monocytic subset within the tumor tissue exhibited at least three distinct features which might support tumor progression: (i) increased expression of the suppressive factors arginase-1 and iNOS, whose activities are connected with T cell suppression (ii) pro-inflammatory phenotype distinguished by elevated levels of CD14, TLR-4 and Dectin-2 that are known to promote tumor progression and (iii) production of the chemokines CCL3, CCL4 and CCL5 at the tumor site, which might support the recruitment of pro-tumoral effector cells.

7.2 Tumor-infiltrating MDSC subpopulations

Tumors use a variety of suppressive strategies to escape from immune responses. One of the common features of tumor progression is the dysregulation of myelopoiesis and the induction and the expansion of MDSCs. It is well established that MDSCs accumulate in bone marrow, blood and spleen of tumor-bearing mice and cancer patients and suppress T cell function [115], [156]. They comprise a heterogeneous population consisting of monocytes, macrophages, granulocytes and dendritic cells. Due to the heterogeneity of MDSCs no common marker has been described so far [157]. Movahedi *et al.* demonstrated that in mice splenic Gr-1⁺CD11b⁺MDSCs consisted of a Ly6G⁺SSC^{high} polymorphonuclear (PMN) and a Ly6G⁻SSC^{low} mononuclear (MO) fraction. MO-MDSCs express the macrophage marker F4/80 that was absent on the PMN-MDSC subset [64]. Since most studies had been focused on MDSCs that accumulate in spleen of different tumor models, we characterized the phenotype of discrete tumor-infiltrating MDSC subsets from the TAP2-deficient RMA-S lymphoma.

We demonstrated that MDSCs accumulated in blood, spleen and tumors. In concordance with the findings of Movahedi *et al.*, two major subsets of tumor-infiltrating MDSCs from RMA-S were identified [64]. Differential expression of Ly6G and Ly6C as well as different morphologies defined these two subsets as mononuclear (MO) and polymorphonuclear (PMN) MDSCs. Our experiments, addressing dynamics of these two subpopulations revealed a high turnover rate of MO-MDSCs in bone marrow, spleen and tumor and only low proliferation levels in blood (Figure 6.4). We assume that this population migrates from bone marrow through the blood stream and infiltrates into peripheral organs such as spleen and tumor, where they further proliferate. In our preliminary experiment, PMN-MDSC expanded neither in bone marrow or blood, nor in spleen and tumors, suggesting that these cells arise in situ from precursors other than Gr-1⁺CD11b⁺F4/80⁻ (Figure 6.4).

Our further characterizations by flow cytometry described MO-MDSCs by high expression of CD124 and CD115 and high levels of the adhesion molecules CD54, CD43 and CD31. CD54 is a glycoprotein that can be induced by IL-1 and TNF- α . It binds the integrins Mac-1 and LFA-1, which are expressed by activated leukocytes [158], and plays an important role in intercellular adhesion. Moreover, MO-MDSC exhibited high expression of several molecules involved in antigen presentation. Several studies demonstrated the ability of MDSCs to induce antigen-specific T cell tolerance in cancer. Upon antigen uptake, MDSCs migrate to peripheral lymphoid organs and present these antigens to T cells [159], [160]. Corzo *et al.* discovered functional differences in T cell suppression dependent on the organ infiltrated by MDSCs. MDSCs from peripheral lymphoid organs suppressed only antigen-specific CD8⁺ T cells, whereas tumor-infiltrating suppressed both antigen-specific and unspecific T cell activity due to high levels of the transcription factor HIF-1 α (hypoxia inducible factor 1 α) expression in tumor-infiltrating MDSCs [161]. Furthermore, Serafini *et al.* showed that MDSCs took up and processed tumor-associated antigens and thereby, induced Treg expansion [87]. In our study, tumor-infiltrating MO-MDSCs expressed high levels of MHC class I and II, CD40 and CD86, which increased expressions were confirmed in our microarray analysis. These findings suggest that the MO-MDSC subset might interact with certain T cell populations in an antigen specific manner. The functional outcome of such an interaction has to be investigated in future studies.

7.2.1 Genetic profile of tumor-infiltrating MDSC subsets

In addition to the analysis of surface markers that were previously described to be expressed by MDSCs [64], we performed a gene expression profile of blood and tumor-infiltrating MDSC subpopulations using whole genome microarrays. Functional classification of differently expressed targets between blood and tumor-infiltrating MDSCs revealed several genes, which were involved in distinct pathways. Compared to blood MO-MDSC, the tumor-infiltrating subset showed upregulations in the MAPK signaling pathway, including surface molecules like CD14 and downstream molecules such as Jun, Hras1, Raf1, and Akt2. It is known that triggering of TLR-4, the co-receptor of CD14, also activates different inflammatory responses via the transcription factor NF κ B. Once activated, NF κ B leads to the expression of several inflammatory mediators such as TNF- α , IL-6 and IL-1 β [162], [163]. We found IL-1 β to be upregulated at mRNA level, suggesting that the above mentioned pathways might be functional in MO-MDSCs and contribute to a pro-inflammatory environment within the tumor. Ostrand-Rosenberg and colleagues observed that MDSC accumulation in spleen and activation was driven by IL-1 β [120]. Mice inoculated with mammary carcinoma or fibrosarcoma cells secreting IL-1 β , developed significantly higher levels of Gr-1⁺CD11b⁺ MDSCs compared to mice inoculated with non-secreting cells. Our data suggest that MDSC might support their own accumulation at the tumor site by producing high levels of pro-inflammatory cytokines and thereby providing an autocrine feedback loop that sustains the accumulation and retention of MDSCs.

In addition to MAPK signaling, genes involved in T cell receptor signaling were differently regulated in tumor-infiltrating MDSCs, including CD3 ϵ , ZAP70, Itk and NFAT. CD3 molecules are

known to associate with the T cell receptor and transduce the TCR signal into the cell via phosphorylation of ITAMs, which subsequently activates the tyrosine kinase ZAP70 and the transcription factor NFAT [164]. Of importance, also CD3 δ and CD3 γ were upregulated at transcriptional level and we confirmed the surface expression of CD3 ϵ on MDSCs by flow cytometry (data not shown). It will be important to investigate, to which receptor (other than T cell receptor) these CD3 molecules might couple onto MDSCs. At least for CD3 ζ , it has been shown that it associates with several receptors expressed by NK cells [165], [166]. Whether MDSCs express CD3 molecules has not been investigated so far. Further analysis of the CD3 signaling pathway might reveal new functions of MDSCs and their contribution to the tumor progression.

The most striking observation of gene expression profiling was that the tumor-infiltrating MO-MDSC subset showed pronounced differences when compared to all other subsets including blood of naïve and tumor-bearing mice. 411 genes were found to be explicitly upregulated only in tumor-infiltrating MO-MDSCs. Briefly, three main features were further investigated. First, MO-MDSCs within the tumor displayed high levels of the suppressive enzyme arginase-1. Second, we observed an upregulation of several genes involved in pro-inflammatory signaling. And the third group comprised several chemokines, which were highly upregulated only in tumor-infiltrating MO-MDSCs. These findings will be discussed in the following sections.

7.2.2 Suppressive factors and their influence on immune cells

The role of MDSCs as suppressor cells that downregulate antitumor immunity has been well established by several studies. They are potent inhibitors of both antigen-specific and non-specific T cells activation. Both T cells subsets, CD4⁺ and CD8⁺ T cells, are defined as targets of suppression that requires cell-cell contact [118]. *In vivo* treatment of tumor-bearing mice with chemotherapeutic drugs, antibodies to Gr-1 or retinoic acid reduced the amount of MDSCs, reversed T cell suppression and delayed tumor growth [111], [167]. One of the aims of our project was to determine the interaction of tumor-infiltrating MDSC subsets with T cells. Microarray analysis revealed that the expression of arginase-1 was significantly upregulated in MO-MDSCs within the tumor compared to blood, and its enzymatic activity was confirmed at protein level (Figure 6.8). In addition, the same subset displayed high iNOS activity, which was increased by three fold compared to the MO-MDSC subset from blood (Figure 6.9A). However, our present study showed that tumor-infiltrating MDSC subsets did not exert T cell suppression but rather supported their proliferation (Figure 6.18). At the same time, we were unable to reproduce the previous results of Nausch *et al.* demonstrating that splenic MO-MDSCs from RMA-S tumor-bearing mice diminished T cell proliferation [91]. In our study, MDSCs isolated from blood or spleen from RMA-S tumor bearing mice had no effect on T cell activation or moderately enhanced T cell proliferation. Similar results were repeatedly observed and the effect was dose-dependent. Several possibilities have been considered and are currently under investigation:

(i) Several studies demonstrated that both human and murine MDSCs induced the development, recruitment and expansion of Tregs. Dependent on the tumor type, Treg induction was either TGF- β - and IL-10-dependent [68], mediated via arginase-1 [87] or driven by CD40 expression on MDSCs [103]. In our study, high arginase-1 activity as well as expression of CD40 was detected in tumor-infiltrating MO-MDSCs. It is therefore possible that tumor-infiltrating MO-MDSCs support the proliferation of Tregs in the tumor tissue and use the same mechanisms to support T cell proliferation in our *in vitro* system. The effects observed with splenic and blood MDSCs were much less pronounced. Discrepancy with the previous report might be the consequence of differential induction of Tregs in MDSC co-culture experiments. Further experiments need to be performed to analyze whether Treg induction and expansion play a role in T cell suppression mediated by splenic and tumor-infiltrating MDSC subsets.

(ii) An alternative possibility is that MDSCs, once infiltrated into the tumor tissue, change their suppressive potential due to the tumor microenvironment. The study from Haverkamp *et al.* analyzed the influence of tissue-specific inflammatory response on MDSC-mediated T cell suppression [168]. These data demonstrated that the regulation of T cell function by MDSCs was restricted *in vivo* to the site of ongoing immune responses, while MDSCs from peripheral tissues were not suppressive without activation of iNOS by exposure to IFN- γ . The main producers of IFN- γ are NK cells, activated T cells and macrophages polarized towards M1 phenotype. It is, however, well established that tumor microenvironment negatively affects the effector functions of all three cell subsets, including IFN- γ secretion [30]. As discussed in section 4.3, TAMs resemble the M2 phenotype, which mainly produces IL-10 and IL-1 receptor antagonists while inhibiting pro-inflammatory responses. It is therefore possible that MDSCs derived from the tumor tissue were not exposed to pro-inflammatory stimuli and therefore failed to suppress T cells *in vitro*. Whether the exogenous stimuli might reactivate their suppressive function needs to be further analyzed. Of note, Gabrilovich and colleagues reported an increased suppressive potential of tumor-infiltrating MDSCs in the EL-4 lymphoma tumor generated as ascites [161]. It is important to analyze whether the inflammatory microenvironment of ascites might be different compared to established solid tumor and thus favor the MDSC suppressive phenotype.

(iii) Ribechini *et al.* reported that the α -Gr-1 mAb transmitted signals via STAT-1, STAT-3 and STAT-5 into bone marrow cells *in vitro* and remained attached to the cell surface for at least four days [110]. In addition, α -Gr-1 mAb injection *in vivo* induced signals leading to myelopoiesis and reduced MDSC suppressive activity. For the isolation of MDSCs from tumor bearing mice we have used the α -Gr-1 mAb and the antibody was still detectable on the surface of MDSCs after co-culture with T cells. Therefore, it is possible that the α -Gr-1 mAb induced differentiation of isolated tumor-infiltrating MDSCs *in vitro* and subsequently abrogate the suppressive potential of these cells. However, an alternative isolation procedure without Gr-1 engagement led to similar results, thus excluding its signaling effect on MDSCs.

In our previous report, we described that MO-MDSCs from blood expressed Rae-1 and induced IFN- γ release by NK cells. IFN- γ production in co-culture of MO-MDSCs and NK cells was partially blocked by addition of an α -NKG2D mAb [91]. As in blood MO-MDSCs, we detected high levels of the NKG2D ligand Rae-1, which was exclusively expressed on the monocytic subpopulation. In addition, we showed that tumor-infiltrating MO-MDSCs also induced IFN- γ release by NK cells. Due to high expression of Rae-1 on the monocytic population in the tumor, an interaction with NKG2D on NK cells might also lead to IFN- γ induction. Rae-1/NKG2D interaction may delineate a mechanism by which MO-MDSCs and NK cells directly interact. It has been shown that IFN- γ is essential for activating the suppressive function of MDSCs and blocking of IFN- γ reversed the T cell suppression mediated by MO-MDSCs [64]. Therefore, elevated IFN- γ production by NK cells in co-culture with MO-MDSCs might further increase the suppressive potential on T cell responses.

Whether human MDSCs express NKG2D ligands, has not been reported so far. Compared to murine MDSCs, MDSCs in humans are still poorly defined. Due to the lack of a Gr-1 homologue, several combinations of surface molecules have been used to describe MDSCs in cancer patients. In melanoma patients, the monocytic fraction, which express CD14⁺CD11b⁺HLA-DR⁺CD124⁺, was identified to mediate immune suppression [72],[75]. Nowbakht et al. reported that CD14⁺ immature human myeloid cells expressed NKG2D ligands [169]. Since MDSCs are comprised of different myeloid cell populations, MDSCs from melanoma patients might express potential ligands for NKG2D, suggesting a possibility for MDSC – NK cell cross-talk also in humans.

In addition to NK cells, CD8⁺ T cells and $\gamma\delta$ T cells express the NKG2D receptor [170]. Therefore, interactions with Rae-1 expressed on MO-MDSCs might not be restricted to NK cells. Future studies with NKG2D expressing immune cells will further investigate the influence of MDSCs on activation on distinct immune responses. *Vice versa*, MO-MDSCs might also suppress immune responses via Rae-1. Shedding of NKG2D ligands as soluble molecules has been studied extensively. Tumor cells evade NKG2D surveillance by releasing matrix metalloproteinases (MMPs) that cleave NKG2D ligands from the cell surface resulting in downmodulation of the NKG2D receptor on NK cells and inhibition of anti-tumor immune responses. It has been shown that the presence of soluble NKG2D ligands in sera was correlated with compromised immune responses and accelerated tumor progression [171], [172]. Of interest, several members of the MMP family were upregulated on transcriptional levels in tumor-infiltrating MO-MDSCs. Microarray analysis revealed that MMP12, MMP13 and MMP14 were significantly increased (data not shown). Therefore, it might be possible that tumor-infiltrating MO-MDSCs suppress immune responses via shedding of Rae-1.

7.2.3 Pro-inflammatory phenotype

It is well established that chronic inflammation increases cancer risk and promotes tumor progression by causing genetic alterations, fostering neoangiogenesis, altering responses to growth signals and inducing cell proliferation accompanied by altered cell recruitment [173].

Recently it became clear, that MDSCs are induced by tumor-secreted and host-secreted molecules, many of which are pro-inflammatory factors. In addition to responding to pro-inflammatory signals, MDSCs contribute to the inflammatory tumor microenvironment by secreting pro-inflammatory molecules themselves. By analysis of the transcription profile of tumor-infiltrating MO-MDSCs we observed an upregulation of CD14 and TLR-4 as well as potential target genes of this pathway (Figure 6.10 and 6.11; Table 6.3). To investigate whether TLR-4 signaling on MDSCs might contribute to an inflammatory environment, tumor-infiltrating MDSC subsets were stimulated with LPS. In addition to high levels of TNF- α and CXCL2 secretion, we detected an increased expression of Rae-1 upon stimulation. The exact mechanism leading to the upregulation of Rae-1 on MDSCs is unknown. Hamerman *et al.* reported that several pathogens triggered TLR/MyD88 signaling resulting in upregulation of Rae-1 [134].

Recently, S100A8 and S100A9, two members of the S100 protein family, have been identified as important DAMPs (damage-associated molecular pattern) released by activated phagocytes and recognized by TLR-4 on monocytes [135]. Several studies confirmed an implication of S100A8/A9 in tumor biology. In mice, these molecules promote tumor growth as well as metastasis. Mice deficient in S100A9 exhibited reduced growth and lacked the accumulation of MDSCs in lymphomas and sarcomas. Furthermore, upregulation of S100A8/A9 was observed in splenocytes from tumor-bearing mice and was restricted to the Gr-1⁺ population [81]. Of note, we detected increased levels of S100A8/A9 in tumor-infiltrating MDSCs on transcriptional level (data not shown). Secretion of S100A8/A9 by MDSCs and binding to TLR-4 on MDSCs indicate a potential autocrine effect. Sinha *et al.* observed that antibody treatment of mice, which block the S100A8/A9-binding sites on MDSCs, reduced MDSC recruitment and accumulation as well as S100A8/A9 serum levels [82]. However, the relative contribution of extracellular and intracellular effects of S100 proteins for MDSC-mediated immune suppression remains elusive. In our studies, we discovered that *in vitro* treatment of tumor-infiltrating MO-MDSCs with S100 proteins induced the upregulation of Rae-1, which was more potent than LPS stimulation itself (Figure 6.21). Future experiments with TLR-4 deficient MDSCs will clarify whether this induction results from TLR-4 triggering. Several reports speculated about the existence of more than one S100A8/A9 receptor. It has been assumed that the molecules CD36 and RAGE (receptor of advanced glycation end-products) might be two additional receptors for S100A8/A9 [174-175].

Whether other TLR-4 ligands are involved in Rae-1 regulation on tumor-infiltrating MO-MDSCs is currently under investigation. Hiratsuka *et al.* identified SAA3 as an endogenous ligand of TLR-4. In their study, SAA3 induced chemotaxis of tumor cells and phagocytes and was an important downstream target of S100A8/A9. They concluded that S100A8/A9, SAA3 and TLR-4 might represent a paracrine positive feedback cascade involved in inflammatory responses [136]. Recently, it has been shown that the interaction of high mobility group box 1 protein (HMGB1) released from dying tumor cells triggered TLR-4 on DCs, which was required for the cross-presentation of tumor antigens and the promotion of tumor specific cytotoxic T-cell responses [176]. Therefore, HMGB1 might be another TLR-4 ligand leading to Rae-1 induction.

In addition to TLR-4 and CD14, another receptor, Dectin-2, involved in inflammatory responses was detected on tumor-infiltrating MDSCs. While Dectin-2 was only slightly expressed on blood MDSCs, increased levels were displayed on tumor-infiltrating MDSCs from RMA-S tumor-bearing mice. Dectin-2 belongs to the Dectin-2 family of C-type lectins, which is comprised of Dectin-2, DCIR (dendritic cell immunoreceptor), DCAR (dendritic cell immunostimulating receptor), BDCA-2 (blood dendritic cell antigen 2), Mincle and Clecsf8. Dectin-2 recognizes zymosan, numerous pathogens and mannose and its triggering leads to the activation of the transcription factor NF κ B and the production of TNF- α [177]. So far, the role of Dectin-2 in the tumor microenvironment is unclear. Whether potential ligands of Dectin-2 can be found within the tumor environment will be investigated. It is possible that Dectin-2 binds necrotic particles released from tumor cells, which has been discovered for its family member Mincle. Yamasaki et al. proposed in their study that Mincle recognized SAP130, a soluble protein released from necrotic cells, which resulted in cytokine production by macrophages and subsequent neutrophil infiltration into the tissue [178]. Of interest, elevated gene expression of Mincle and Clecsf8 was also detected in tumor-infiltrating MO-MDSCs in our microarray study (data not shown).

7.2.4 Chemokine-mediated migration

Among different factors that influence tumor progression and metastasis, a major focus in our study had been put on chemokines and their receptors. Chemokines play a dual role in cancer: on the one hand they possess promalignant potential, on the other hand some chemokines were found to act anti-tumorigenic. However, some chemokines exert distinct roles under different conditions. The effect of each specific chemokine in tumorigenesis depends to a large extent on the tumor type and the tumor model [179], [180], [181].

In our microarray experiment, we observed that tumor-infiltrating MO-MDSCs exhibited high transcript levels of the chemokines CCL3, CCL4, CXCL2, CXCL9, CCL7 and CCL24 compared to the other subsets from blood and tumor. Bioplex analysis revealed that most of these changes were also present at protein levels (Figure 6.16). The most highly induced chemokines, produced by tumor-infiltrating MO-MDSCs were CCL3, CCL4 and CCL5. The latter was additionally included in our study, since all three chemokines bind the same receptor, CCR5.

CCL3 (MIP-1 α) and CCL4 (MIP-1 β) belong to the macrophage inflammatory protein (MIP) group of the CC chemokine subfamily. Despite their structural similarities, CCL3 and CCL4 show diverging signaling capacities. CCL3 mRNA is expressed at low levels in resting monocytes and macrophages, but increased upon stimulation with LPS, IL-1 β or IFN- γ [182], [183]. As previously discussed LPS, IL-1 β and IFN- γ played an important role in the regulation of MO-MDSCs. Therefore it might be possible that these molecules and their signaling pathways are involved in CCL3 regulation. Moreover, secretion of CCL3 is known to be enhanced during monocyte-endothelial cell interaction, which was ICAM-1-mediated [184]. CCL3 has been found to reversibly inhibit the proliferation of certain murine hematopoietic stem cells *in vitro* as well as *in vivo*. This effect was dependent on the developmental stage of the progenitor cells and the cytokines used as growth

stimulators [185]. Like CCL3, CCL4 is produced by monocytes in high amounts upon stimulation with LPS or IL-7 [186] and it acts as the chemoattractant mainly for Tregs and monocytes [187]. CCL5 (RANTES) attracts T cells, granulocytes, monocytes and macrophages (in particular TAMs: see section 3.4) and plays an important role in recruiting leukocytes to inflammatory sites. Tan *et al.* observed that Tregs were recruited by CCL5 in a murine model of pancreatic cancer [140]. In melanoma and in papillary thyroid carcinoma, increased CCL5 levels resulted in high infiltration of CD8⁺ T cells [188] and DCs [189], however, their prognostic value remained unclear. In addition to its chemoattracting potential, CCL5 also acts as a regulatory molecule by inducing proliferation and activation of NK cells to form so called CC chemokine-activated killer cells (CHAK) [190].

All three chemokines share the chemokine receptor CCR5 as common receptor. It is known that CCR5 can be expressed on monocytes, macrophages, activated T cells and NK cells mainly under inflammatory conditions [191]. In our RMA-S lymphoma model, CCR5 expression was observed on splenic and tumor-infiltrating Tregs as well as on tumor-infiltrating MDSCs. No expression was detected on immune cells in the blood (Figure 6.22). Of interest, CD4⁺ and CD8⁺ T cells expressed CCR5 only when infiltrated into the tumor tissue (data not shown). Therefore, we hypothesized that Tregs might be recruited via CCR5 from the periphery to the tumor. To confirm our hypothesis, the recombinant chemokines CCL3, CCL4 or CCL5 were intratumorally injected into RMA-S tumor-bearing mice. Analysis of the tumor infiltrates revealed higher levels of Tregs when CCL4 or CCL5 was injected. Moreover, the ratio of CD4/Treg and CD8/Treg was reduced in chemokine-injected mice, suggesting that Tregs might be preferentially recruited to the tumor site via CCL4 and CCL5. Repeated injection of chemokines resulted in accelerated tumor growth and shortened survival compared to PBS injected mice. Recently, Li *et al.* reported that Treg depletion resulted in complete regression of large established tumors. The depletion induced activation of tumor-specific CD8⁺ T cell and enhanced infiltration of these cells into the tumor [192]. Galani *et al.* demonstrated that Treg depletion in RMA-S tumor bearing mice led to tumor rejection, which was dependent on T cells, NK cells and IFN- γ [193]. Therefore, it might be possible that in our RMA-S tumor model increased levels of Tregs upon chemokine injection suppress anti-tumor immune responses resulting in accelerated tumor growth. Since CCL3 and CCL5 are chemokines that bind to several receptors with different affinities (CCL3 binds CCR1 and CCR5; CCL5 binds CCR1, CCR3 and CCR5), it has to be considered that other immune cells might be additionally recruited via CCR5-independent mechanisms.

7.2.5 The role of CCR5 in tumor progression

The role of CCR5 in cancer remains controversial. While CCR5 expression on tumor epithelia had been connected to tumorigenesis [137], some tumor therapies required a functional CCR5 signaling pathway [138]. Whether our RMA-S cell line express CCR5 has to be analyzed. To investigate the role of CCR5 in our model, we took advantage of these mice. Tumor inoculation resulted in reduced tumor burden and prolonged survival of CCR5 deficient mice (Figure 6.25A/B), which correlated with an increased accumulation of CD4⁺ and CD8⁺ T cells compared to wild type mice. Of note, tumor-infiltrating CD8⁺ T cells were shown to play an important role in the control

of RMA-S tumor progression (I. Galani, unpublished data). Molon *et al.* reported that binding of CCL3 and CCL4 to CCR5 on T cells reduced the T cell responsiveness to other chemokines [194]. It might be possible that due to the absence of CCR5, T cells from knockout mice express a different chemokine receptor repertoire or respond differently to other chemokines. Their effector potential in anti-tumor immunity remains to be investigated.

Whether human MDSCs secrete CCR5 ligands and how these chemokines influence tumorigenesis has not been reported. So far, production of CCL3, CCL4 and CCL5 was pinpointed to tumor cells of multiple myeloma [195], breast cancer [196], melanoma [197] and gastric cancer [198]. In addition to CCR5 expression on human memory T cells and NK cells, CCR5 was also expressed on CD34⁺ hematopoietic progenitor cells [199]. Since human MDSCs are comprised of different myeloid progenitors expressing CD34⁺, it might be interesting to see if human MDSCs express CCR5 and if they could be recruited via CCR5 receptors.

7.3 Therapeutic implications

Since no marker is known, which is exclusively expressed on MDSCs, tools to specifically eliminate MDSCs are lacking. As discussed in section 3.5.7, several approaches have been made to either mature MDSCs by differentiating them into macrophages and dendritic cells, reduce their accumulation or inhibit their suppressive function. Many of these strategies were used in combination to achieve more effective cancer therapies [118], [200]. In our study, all-*trans* retinoic acid (ATRA) was used to differentiate MDSCs and thereby reduce their potential to secrete chemokines. Kusmartsev *et al.* showed that *in vivo* administration of ATRA did not only reduce the amount of MDSCs but also increase the level of mature cells, including macrophages, dendritic cells and granulocytes. Combination of ATRA and DC vaccine significantly prolonged the survival rate and reduced tumor growth in the DA3 mouse model of mammary carcinoma [107].

We implanted ATRA or placebo pellets into RMA-S tumor-bearing mice to assess the effect on MDSC differentiation and tumor growth. Eight days after implantation, ATRA efficiently differentiated MDSCs into macrophages. However, no therapeutic effect on tumor burden was observed (Figure 6.26A/B). This observation might be caused by increased levels of macrophages within the tumor tissue detected upon ATRA treatment. The generated macrophages might function as tumor-associated macrophages, thereby supporting tumor progression. These findings are in concordance with previous studies that ATRA did not directly inhibit the growth of solid tumors and combination therapies were necessary [200].

To investigate the role of chemokine secretion by MDSCs, tumor lysates of ATRA- and placebo-implanted mice were analyzed. While ATRA treatment significantly reduced the overall secretion of CCL3 in the tumor tissue, no effect was seen for CCL4 and CCL5 production. We assume that due to differentiation of MDSCs, matured macrophages generated by ATRA treatment, might be

an additional producer of these chemokines. Our previous Bioplex analysis showed that TAMs were also potential chemokine producers within the tumor (Figure 6.16). Therefore, a combination therapy should be considered, to first reduce the amount of MDSCs (like ATRA), and second to decrease the level of differentiated macrophages at the tumor site. Using either CpG, the ligand for TLR9, which shifts TAMs towards M1 phenotype [57], or clodronate to deplete macrophages [201], might be a promising strategy to reduce both MDSC and macrophage levels in the tumor tissue. This combination might efficiently decrease the chemokine level and subsequently enhance anti-tumor immune responses.

7.4 Concluding remarks

Myeloid-derived suppressor cells play a crucial role in the cellular network that regulates immune responses in cancer, inflammation and in other pathological conditions. One of the most important hallmarks of MDSCs is the morphological, phenotypic and functional heterogeneity. Therefore, the roles of specific MDSC subsets in mediating T cell suppression and the molecular mechanisms for their accumulation need to be elucidated. In this study we discovered new factors, which might be involved in Treg-mediated T cell suppression. We demonstrated that tumor-infiltrating MO-MDSCs secreted high levels of the chemokines CCL3, CCL4 and CCL5 that were able to chemoattract CCR5⁺ regulatory T cells to the tumor site and change the Treg/T cell ratio. In summary, we defined a new regulatory role of MDSCs in recruiting Tregs, which might be clinically relevant in developing novel immunotherapeutic strategies for cancer patients.

8 REFERENCES

1. Kawai, T. and S. Akira, *The role of pattern-recognition receptors in innate immunity: update on Toll-like receptors*. Nat Immunol, 2010. **11**(5): p. 373-84.
2. McBlane, J.F., et al., *Cleavage at a V(D)J recombination signal requires only RAG1 and RAG2 proteins and occurs in two steps*. Cell, 1995. **83**(3): p. 387-95.
3. Burnet, M., *Cancer; a biological approach. I. The processes of control*. Br Med J, 1957. **1**(5022): p. 779-86.
4. Swann, J.B. and M.J. Smyth, *Immune surveillance of tumors*. J Clin Invest, 2007. **117**(5): p. 1137-46.
5. Dunn, G.P., et al., *Cancer immunoediting: from immunosurveillance to tumor escape*. Nat Immunol, 2002. **3**(11): p. 991-8.
6. Dunn, G.P., L.J. Old, and R.D. Schreiber, *The three Es of cancer immunoediting*. Annu Rev Immunol, 2004. **22**: p. 329-60.
7. Hanahan, D. and R.A. Weinberg, *The hallmarks of cancer*. Cell, 2000. **100**(1): p. 57-70.
8. Pawelec, G., J. Zeuthen, and R. Kiessling, *Escape from host-antitumor immunity*. Crit Rev Oncog, 1997. **8**(2-3): p. 111-41.
9. Shankaran, V., et al., *IFN γ and lymphocytes prevent primary tumour development and shape tumour immunogenicity*. Nature, 2001. **410**(6832): p. 1107-11.
10. Smyth, M.J., et al., *NKG2D function protects the host from tumor initiation*. J Exp Med, 2005. **202**(5): p. 583-8.
11. Smyth, M.J., et al., *NKT cells - conductors of tumor immunity?* Curr Opin Immunol, 2002. **14**(2): p. 165-71.
12. Sallusto, F., C.R. Mackay, and A. Lanzavecchia, *The role of chemokine receptors in primary, effector, and memory immune responses*. Annu Rev Immunol, 2000. **18**: p. 593-620.
13. Smyth, M.J., G.P. Dunn, and R.D. Schreiber, *Cancer immunosurveillance and immunoediting: the roles of immunity in suppressing tumor development and shaping tumor immunogenicity*. Adv Immunol, 2006. **90**: p. 1-50.
14. Marincola, F.M., et al., *Escape of human solid tumors from T-cell recognition: molecular mechanisms and functional significance*. Adv Immunol, 2000. **74**: p. 181-273.
15. Seliger, B., M.J. Maeurer, and S. Ferrone, *Antigen-processing machinery breakdown and tumor growth*. Immunol Today, 2000. **21**(9): p. 455-64.
16. Spiotto, M.T., D.A. Rowley, and H. Schreiber, *Bystander elimination of antigen loss variants in established tumors*. Nat Med, 2004. **10**(3): p. 294-8.
17. Gajewski, T.F., et al., *Immune resistance orchestrated by the tumor microenvironment*. Immunol Rev, 2006. **213**: p. 131-45.
18. Kim, R., M. Emi, and K. Tanabe, *Cancer cell immune escape and tumor progression by exploitation of anti-inflammatory and pro-inflammatory responses*. Cancer Biol Ther, 2005. **4**(9): p. 924-33.
19. Gabrilovich, D., et al., *Vascular endothelial growth factor inhibits the development of dendritic cells and dramatically affects the differentiation of multiple hematopoietic lineages in vivo*. Blood, 1998. **92**(11): p. 4150-66.
20. Groh, V., et al., *Tumour-derived soluble MIC ligands impair expression of NKG2D and T-cell activation*. Nature, 2002. **419**(6908): p. 734-8.
21. Sica, A., et al., *Macrophage polarization in tumour progression*. Semin Cancer Biol, 2008. **18**(5): p. 349-55.

22. Solinas, G., et al., *Tumor-associated macrophages (TAM) as major players of the cancer-related inflammation*. J Leukoc Biol, 2009. **86**(5): p. 1065-73.
23. Mantovani, A., et al., *Macrophage polarization: tumor-associated macrophages as a paradigm for polarized M2 mononuclear phagocytes*. Trends Immunol, 2002. **23**(11): p. 549-55.
24. Biswas, S.K. and A. Mantovani, *Macrophage plasticity and interaction with lymphocyte subsets: cancer as a paradigm*. Nat Immunol, 2010. **11**(10): p. 889-96.
25. Allavena, P., et al., *The inflammatory micro-environment in tumor progression: the role of tumor-associated macrophages*. Crit Rev Oncol Hematol, 2008. **66**(1): p. 1-9.
26. Mantovani, A., A. Sica, and M. Locati, *Macrophage polarization comes of age*. Immunity, 2005. **23**(4): p. 344-6.
27. Geissmann, F., S. Jung, and D.R. Littman, *Blood monocytes consist of two principal subsets with distinct migratory properties*. Immunity, 2003. **19**(1): p. 71-82.
28. Hu, X., et al., *Crosstalk among Jak-STAT, Toll-like receptor, and ITAM-dependent pathways in macrophage activation*. J Leukoc Biol, 2007. **82**(2): p. 237-43.
29. Gordon, S. and P.R. Taylor, *Monocyte and macrophage heterogeneity*. Nat Rev Immunol, 2005. **5**(12): p. 953-64.
30. Qian, B.Z. and J.W. Pollard, *Macrophage diversity enhances tumor progression and metastasis*. Cell, 2010. **141**(1): p. 39-51.
31. Ryder, M., et al., *Increased density of tumor-associated macrophages is associated with decreased survival in advanced thyroid cancer*. Endocr Relat Cancer, 2008. **15**(4): p. 1069-74.
32. Zhu, X.D., et al., *High expression of macrophage colony-stimulating factor in peritumoral liver tissue is associated with poor survival after curative resection of hepatocellular carcinoma*. J Clin Oncol, 2008. **26**(16): p. 2707-16.
33. Lin, E.Y., et al., *Colony-stimulating factor 1 promotes progression of mammary tumors to malignancy*. J Exp Med, 2001. **193**(6): p. 727-40.
34. Sapi, E. and B.M. Kacinski, *The role of CSF-1 in normal and neoplastic breast physiology*. Proc Soc Exp Biol Med, 1999. **220**(1): p. 1-8.
35. Abraham, D., et al., *Stromal cell-derived CSF-1 blockade prolongs xenograft survival of CSF-1-negative neuroblastoma*. Int J Cancer, 2010. **126**(6): p. 1339-52.
36. Allavena, P., et al., *IL-10 prevents the differentiation of monocytes to dendritic cells but promotes their maturation to macrophages*. Eur J Immunol, 1998. **28**(1): p. 359-69.
37. Bell, D., et al., *In breast carcinoma tissue, immature dendritic cells reside within the tumor, whereas mature dendritic cells are located in peritumoral areas*. J Exp Med, 1999. **190**(10): p. 1417-26.
38. Sica, A., et al., *Autocrine production of IL-10 mediates defective IL-12 production and NF-kappa B activation in tumor-associated macrophages*. J Immunol, 2000. **164**(2): p. 762-7.
39. Klimp, A.H., et al., *Expression of cyclooxygenase-2 and inducible nitric oxide synthase in human ovarian tumors and tumor-associated macrophages*. Cancer Res, 2001. **61**(19): p. 7305-9.
40. Biswas, S.K., et al., *A distinct and unique transcriptional program expressed by tumor-associated macrophages (defective NF-kappaB and enhanced IRF-3/STAT1 activation)*. Blood, 2006. **107**(5): p. 2112-22.
41. Schoppmann, S.F., et al., *Tumor-associated macrophages express lymphatic endothelial growth factors and are related to peritumoral lymphangiogenesis*. Am J Pathol, 2002. **161**(3): p. 947-56.
42. Vignaud, J.M., et al., *The role of platelet-derived growth factor production by tumor-associated macrophages in tumor stroma formation in lung cancer*. Cancer Res, 1994. **54**(20): p. 5455-63.

43. Balkwill, F., *Cancer and the chemokine network*. Nat Rev Cancer, 2004. **4**(7): p. 540-50.
44. Strieter, R.M., et al., *CXC chemokines in angiogenesis of cancer*. Semin Cancer Biol, 2004. **14**(3): p. 195-200.
45. Murdoch, C., A. Giannoudis, and C.E. Lewis, *Mechanisms regulating the recruitment of macrophages into hypoxic areas of tumors and other ischemic tissues*. Blood, 2004. **104**(8): p. 2224-34.
46. Nagakawa, Y., et al., *Histologic features of venous invasion, expression of vascular endothelial growth factor and matrix metalloproteinase-2 and matrix metalloproteinase-9, and the relation with liver metastasis in pancreatic cancer*. Pancreas, 2002. **24**(2): p. 169-78.
47. Locati, M., et al., *Analysis of the gene expression profile activated by the CC chemokine ligand 5/RANTES and by lipopolysaccharide in human monocytes*. J Immunol, 2002. **168**(7): p. 3557-62.
48. Hagemann, T., et al., *Enhanced invasiveness of breast cancer cell lines upon co-cultivation with macrophages is due to TNF-alpha dependent up-regulation of matrix metalloproteases*. Carcinogenesis, 2004. **25**(8): p. 1543-9.
49. Mantovani, A., et al., *The origin and function of tumor-associated macrophages*. Immunol Today, 1992. **13**(7): p. 265-70.
50. Schutysse, E., et al., *Identification of biologically active chemokine isoforms from ascitic fluid and elevated levels of CCL18/pulmonary and activation-regulated chemokine in ovarian carcinoma*. J Biol Chem, 2002. **277**(27): p. 24584-93.
51. Curiel, T.J., et al., *Specific recruitment of regulatory T cells in ovarian carcinoma fosters immune privilege and predicts reduced survival*. Nat Med, 2004. **10**(9): p. 942-9.
52. Allavena, P., et al., *Anti-inflammatory properties of the novel antitumor agent yondelis (trabectedin): inhibition of macrophage differentiation and cytokine production*. Cancer Res, 2005. **65**(7): p. 2964-71.
53. Robinson, S.C., et al., *A chemokine receptor antagonist inhibits experimental breast tumor growth*. Cancer Res, 2003. **63**(23): p. 8360-5.
54. Dineen, S.P., et al., *Vascular endothelial growth factor receptor 2 mediates macrophage infiltration into orthotopic pancreatic tumors in mice*. Cancer Res, 2008. **68**(11): p. 4340-6.
55. Giraud, E., M. Inoue, and D. Hanahan, *An amino-bisphosphonate targets MMP-9-expressing macrophages and angiogenesis to impair cervical carcinogenesis*. J Clin Invest, 2004. **114**(5): p. 623-33.
56. Krieg, A.M., *Therapeutic potential of Toll-like receptor 9 activation*. Nat Rev Drug Discov, 2006. **5**(6): p. 471-84.
57. Guiducci, C., et al., *Redirecting in vivo elicited tumor infiltrating macrophages and dendritic cells towards tumor rejection*. Cancer Res, 2005. **65**(8): p. 3437-46.
58. Roder, J.C., et al., *Immunological senescence. I. The role of suppressor cells*. Immunology, 1978. **35**(5): p. 837-47.
59. Subiza, J.L., et al., *Development of splenic natural suppressor (NS) cells in Ehrlich tumor-bearing mice*. Int J Cancer, 1989. **44**(2): p. 307-14.
60. Strober, S., *Natural suppressor (NS) cells, neonatal tolerance, and total lymphoid irradiation: exploring obscure relationships*. Annu Rev Immunol, 1984. **2**: p. 219-37.
61. Gabrilovich, D.I., et al., *The terminology issue for myeloid-derived suppressor cells*. Cancer Res, 2007. **67**(1): p. 425; author reply 426.
62. Bronte, V., et al., *Apoptotic death of CD8+ T lymphocytes after immunization: induction of a suppressive population of Mac-1+/Gr-1+ cells*. J Immunol, 1998. **161**(10): p. 5313-20.
63. Havran, W.L., et al., *Characterization of an anti-Ly-6 monoclonal antibody which defines and activates cytolytic T lymphocytes*. J Immunol, 1988. **140**(4): p. 1034-42.

64. Movahedi, K., et al., *Identification of discrete tumor-induced myeloid-derived suppressor cell subpopulations with distinct T cell-suppressive activity*. *Blood*, 2008. **111**(8): p. 4233-44.
65. Youn, J.I., et al., *Subsets of myeloid-derived suppressor cells in tumor-bearing mice*. *J Immunol*, 2008. **181**(8): p. 5791-802.
66. Dolcetti, L., et al., *Hierarchy of immunosuppressive strength among myeloid-derived suppressor cell subsets is determined by GM-CSF*. *Eur J Immunol*, 2010. **40**(1): p. 22-35.
67. Yang, R., et al., *CD80 in immune suppression by mouse ovarian carcinoma-associated Gr-1+CD11b+ myeloid cells*. *Cancer Res*, 2006. **66**(13): p. 6807-15.
68. Huang, B., et al., *Gr-1+CD115+ immature myeloid suppressor cells mediate the development of tumor-induced T regulatory cells and T-cell anergy in tumor-bearing host*. *Cancer Res*, 2006. **66**(2): p. 1123-31.
69. Gallina, G., et al., *Tumors induce a subset of inflammatory monocytes with immunosuppressive activity on CD8+ T cells*. *J Clin Invest*, 2006. **116**(10): p. 2777-90.
70. Mirza, N., et al., *All-trans-retinoic acid improves differentiation of myeloid cells and immune response in cancer patients*. *Cancer Res*, 2006. **66**(18): p. 9299-307.
71. Ochoa, A.C., et al., *Arginase, prostaglandins, and myeloid-derived suppressor cells in renal cell carcinoma*. *Clin Cancer Res*, 2007. **13**(2 Pt 2): p. 721s-726s.
72. Filipazzi, P., et al., *Identification of a new subset of myeloid suppressor cells in peripheral blood of melanoma patients with modulation by a granulocyte-macrophage colony-stimulation factor-based antitumor vaccine*. *J Clin Oncol*, 2007. **25**(18): p. 2546-53.
73. Hoechst, B., et al., *A new population of myeloid-derived suppressor cells in hepatocellular carcinoma patients induces CD4(+)/CD25(+)/Foxp3(+) T cells*. *Gastroenterology*, 2008. **135**(1): p. 234-43.
74. Liu, C.Y., et al., *Population alterations of L: -arginase- and inducible nitric oxide synthase-expressed CD11b(+)/CD14 (-)/CD15 (+)/CD33 (+) myeloid-derived suppressor cells and CD8 (+) T lymphocytes in patients with advanced-stage non-small cell lung cancer*. *J Cancer Res Clin Oncol*, 2009.
75. Mandruzzato, S., et al., *IL4Ralpha+ myeloid-derived suppressor cell expansion in cancer patients*. *J Immunol*, 2009. **182**(10): p. 6562-8.
76. Rodriguez, P.C., et al., *Arginase I-producing myeloid-derived suppressor cells in renal cell carcinoma are a subpopulation of activated granulocytes*. *Cancer Res*, 2009. **69**(4): p. 1553-60.
77. Imada, K. and W.J. Leonard, *The Jak-STAT pathway*. *Mol Immunol*, 2000. **37**(1-2): p. 1-11.
78. Cheng, F., et al., *A critical role for Stat3 signaling in immune tolerance*. *Immunity*, 2003. **19**(3): p. 425-36.
79. Kortylewski, M., et al., *Inhibiting Stat3 signaling in the hematopoietic system elicits multicomponent antitumor immunity*. *Nat Med*, 2005. **11**(12): p. 1314-21.
80. Foell, D., et al., *S100 proteins expressed in phagocytes: a novel group of damage-associated molecular pattern molecules*. *J Leukoc Biol*, 2007. **81**(1): p. 28-37.
81. Cheng, P., et al., *Inhibition of dendritic cell differentiation and accumulation of myeloid-derived suppressor cells in cancer is regulated by S100A9 protein*. *J Exp Med*, 2008. **205**(10): p. 2235-49.
82. Sinha, P., et al., *Proinflammatory S100 proteins regulate the accumulation of myeloid-derived suppressor cells*. *J Immunol*, 2008. **181**(7): p. 4666-75.
83. Marigo, I., et al., *Tumor-induced tolerance and immune suppression depend on the C/EBPbeta transcription factor*. *Immunity*, 2010. **32**(6): p. 790-802.
84. Condamine, T. and D.I. Gaborilovich, *Molecular mechanisms regulating myeloid-derived suppressor cell differentiation and function*. *Trends Immunol*, 2011. **32**(1): p. 19-25.

85. Kusmartsev, S. and D.I. Gabrilovich, *STAT1 signaling regulates tumor-associated macrophage-mediated T cell deletion*. J Immunol, 2005. **174**(8): p. 4880-91.
86. Bronte, V., et al., *IL-4-induced arginase 1 suppresses alloreactive T cells in tumor-bearing mice*. J Immunol, 2003. **170**(1): p. 270-8.
87. Serafini, P., et al., *Myeloid-derived suppressor cells promote cross-tolerance in B-cell lymphoma by expanding regulatory T cells*. Cancer Res, 2008. **68**(13): p. 5439-49.
88. Delano, M.J., et al., *MyD88-dependent expansion of an immature GR-1(+)/CD11b(+) population induces T cell suppression and Th2 polarization in sepsis*. J Exp Med, 2007. **204**(6): p. 1463-74.
89. Liu, C., et al., *Expansion of spleen myeloid suppressor cells represses NK cell cytotoxicity in tumor-bearing host*. Blood, 2007. **109**(10): p. 4336-42.
90. Li, H., et al., *Cancer-expanded myeloid-derived suppressor cells induce anergy of NK cells through membrane-bound TGF-beta 1*. J Immunol, 2009. **182**(1): p. 240-9.
91. Nausch, N., et al., *Mononuclear myeloid-derived "suppressor" cells express RAE-1 and activate natural killer cells*. Blood, 2008. **112**(10): p. 4080-9.
92. Sinha, P., et al., *Cross-talk between myeloid-derived suppressor cells and macrophages subverts tumor immunity toward a type 2 response*. J Immunol, 2007. **179**(2): p. 977-83.
93. Marigo, I., et al., *Tumor-induced tolerance and immune suppression by myeloid derived suppressor cells*. Immunol Rev, 2008. **222**: p. 162-79.
94. Bronte, V. and P. Zanovello, *Regulation of immune responses by L-arginine metabolism*. Nat Rev Immunol, 2005. **5**(8): p. 641-54.
95. Bogdan, C., *Nitric oxide and the immune response*. Nat Immunol, 2001. **2**(10): p. 907-16.
96. Rodriguez, P.C., et al., *Arginase I production in the tumor microenvironment by mature myeloid cells inhibits T-cell receptor expression and antigen-specific T-cell responses*. Cancer Res, 2004. **64**(16): p. 5839-49.
97. Fischer, T.A., et al., *Activation of cGMP-dependent protein kinase Ibeta inhibits interleukin 2 release and proliferation of T cell receptor-stimulated human peripheral T cells*. J Biol Chem, 2001. **276**(8): p. 5967-74.
98. Szabo, C., H. Ischiropoulos, and R. Radi, *Peroxyne nitrite: biochemistry, pathophysiology and development of therapeutics*. Nat Rev Drug Discov, 2007. **6**(8): p. 662-80.
99. Sauer, H., M. Wartenberg, and J. Hescheler, *Reactive oxygen species as intracellular messengers during cell growth and differentiation*. Cell Physiol Biochem, 2001. **11**(4): p. 173-86.
100. Ostrand-Rosenberg, S., *Myeloid-derived suppressor cells: more mechanisms for inhibiting antitumor immunity*. Cancer Immunol Immunother, 2010. **59**(10): p. 1593-600.
101. Srivastava, M.K., et al., *Myeloid-derived suppressor cells inhibit T-cell activation by depleting cystine and cysteine*. Cancer Res, 2010. **70**(1): p. 68-77.
102. Hanson, E.M., et al., *Myeloid-derived suppressor cells down-regulate L-selectin expression on CD4+ and CD8+ T cells*. J Immunol, 2009. **183**(2): p. 937-44.
103. Pan, P.Y., et al., *Immune stimulatory receptor CD40 is required for T-cell suppression and T regulatory cell activation mediated by myeloid-derived suppressor cells in cancer*. Cancer Res, 2010. **70**(1): p. 99-108.
104. Song, H., et al., *A low-molecular-weight compound discovered through virtual database screening inhibits Stat3 function in breast cancer cells*. Proc Natl Acad Sci U S A, 2005. **102**(13): p. 4700-5.
105. van Cruysen, H., et al., *Sunitinib-induced myeloid lineage redistribution in renal cell cancer patients: CD1c+ dendritic cell frequency predicts progression-free survival*. Clin Cancer Res, 2008. **14**(18): p. 5884-92.
106. Finke, J.H., et al., *Sunitinib reverses type-1 immune suppression and decreases T-regulatory cells in renal cell carcinoma patients*. Clin Cancer Res, 2008. **14**(20): p. 6674-82.

107. Kusmartsev, S., et al., *All-trans-retinoic acid eliminates immature myeloid cells from tumor-bearing mice and improves the effect of vaccination*. *Cancer Res*, 2003. **63**(15): p. 4441-9.
108. Nefedova, Y., et al., *Mechanism of all-trans retinoic acid effect on tumor-associated myeloid-derived suppressor cells*. *Cancer Res*, 2007. **67**(22): p. 11021-8.
109. Lathers, D.M., et al., *Phase 1B study to improve immune responses in head and neck cancer patients using escalating doses of 25-hydroxyvitamin D3*. *Cancer Immunol Immunother*, 2004. **53**(5): p. 422-30.
110. Ribechini, E., P.J. Leenen, and M.B. Lutz, *Gr-1 antibody induces STAT signaling, macrophage marker expression and abrogation of myeloid-derived suppressor cell activity in BM cells*. *Eur J Immunol*, 2009. **39**(12): p. 3538-51.
111. Suzuki, E., et al., *Gemcitabine selectively eliminates splenic Gr-1+/CD11b+ myeloid suppressor cells in tumor-bearing animals and enhances antitumor immune activity*. *Clin Cancer Res*, 2005. **11**(18): p. 6713-21.
112. Vincent, J., et al., *5-Fluorouracil selectively kills tumor-associated myeloid-derived suppressor cells resulting in enhanced T cell-dependent antitumor immunity*. *Cancer Res*, 2010. **70**(8): p. 3052-61.
113. De Santo, C., et al., *Nitroaspirin corrects immune dysfunction in tumor-bearing hosts and promotes tumor eradication by cancer vaccination*. *Proc Natl Acad Sci U S A*, 2005. **102**(11): p. 4185-90.
114. Serafini, P., et al., *Phosphodiesterase-5 inhibition augments endogenous antitumor immunity by reducing myeloid-derived suppressor cell function*. *J Exp Med*, 2006. **203**(12): p. 2691-702.
115. Bronte, V., et al., *Identification of a CD11b(+)/Gr-1(+)/CD31(+) myeloid progenitor capable of activating or suppressing CD8(+) T cells*. *Blood*, 2000. **96**(12): p. 3838-46.
116. Young, M.R., M.E. Young, and K. Kim, *Regulation of tumor-induced myelopoiesis and the associated immune suppressor cells in mice bearing metastatic Lewis lung carcinoma by prostaglandin E2*. *Cancer Res*, 1988. **48**(23): p. 6826-31.
117. Kusmartsev, S.A., Y. Li, and S.H. Chen, *Gr-1+ myeloid cells derived from tumor-bearing mice inhibit primary T cell activation induced through CD3/CD28 costimulation*. *J Immunol*, 2000. **165**(2): p. 779-85.
118. Gabrilovich, D.I. and S. Nagaraj, *Myeloid-derived suppressor cells as regulators of the immune system*. *Nat Rev Immunol*, 2009. **9**(3): p. 162-74.
119. Sica, A. and V. Bronte, *Altered macrophage differentiation and immune dysfunction in tumor development*. *J Clin Invest*, 2007. **117**(5): p. 1155-66.
120. Bunt, S.K., et al., *Inflammation induces myeloid-derived suppressor cells that facilitate tumor progression*. *J Immunol*, 2006. **176**(1): p. 284-90.
121. Song, X., et al., *CD11b+/Gr-1+ immature myeloid cells mediate suppression of T cells in mice bearing tumors of IL-1beta-secreting cells*. *J Immunol*, 2005. **175**(12): p. 8200-8.
122. Kitchens, R.L., *Role of CD14 in cellular recognition of bacterial lipopolysaccharides*. *Chem Immunol*, 2000. **74**: p. 61-82.
123. Loser, K., et al., *The Toll-like receptor 4 ligands Mrp8 and Mrp14 are crucial in the development of autoreactive CD8+ T cells*. *Nat Med*, 2010. **16**(6): p. 713-7.
124. O'Neill, L.A. and A.G. Bowie, *The family of five: TIR-domain-containing adaptors in Toll-like receptor signalling*. *Nat Rev Immunol*, 2007. **7**(5): p. 353-64.
125. Drickamer, K., *Two distinct classes of carbohydrate-recognition domains in animal lectins*. *J Biol Chem*, 1988. **263**(20): p. 9557-60.
126. Taylor, P.R., et al., *Dectin-2 is predominantly myeloid restricted and exhibits unique activation-dependent expression on maturing inflammatory monocytes elicited in vivo*. *Eur J Immunol*, 2005. **35**(7): p. 2163-74.

127. McGreal, E.P., et al., *The carbohydrate-recognition domain of Dectin-2 is a C-type lectin with specificity for high mannose*. Glycobiology, 2006. **16**(5): p. 422-30.
128. Sato, K., et al., *Dectin-2 is a pattern recognition receptor for fungi that couples with the Fc receptor gamma chain to induce innate immune responses*. J Biol Chem, 2006. **281**(50): p. 38854-66.
129. Aragane, Y., et al., *Involvement of dectin-2 in ultraviolet radiation-induced tolerance*. J Immunol, 2003. **171**(7): p. 3801-7.
130. Lazennec, G. and A. Richmond, *Chemokines and chemokine receptors: new insights into cancer-related inflammation*. Trends Mol Med, 2010. **16**(3): p. 133-44.
131. Sawanobori, Y., et al., *Chemokine-mediated rapid turnover of myeloid-derived suppressor cells in tumor-bearing mice*. Blood, 2008. **111**(12): p. 5457-66.
132. Huang, B., et al., *CCL2/CCR2 pathway mediates recruitment of myeloid suppressor cells to cancers*. Cancer Lett, 2007. **252**(1): p. 86-92.
133. Nagaraj, S., et al., *Altered recognition of antigen is a mechanism of CD8+ T cell tolerance in cancer*. Nat Med, 2007. **13**(7): p. 828-35.
134. Hamerman, J.A., K. Ogasawara, and L.L. Lanier, *Cutting edge: Toll-like receptor signaling in macrophages induces ligands for the NKG2D receptor*. J Immunol, 2004. **172**(4): p. 2001-5.
135. Vogl, T., et al., *Mrp8 and Mrp14 are endogenous activators of Toll-like receptor 4, promoting lethal, endotoxin-induced shock*. Nat Med, 2007. **13**(9): p. 1042-9.
136. Hiratsuka, S., et al., *The S100A8-serum amyloid A3-TLR4 paracrine cascade establishes a pre-metastatic phase*. Nat Cell Biol, 2008. **10**(11): p. 1349-55.
137. Azenshtein, E., et al., *The CC chemokine RANTES in breast carcinoma progression: regulation of expression and potential mechanisms of promalignant activity*. Cancer Res, 2002. **62**(4): p. 1093-102.
138. Lavergne, E., et al., *Intratumoral CC chemokine ligand 5 overexpression delays tumor growth and increases tumor cell infiltration*. J Immunol, 2004. **173**(6): p. 3755-62.
139. Laubli, H., K.S. Spanaus, and L. Borsig, *Selectin-mediated activation of endothelial cells induces expression of CCL5 and promotes metastasis through recruitment of monocytes*. Blood, 2009. **114**(20): p. 4583-91.
140. Tan, M.C., et al., *Disruption of CCR5-dependent homing of regulatory T cells inhibits tumor growth in a murine model of pancreatic cancer*. J Immunol, 2009. **182**(3): p. 1746-55.
141. Breitman, T.R., S.J. Collins, and B.R. Keene, *Terminal differentiation of human promyelocytic leukemic cells in primary culture in response to retinoic acid*. Blood, 1981. **57**(6): p. 1000-4.
142. Castaigne, S., et al., *All-trans retinoic acid as a differentiation therapy for acute promyelocytic leukemia. I. Clinical results*. Blood, 1990. **76**(9): p. 1704-9.
143. Palucka, K., H. Ueno, and J. Banchereau, *Recent developments in cancer vaccines*. J Immunol, 2011. **186**(3): p. 1325-31.
144. Rosenberg, S.A., et al., *Adoptive cell transfer: a clinical path to effective cancer immunotherapy*. Nat Rev Cancer, 2008. **8**(4): p. 299-308.
145. Oble, D.A., et al., *Focus on TILs: prognostic significance of tumor infiltrating lymphocytes in human melanoma*. Cancer Immun, 2009. **9**: p. 3.
146. Albertsson, P.A., et al., *NK cells and the tumour microenvironment: implications for NK-cell function and anti-tumour activity*. Trends Immunol, 2003. **24**(11): p. 603-9.
147. Day, C.L., Jr., et al., *A prognostic model for clinical stage I melanoma of the upper extremity. The importance of anatomic subsites in predicting recurrent disease*. Ann Surg, 1981. **193**(4): p. 436-40.
148. Simpson, J.A., et al., *Intratumoral T cell infiltration, MHC class I and STAT1 as biomarkers of good prognosis in colorectal cancer*. Gut, 2010. **59**(7): p. 926-33.

149. Fukunaga, A., et al., *CD8+ tumor-infiltrating lymphocytes together with CD4+ tumor-infiltrating lymphocytes and dendritic cells improve the prognosis of patients with pancreatic adenocarcinoma*. *Pancreas*, 2004. **28**(1): p. e26-31.
150. Kim, S., et al., *In vivo natural killer cell activities revealed by natural killer cell-deficient mice*. *Proc Natl Acad Sci U S A*, 2000. **97**(6): p. 2731-6.
151. Smyth, M.J., et al., *New aspects of natural-killer-cell surveillance and therapy of cancer*. *Nat Rev Cancer*, 2002. **2**(11): p. 850-61.
152. Liyanage, U.K., et al., *Prevalence of regulatory T cells is increased in peripheral blood and tumor microenvironment of patients with pancreas or breast adenocarcinoma*. *J Immunol*, 2002. **169**(5): p. 2756-61.
153. Viguier, M., et al., *Foxp3 expressing CD4+CD25(high) regulatory T cells are overrepresented in human metastatic melanoma lymph nodes and inhibit the function of infiltrating T cells*. *J Immunol*, 2004. **173**(2): p. 1444-53.
154. Yang, Z.Z., et al., *Intratumoral CD4+CD25+ regulatory T-cell-mediated suppression of infiltrating CD4+ T cells in B-cell non-Hodgkin lymphoma*. *Blood*, 2006. **107**(9): p. 3639-46.
155. Shimizu, J., S. Yamazaki, and S. Sakaguchi, *Induction of tumor immunity by removing CD25+CD4+ T cells: a common basis between tumor immunity and autoimmunity*. *J Immunol*, 1999. **163**(10): p. 5211-8.
156. Gabrilovich, D.I., et al., *Mechanism of immune dysfunction in cancer mediated by immature Gr-1+ myeloid cells*. *J Immunol*, 2001. **166**(9): p. 5398-406.
157. Youn, J.I. and D.I. Gabrilovich, *The biology of myeloid-derived suppressor cells: the blessing and the curse of morphological and functional heterogeneity*. *Eur J Immunol*, 2010. **40**(11): p. 2969-75.
158. Yang, L., et al., *ICAM-1 regulates neutrophil adhesion and transcellular migration of TNF-alpha-activated vascular endothelium under flow*. *Blood*, 2005. **106**(2): p. 584-92.
159. Kusmartsev, S., S. Nagaraj, and D.I. Gabrilovich, *Tumor-associated CD8+ T cell tolerance induced by bone marrow-derived immature myeloid cells*. *J Immunol*, 2005. **175**(7): p. 4583-92.
160. Nagaraj, S., et al., *Mechanism of T cell tolerance induced by myeloid-derived suppressor cells*. *J Immunol*, 2010. **184**(6): p. 3106-16.
161. Corzo, C.A., et al., *HIF-1alpha regulates function and differentiation of myeloid-derived suppressor cells in the tumor microenvironment*. *J Exp Med*, 2010. **207**(11): p. 2439-53.
162. Campo, G.M., et al., *Small hyaluronan oligosaccharides induce inflammation by engaging both toll-like-4 and CD44 receptors in human chondrocytes*. *Biochem Pharmacol*, 2010. **80**(4): p. 480-90.
163. Konat, G.W., A. Krasowska-Zoladek, and M. Kraszpulski, *Statins enhance toll-like receptor 4-mediated cytokine gene expression in astrocytes: implication of Rho proteins in negative feedback regulation*. *J Neurosci Res*, 2008. **86**(3): p. 603-9.
164. Abram, C.L. and C.A. Lowell, *The expanding role for ITAM-based signaling pathways in immune cells*. *Sci STKE*, 2007. **2007**(377): p. re2.
165. Pende, D., et al., *Identification and molecular characterization of NKp30, a novel triggering receptor involved in natural cytotoxicity mediated by human natural killer cells*. *J Exp Med*, 1999. **190**(10): p. 1505-16.
166. Vitale, M., et al., *NKp44, a novel triggering surface molecule specifically expressed by activated natural killer cells, is involved in non-major histocompatibility complex-restricted tumor cell lysis*. *J Exp Med*, 1998. **187**(12): p. 2065-72.
167. Terabe, M., et al., *Transforming growth factor-beta production and myeloid cells are an effector mechanism through which CD1d-restricted T cells block cytotoxic T lymphocyte-mediated tumor immunosurveillance: abrogation prevents tumor recurrence*. *J Exp Med*, 2003. **198**(11): p. 1741-52.

168. Haverkamp, J.M., et al., *In vivo suppressive function of myeloid-derived suppressor cells is limited to the inflammatory site*. Eur J Immunol, 2011. **41**(3): p. 749-59.
169. Nowbakht, P., et al., *Ligands for natural killer cell-activating receptors are expressed upon the maturation of normal myelomonocytic cells but at low levels in acute myeloid leukemias*. Blood, 2005. **105**(9): p. 3615-22.
170. Jamieson, A.M., et al., *The role of the NKG2D immunoreceptor in immune cell activation and natural killing*. Immunity, 2002. **17**(1): p. 19-29.
171. Fernandez-Messina, L., et al., *Differential mechanisms of shedding of the glycosylphosphatidylinositol (GPI)-anchored NKG2D ligands*. J Biol Chem, 2010. **285**(12): p. 8543-51.
172. Ashiru, O., et al., *Natural killer cell cytotoxicity is suppressed by exposure to the human NKG2D ligand MICA*008 that is shed by tumor cells in exosomes*. Cancer Res, 2010. **70**(2): p. 481-9.
173. Mantovani, A., et al., *Cancer-related inflammation*. Nature, 2008. **454**(7203): p. 436-44.
174. Roth, J., et al., *Phagocyte-specific S100 proteins: a novel group of proinflammatory molecules*. Trends Immunol, 2003. **24**(4): p. 155-8.
175. Kerkhoff, C., et al., *Interaction of S100A8/S100A9-arachidonic acid complexes with the scavenger receptor CD36 may facilitate fatty acid uptake by endothelial cells*. Biochemistry, 2001. **40**(1): p. 241-8.
176. Brusa, D., et al., *Post-apoptotic tumors are more palatable to dendritic cells and enhance their antigen cross-presentation activity*. Vaccine, 2008. **26**(50): p. 6422-32.
177. Graham, L.M. and G.D. Brown, *The Dectin-2 family of C-type lectins in immunity and homeostasis*. Cytokine, 2009. **48**(1-2): p. 148-55.
178. Yamasaki, S., et al., *Mincle is an ITAM-coupled activating receptor that senses damaged cells*. Nat Immunol, 2008. **9**(10): p. 1179-88.
179. Ben-Baruch, A., *The multifaceted roles of chemokines in malignancy*. Cancer Metastasis Rev, 2006. **25**(3): p. 357-71.
180. Zlotnik, A., *Involvement of chemokine receptors in organ-specific metastasis*. Contrib Microbiol, 2006. **13**: p. 191-9.
181. Wong, M.M. and E.N. Fish, *Chemokines: attractive mediators of the immune response*. Semin Immunol, 2003. **15**(1): p. 5-14.
182. Berkman, N., et al., *Inhibition of macrophage inflammatory protein-1 alpha expression by IL-10. Differential sensitivities in human blood monocytes and alveolar macrophages*. J Immunol, 1995. **155**(9): p. 4412-8.
183. Hariharan, D., et al., *Interferon-gamma upregulates CCR5 expression in cord and adult blood mononuclear phagocytes*. Blood, 1999. **93**(4): p. 1137-44.
184. Lukacs, N.W., et al., *Intercellular adhesion molecule-1 mediates the expression of monocyte-derived MIP-1 alpha during monocyte-endothelial cell interactions*. Blood, 1994. **83**(5): p. 1174-8.
185. Broxmeyer, H.E. and C.H. Kim, *Regulation of hematopoiesis in a sea of chemokine family members with a plethora of redundant activities*. Exp Hematol, 1999. **27**(7): p. 1113-23.
186. Ziegler, S.F., et al., *Induction of macrophage inflammatory protein-1 beta gene expression in human monocytes by lipopolysaccharide and IL-7*. J Immunol, 1991. **147**(7): p. 2234-9.
187. Bystry, R.S., et al., *B cells and professional APCs recruit regulatory T cells via CCL4*. Nat Immunol, 2001. **2**(12): p. 1126-32.
188. Harlin, H., et al., *Chemokine expression in melanoma metastases associated with CD8+ T-cell recruitment*. Cancer Res, 2009. **69**(7): p. 3077-85.
189. Scarpino, S., et al., *Papillary carcinoma of the thyroid: hepatocyte growth factor (HGF) stimulates tumor cells to release chemokines active in recruiting dendritic cells*. Am J Pathol, 2000. **156**(3): p. 831-7.

190. Maghazachi, A.A., A. Al-Aoukaty, and T.J. Schall, *CC chemokines induce the generation of killer cells from CD56+ cells*. Eur J Immunol, 1996. **26**(2): p. 315-9.
191. Mantovani, A., et al., *The chemokine system in cancer biology and therapy*. Cytokine Growth Factor Rev, 2010. **21**(1): p. 27-39.
192. Li, X., et al., *Efficient Treg depletion induces T-cell infiltration and rejection of large tumors*. Eur J Immunol, 2010. **40**(12): p. 3325-35.
193. Galani, I.E., et al., *Regulatory T cells control macrophage accumulation and activation in lymphoma*. Int J Cancer, 2010. **127**(5): p. 1131-40.
194. Molon, B., et al., *T cell costimulation by chemokine receptors*. Nat Immunol, 2005. **6**(5): p. 465-71.
195. Abe, M., et al., *Role for macrophage inflammatory protein (MIP)-1alpha and MIP-1beta in the development of osteolytic lesions in multiple myeloma*. Blood, 2002. **100**(6): p. 2195-202.
196. Luboshits, G., et al., *Elevated expression of the CC chemokine regulated on activation, normal T cell expressed and secreted (RANTES) in advanced breast carcinoma*. Cancer Res, 1999. **59**(18): p. 4681-7.
197. Mattei, S., et al., *Expression of cytokine/growth factors and their receptors in human melanoma and melanocytes*. Int J Cancer, 1994. **56**(6): p. 853-7.
198. Kim, H.K., et al., *Elevated levels of circulating platelet microparticles, VEGF, IL-6 and RANTES in patients with gastric cancer: possible role of a metastasis predictor*. Eur J Cancer, 2003. **39**(2): p. 184-91.
199. Ruiz, M.E., et al., *Peripheral blood-derived CD34+ progenitor cells: CXC chemokine receptor 4 and CC chemokine receptor 5 expression and infection by HIV*. J Immunol, 1998. **161**(8): p. 4169-76.
200. Ugel, S., et al., *Therapeutic targeting of myeloid-derived suppressor cells*. Curr Opin Pharmacol, 2009. **9**(4): p. 470-81.
201. Zeisberger, S.M., et al., *Clodronate-liposome-mediated depletion of tumour-associated macrophages: a new and highly effective antiangiogenic therapy approach*. Br J Cancer, 2006. **95**(3): p. 272-81.

9 ABBREVIATIONS

µg	Microgram
µl	Microliter
µM	Micromolar
7-AAD	7-Aminoactinomycin D
ACK	Ammonium chloride potassium phosphate
Ag	Antigen
APC	Allophycocyanin
APC(s)	Antigen presenting cell(s)
ATRA	all- <i>trans</i> retinoic acid
BCR	B cell receptor
BM	Bone marrow
BrdU	Bromodeoxyuridine
CD	Cluster of differentiation
cDNA	complementary DNA
CFSE	Carboxyfluorescein succinimidyl ester
Cpm	Counts per minute
CTL(s)	Cytotoxic T lymphocyte(s)
Cy	Cyanine
d	Day(s)
DC(s)	Dendritic cell(s)
ddH ₂ O	Double distilled water
DMEM	Dulbecco/Vogt modified Eagle's minimal essential medium
DMSO	Dimethylsulfoxide
DNA	Desoxyribonucleic acid
EDTA	Ethylenediaminetetraacetic acid
ELISA	Enzyme-linked immunosorbent assay
FACS	Fluorescence-activated cell sorting
FCS	Fetal calf serum
FITC	Fluorescein-isothiocyanate
FSC	Forward scatter
g	Gram(s)
GM-CSF	Granulocyte-macrophage colony stimulating factor
h	Hour(s)
HLA	Human leukocyte antigen
i.p.	Intraperitoneal
ICAM	Intercellular adhesion molecule
iDC	Immature dendritic cells
IFN	Interferon
Ig	Immunoglobulin
IL	Interleukin
ITAM	Immunoreceptor tyrosine-based activation motif
ITIM	Immunoreceptor tyrosine-based inhibitory motif
KEGG	Kyoto Encyclopedia of Genes and Genomes
KO	Knock out

L	Liter
LPS	Lipopolysaccharide
M	Molar concentration
mAb(s)	monoclonal antibody(ies)
MACS	Magnetic cell sorting
mDC(s)	Mature dendritic cell(s)
MDSCs	Myeloid derived suppressor cell(s)
MFI	Mean fluorescence intensity
M ϕ	Macrophage
MHC	Major histocompatibility complex
min	Minute(s)
mg	Miligram
ml	Mililitre
mM	Milimolar
MMP	Matrix metalloproteinase
MO	Mononuclear
mRNA	Messenger RNA
NF	Nuclear factor
NFAT	Nuclear factor of activated T cells
NK	Natural killer
NKG2	NK group 2 member
NOS	Nitric oxide syntase
ORA	Over-representation approach
PAMP	Pathogen-associated molecular patterns
PBMC	Peripheral blood mononuclear cells
PBS	Phosphate buffered saline
PE	Phycoerythrin
PerCP-Cy5.5	Peridinin-chlorophyll-protein-complex-cyanine 5.5
pH	Potential hydrogen
PI	Propidium iodide
PI3K	Phosphoinositide 3-kinase
PMN	Polymorphonuclear
PRR(s)	Pattern Recognition Receptor(s)
Rae-1	Retinoic acid early inducible-1
RAG	Recombination activation gene
RNA	Ribonucleic acid
ROS	Reactive oxygen species
rpm	Rounds per minute
RPMI	Roswell park memorial institute medium
RT	Room temperature
SAM	Statistical analysis of microarrays
s.c.	Subcutaneous
SD	Standard deviation
SSC	Side scatter
TAP	Transporter associated with antigen processing
TCR	T cell receptor
TF	Transcription Factor
TGF- β	Transforming growth factor β
Th	T helper
TLR	Toll-like receptor

TNF	Tumor necrosis factor
Treg	Regulatory T cell
U	Unit
ULBP	UL16-binding protein
UV	Ultraviolet
VEGF	Vascular endothelial growth factor
W/O	Without
WT	Wild type
ZAP70	zeta-chain-associated protein kinase 70

10 ACKNOWLEDGEMENTS

At the end of my thesis, I would like to thank all people who made this thesis possible and enjoyable for me:

First of all, I would like to thank PD Dr. Adelheid Cerwenka for the interesting and challenging PhD project, her scientific guidance and continuous support. I'm thankful for all her encouragement and for the opportunities to present my work in scientific conferences.

In addition, my special gratitude goes to my first referee and member of my PhD committee Prof. Dr. Viktor Umansky for his valuable input and scientific guidance.

Moreover, I would like to acknowledge PD Dr. Christine Falk and Christian Quack for their great collaboration, technical support and helpful discussions.

Special thanks to Klaus Hexel, Steffen Schmitt and Gelo de la Cruz from the Flow Cytometry Unit of the DKFZ.

Many, many thanks to all my former and current colleagues from D080 – in particular to Alex, Annette, Kathi, Kitty, Matthias, Sonja, Nathalie and Tereza for the great and friendly atmosphere, helpful advices/discussions and their support in having coffees.

In the same way, I would like to thank my best friends from Munich and Illertissen, for being there in all "circumstances" during the last 28 years of my life.

The biggest "Thank you" ever to the little mole and tallest girl in the lab, who helped and supported me throughout my whole thesis ... for being there, days and sometimes nights ... but just to tell you, I haven't passed the door ...

Finally, I would like to thank my family for all their support and motivations and - to the best (bio)informatical belly ever, for being there 24/7 :-*

Sorry, for those I forgot!!!